CHARACTERIZATION OF QUARTZ IN SOME POTENTIAL HIGH PURITY QUARTZ DEPOSITS IN THE DAMARA OROGENIC BELT.

A MINI THESIS SUBMITTED IN PARTIAL FULFILMENT

OF THE REQUIREMENTS FOR THE DEGREE OF

MASTER OF SCIENCE (APPLIED GEOLOGY)

OF

THE UNIVERSITY OF NAMIBIA

BY

KAMWI RECTOR SISEHO

9808361

April 2016

Main supervisor: Professor A.F. Kamona

Abstract

This research project was aimed at characterizing quartz from selected potential High Purity Quartz (HPQ) deposits in terms of trace element associations, associated trace element concentrations, and growth zones. Six quartz rock samples were collected from three different localities, with two samples collected from each locality. Concentrations of Na, K, Li, Al, Ca, Fe, Ti, B and P were analysed in situ by LA-ICP-MS. This analysis was aimed at finding out whether the total concentrations of these trace elements do not exceed 50 μg g^{-1} as required by the HPQ definition. The Lowest total concentrations obtained from analysed samples were found to be much higher than the required minimum of less than 50 μg $g^{-1}$and are given as follows: sample DB2 from the farm Doornboom 316 yielded 2,144.6 μg g^{-1}, sample ALT2 from the farm Alt-Seeis 133 yielded 726.3 μg g^{-1} and sample MA1 from SP14 pegmatite intrusion in the Cape cross – Uis Pegmatite belt yielded 1,753.5 μg g^{-1}. Analytical results obtained from LA-ICP-MS showed very low Fe concentrations in all three deposits with all samples giving an average of <2μg g^{-1} and is the only trace element that met HPQ definition requirement of <3 μg g^{-1} Fe content. All three deposits showed very high average calcium concentration values varying between 450 and 750 μg g^{-1} and these high concentrations are likely to be associated with the chemistry of the fluids from which the hydrothermal quartz crystallized. Aluminium and alkali metals (Li, Na and K) concentrations were relatively high in all the deposits with fewer exceptions. Average values of lithium were noted as being between 170 and 230 μg g^{-1}, those of sodium as being between 70 and 1600 μg g^{-}

[1], and those of potassium as being between 65 and 120 μg g^{-1}, while aluminium average values were found to be between 150 and 660 μg g^{-1}. Exceptions were exhibited by sample ALT 2 from the hydrothermal vein deposit at the farm Alt Seeis 133, in which all the alkali metals and aluminium average values were found to be less than 63 μg g^{-1}. Titanium content in all samples was found to be relatively low (averaging between 20 and 31 μg g^{-1}). All the samples from deposits under this study do not meet the requirements of the HPQ definition and are thus not HPQ deposits. However a beneficiation study on these deposits is recommended to establish possible industrial applications that may be feasible. Scanning Electron Microscopy - Cathodoluminescence (SEM-CL) images of quartz grains were obtained from polished carbon coated samples. SEM-CL imaging was aimed at revealing replacements, fluid driven overprints and different quartz generations. The transformation of primary to secondary quartz through replacement was very limited in some samples and absent in others. This implies that metamorphic conditions did not have a major impact if any at all on the chemistry of trace elements in quartz. Statistical interpretation of analytical results from SP14 pegmatite intrusions and those from Doornboom indicate significant compositional similarities.

ACKNOWLEDGEMENT

I would like register my vote of thanks to my supervisor Professor Akalemwa Frederick Kamona at the Geology Department of the University of Namibia for his advices, guidance and directions. I would also like to express my appreciation for the service rendered by Central Analytical Facility (CAF) of the Stellenbosch University where the samples were analysed.

DEDICATION

I am dedicating this mini-thesis to my daughter Aimee Namasiku Siseho and my son Ethan Kamwi Siseho.

DECLARATIONS

. I, Kamwi Siseho, declare hereby that this study is a true reflection of my own research, and that this work, or part thereof has not been submitted for a degree in any other institution of higher education.

. I, Kamwi Siseho, grant The University of Namibia the right to reproduce this thesis in whole or in part, in any manner or format, which The University of Namibia may deem fit, for any person or institution requiring it for study and research; providing that The University of Namibia shall waive this right if the whole thesis has been or is being published in a manner satisfactory to the University.

……. [signature] Date……..

[Student's name]

Table of Contents

List of figures

List of Tables

CHAPTER 1

1. Introduction

1.1 Overview

This research paper deals with the study of pegmatite quartz and hydrothermal vein quartz from three deposits in the Pan African Damara Orogenic belt of Namibia. The study focuses on intra-crystalline lattice-bound trace elements which are the major parameters which determine the quality of high purity quartz (HPQ) products. The definition of a trace element according Rollinson (1993) is an element whose concentration in a rock is less than 0.1 wt % i.e. less than 1000 parts per million (ppm). In some instances trace elements will form mineral species in their own right but in most instances they substitute for major elements in rock forming minerals. In this study, concentrations of trace elements in quartz samples were determined and the method used measured the element concentration regardless of whether the element was present as a substitute or as a mineral species.

1.1.1 High purity quartz applications

The demand for high-purity quartz (HPQ) is growing worldwide as a result of increased industrial consumption and increased range of high-technology applications (Müller, Wanvik, and Ihlen, 2012). The main use of HPQ is to manufacture silica glass which has a wide range of applications due to its resistance to extreme fluctuations in temperature, its chemical durability in acidic environments and its ability of transmitting light from near ultraviolet to infrared parts of the electromagnetic spectrum (Larsen, Polvé, and Juve, 2000;Haus, Prinz, and Priess, 2012). In addition silica glass has a wide range of applications in the metallurgical, chemical and optical industries, as well as in communication technology for the production of optical wave-guides and as a raw material in the development of high-performance solar panels for energy production (Larsen et al., 2000).

According to Müller et al. (2012), the definition of HPQ from a commercial position should be based on the concentration limits of elements which have an effect on the quality of the end product. The impurities which determine the quality of quartz are lattice-bound trace elements which cannot be removed by conventional processing. Other impurities are intra-crystalline submicron inclusions (<1 μm), intra-crystalline mineral and fluid micro inclusions (>1 μm) and inter-crystalline impurities which may be present within grain boundaries as micro-crystals or mineral coatings. All other components other than lattice-bound impurities can be removed using different mineral

processing techniques such as initial crushing, optical sorting, comminution, classification to product particle size, autogenous grinding, electrodynamic fragmentation, attrition, magnetic separation, high tension separation, flotation acid washing, leaching, hot chlorination and calcinations, (Ihlen, Muller, Larsen, and Henderson, 2007; Haus, 2005; Haus et al., 2012; Kheloufi et al., 2013).

1.1.2 Negative effects of the presence of some impurities

Müller et al. (2012) stated that the majority of HPQ products are used in applications where the temperature is in excess of 1,400°C. Some end-uses such as laboratory optical devices, lenses for telescopes, photo cameras, ultra-flat TV screens, optical fibers, communication devices, lasers, optical grade glass for halogen vapor lamps, silicon crystals for transistors, diffraction lenses, high quality optical devices, optical fibers, optics for scanning devices and printers, etc. take advantage of the excellent optical properties of silica glass (Platiasa, Vatalisa, and Charalabidisa, 2013). At high temperatures, some impurities if present in excess may negatively affect the quality of the end product in the following ways (Müller et al., 2012): the presence of Ca will result in unwanted crystal nucleation in the quartz glass with time; Na, K and Li diffuse easily through the glass and the presence of Al alters the viscosity of the glass; Ti decreases the UV-light transmission in silica glass; Oxides of heavy elements such as Fe, Mn, Cr, Co, Cu and Ni result in a coloration of the silica glass which decreases its

transmission properties. In addition both P and B cause undesirable effects in photovoltaic or semiconductor products produced from quartz.

1.1.3 High purity quartz definition.

According to Müller et al. (2012) HPQ should contain <50 μg g^{-1} of the following nine elements: Na, K, Li, Al, Ca, Fe, Ti, B and P analysed on quartz crystals (single grain analysis) or processed quartz sand (bulk product analyses). The maximum content of each element was suggested as: Al <30 μg g^{-1}, Ti<10 μg g^{-1}, Na<8 μg g^{-1}, K<8 μg g^{-1}, Li<5 μg g^{-1}, Ca<5 μg g^{-1}, Fe<3 μg g^{-1}, P<2 μg g^{-1} and B<1 μg g^{-1} (Müller et al., 2012).

1.1.4 Analytical techniques for HPQ

Müller et al. (2012) recommended that in exploration of HPQ deposits it is important to characterize unprocessed quartz by in situ analysis of quartz crystals as it gives results not interfered with processing techniques. Trace element concentrations in HPQ products do not necessarily represent 100% lattice-bound elements if processed HPQ sand is analysed by solution ICP-MS for example. Portions of the element concentrations might have their origins from inclusions or other minerals which were not completely removed during beneficiation. The analysis of inclusions or foreign

minerals can be avoided by the application of in situ micro-beam techniques on single quartz crystals such as EPMA, LA-ICP-MS or SIMS (Müller et al., 2012).

The three analytical methods have their advantages and disadvantages and these are stated below as given by Kronz et al. (2012), Müller et al. (2003) and Haus et al. (2012). The advantage of EPMA analysis over other methods is its high spatial resolution and accuracy. In addition its quantitative methods and data reduction procedures are well established. Disadvantages of EPMA analysis are poor detection limits, poor signal/noise ratio and low signal strength in comparison to SIMS or LA-ICPMS. Advantages of La-ICP-MS are low detection limits and relatively straight forward calibration procedures. Its disadvantage is its poor resolution in comparison to both EPMA and SIMS, but this is however only critical in zoned materials. The advantage of SIMS analytical method is its high sensitivity but it has low spatial resolution in comparison to EPMA and this would be a disadvantage if zoned features or alteration domains were involved. EPMA has high resolution but low detection limits and thus give optimum results for zoned features or domains with alterations. This method is ideal for trace element concentrations in excess of 10's of ppm and a scale of <10μm (Müller et al., 2003). La-ICP-MS is ideal for trace elements with very low concentrations in un-zoned or domains without alteration features. SIMS would be ideal for samples which require low detection limit, small sampling size and high precision and it would give optimum results in unzoned features or domains without alterations due to its low resolution.

When analyzing bulk quartz samples by conventional methods, the main source of impurities are Na, K, Cl and Ca from fluid inclusions in quartz (Müller et al., 2012). However, calcination and thermal treatment can be employed to successfully remove these fluid inclusions and their dissolved components during the beneficiation process (Haus, 2005).

1.1.5 Other impurities

Silicate melt inclusions in pegmatitic quartz can contain high concentrations of F, Cl, B, P, Li, Cs and Rb (Thomas et al., 2006). Although silicate melt inclusions trapped within igneous and pegmatitic quartz are scarce in comparison to fluid inclusions (Frezzotti, 2001; Webster, 2006), they are not easily identifiable because they are crystalline and often hidden or overprinted by fluid inclusions (Müller et al., 2012).

Mineral inclusions in igneous quartz are dominantly rutile, mica, Fe-oxides, feldspar, zircon and apatite (Roedder, 1984; Leeder et al., 1987). In metamorphic quartz, the range of mineral inclusions depends on metamorphic conditions e.g. chlorite, muscovite or amphibole occur in low-grade metamorphic rocks, whereas garnet, kyanite or staurolite normally occur in high-grade metamorphic rocks (Müller et al,. 2012). Inclusions of gypsum, calcite, anhydrite, salt minerals and organic matter have been observed in sedimentary authigenic quartz (Hyrsl, and Niedermayr, 2003; Götze, 2012).

1.1.6 Notable effects brought about by the presence of trace elements in quartz

Some trace elements when present in abundance as structural bound trace elements cause color changes in quartz. For example the colour of rose quartz is due to high concentrations of structurally bound Fe^{2+}, $Fe^{3+}$and Ti^{4+}, and amethyst's colour is due to structurally bound $Fe^{2+}$and Fe^{3+} (Hassan, and Cohen, 1974; Cohen, and Makar, 1985) as stated in Larsen et al. (2004). The smoky color is as a result of ionizing radiation from adjacent minerals such as potassium-40 in potassium feldspar (Larsen et al., 1998). In some situations quartz that appears clear and free of inclusions at a glance may contain thousands of parts per million of structurally bound trace elements whereas dark smoky quartz with numerous liquid and solid inclusions may be almost free of lattice bound trace elements (Larsen et al., 2004).

1.1.7 Lattice bound substitutions

Due to the strong configuration of Si–O bonds only a few elements (Al, Na, Li, Ca, B, P, K, Fe, Ti, Ge, Ba, Be, Cr, Cu, U, Mg, Sr, Mn, H, Pb, and Rb) are likely to be substituted into the atomic lattice structure of quartz (Larsen et al., 2004). Substituting trace elements are accommodated in different positions within the atomic structure of quartz depending on their number of unpaired valence electrons. Tetravalent ions ($Ti^{4+}$and

Ge^{4+}), occur in the quartz lattice as simple substitution for Si^{4+} (Fig. 1.1), whereas pentavalent ion (P^{5+}), is accommodated in a coupled substitution together with a trivalent ion (Al^{3+}, Fe^{3+} or B^{3+}), (where the charges are balanced as follows: Al^{3+}+ P^{5+} = Si^{4+} + Si^{4+}) (Larsen et al., 2004, Müller et al., 2012). Monovalent (Li^{+}, K^{+}, $H^{+}$and Na^{+}) and divalent ions (Be^{2+}, Fe^{2+}) occur at interstitial channel positions where they serve as charge compensators for the trivalent (Al^{3+} and Fe^{3+}) and pentavalent substitutional ions (P^{5+}) (Müller et al., 2012).

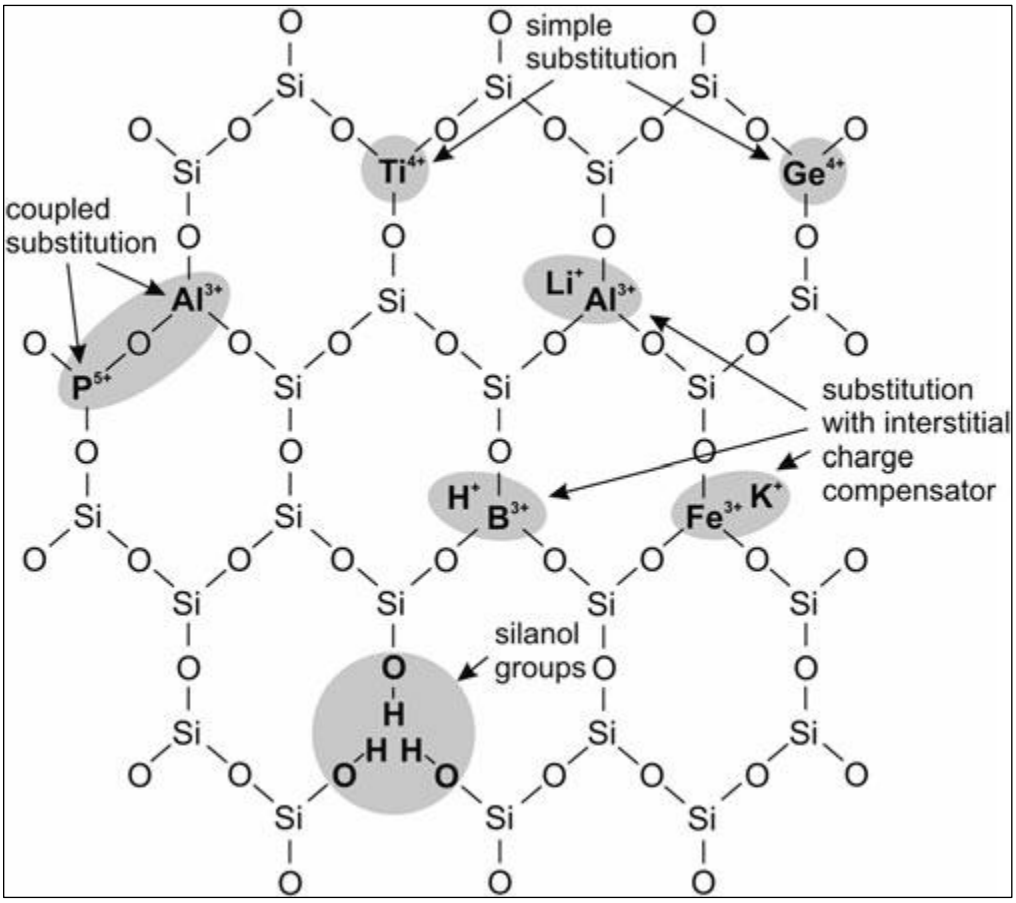

Figure 1.1 Schematic quartz structure showing the configuration of trace elements in the quartz lattice. The substitution of Si^{4+} by four H^{+} is possible (silanol groups). Because of

the two-dimensional illustration the fourth H^+ is not shown on the figure (after Müller et al., 2012).

HPQ is rare in nature and economic quantities (>80,000 t; Fig.1.2) are even rarer (Müller et al., 2012). The few HPQ deposits found around the world include certain types of quartz-rich granitic pegmatite (e.g. IOTA® 2005; Norwegian Crystallites AS 2006) and hydrothermal quartz veins. It is shown in figure 1.2 that the lower the total impurities, the better the quality and consequently the higher the price of quartz. It's also shown that high quality natural quartz deposits are generally smaller in sizes than low quality quartz deposits. The same figure indicates that hyper to low indicates the chemical quality of quartz. HPQ is defined as containing 8–50 μg g^{-1}impurities (grey shaded field). The approximate economic limit of the deposit size shown in figure 1.2 was based on data of active quartz mines

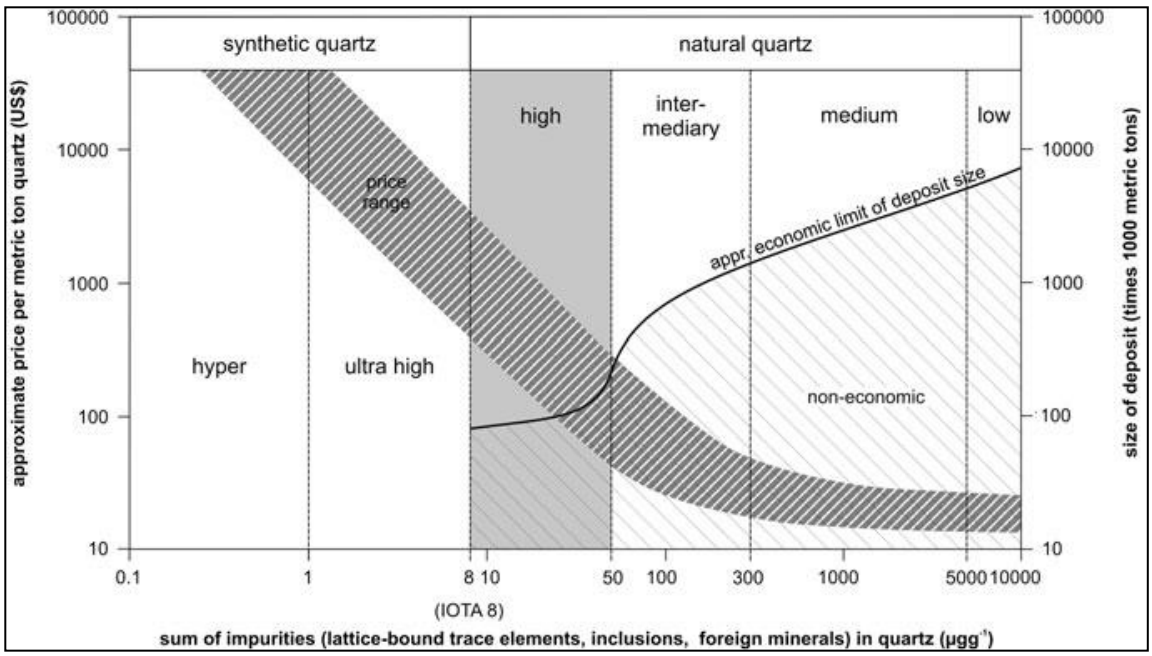

Figure 1.2 Impurity content and quartz quality relationship. Depicted here is generally the relationship between the quality of quartz and the total amount of impurities in quartz. Overlaid on this relationship is its effect on price of quartz (Müller et al., 2012)

1.2 Research problem and objectives

Previous studies on pegmatite and hydrothermal vein quartz deposits within the Damara Orogen have focused mainly on geological, mineralogical, geochemical and genetic aspects, including their potential for gemstones (e.g. Ollila, 1987; Roda et al., 2007, Macey and Harris, 2006; King, 1986; Richards, 1986) and none took the route of researching on high purity quartz (HPQ) mainly due to non-existence of applicable technology at the time. This study is aimed at filling this knowledge gap. Developments in the use of in-situ micro-beam techniques on single quartz crystals such as EPMA, LA-

ICP-MS and SIMS in the recent few years make it possible to carry out this study. The need to assess the potential of deposits of the Damara Orogen of hosting HPQ is warranted by the fact that high quality pegmatite quartz and hydrothermal vein quartz have been documented in the region (King, 1986; Richards, 1986) and the environment is similar to environments where HPQ deposits of substantial potential have been reported elsewhere in the world such as those in Norway (Haus, 2005; Ihlen et al., 2007; Müller et al., 2007; Müller et al., 2012; Larsen et al. 2000).

The main objective of this study was to characterize quartz from selected potential HPQ deposits in terms of trace element concentrations, associated trace elements and growth zones. The hypothesis of the study was based on the idea that tectonic uplift, deformation and / retrogradation of syn-tectonic pegmatites transforms primary pegmatite quartz into HPQ under stipulated conditions such as high water/rock ratios and the infiltration of relatively low-T fluids (Ihlen et al., 2007). The null hypothesis was carried out to determine whether the variances between trace elements from different localities were equal. An F-test and a T-test were carried out for this purpose.

CHAPTER 2

2. Literature review

Studies carried out in other parts of the world have shown that granitic pegmatites, hydrothermal quartz veins and quartzites are promising sources of high-purity quartz. This chapter reviews the literature of similar studies, which were carried out in other parts of the world with focus on geological settings, research methods, trace element concentrations and economic potential of the studied deposits. The deposits dealt with in this chapter are located in Norway and this country was chosen because the country hosts some of the most studied HPQ deposits in the world (Larsen et al., 2004). The chapter will conclude with a synopsis of general conclusions drawn by some of the researchers.

2.1 Similar studies in other parts of world

Studies similar to this research have been carried out in other parts of the world by various researchers. Cases presented under this chapter are studies that were done in Norway, and this country hosts some of the most studied pegmatite and hydrothermal quartz vein fields.

2.1.1 Granitic pegmatites in South Norway

A study on transformation of igneous quartz to high-purity quartz was carried out by Ihlen et al. (2007) on granitic pegmatites in South Norway. These pegmatite fields were developed during the Sveconorwegian orogeny from 1.13 - 0.9 Ga. The study involved syntectonic and anatectic pegmatites which formed at peak-metamorphism roughly 1.1 Ga.

According to Ihlen et al. (2007) the pegmatites can be classified as synkinematic abyssal (AB) biotite pegmatites and muscovite pegmatites, in some areas developed as ABHREE and AB-LREE pegmatites. Zoned pegmatites composed of cores of massive quartz enclosed by blocky feldspar are common while more fractionated types with cleavelandite and sodic aplites are comparatively scarce. The author states that the pegmatites were emplaced during amphibolite (sillimanite grade) to granulite facies metamorphism (1.08 - 1.13 Ga) and show signs of deformation, authenticating their syntectonic development.

Results of trace element concentrations obtained by LA-ICP-MS reveal that most of the pegmatitic quartz exceeds a total impurity content of 50 µg/g and consequently falling outside the range of HPQ. However, quartz intergrown with late cleavelandite and albite was found to be generally low in Ti (<10 µg/g. The concentrations of Al and Ti were found to be highly unpredictable, but scarcely fell within the HPQ requirement limit

with upper limits defined as Al = 25 µg/g and Ti = 10 µg/g (Müller et al., 2005). Quartz in peraluminous muscovite pegmatites was found to contain high concentrations of both Al (25 - 300 µg/g and Ti (<60 µg/g), while quartz in metaluminous biotite pegmatites revealed lower levels of Al (25-100 µg/g) and Ti (<20 µg/g). Quartz in pegmatites that formed under high-grade metamorphic conditions exhibited concentrations of 300 µg/g Al and 100-350 µg/g Ti. According to Ihlen et al. (2007), the trace element characteristics highlight the significance of both temperature (Wark and Watson, 2006) and magma composition (Müller et al., 2002a) on the quartz chemistry. The study showed sample examinations by SEM-CL and optical petrography revealed that the pegmatitic quartz comprises a mixture of multiple quartz generations

In this study Ihlen et al. (2007) gave the following in their conclusions. The transformation of igneous quartz to HPQ in pegmatites is a fluid-induced process which mainly occurs in syntectonic pegmatites. The magmatic quartz recrystallised in conjunction with sub-solidus reactions and episodes of tectonic uplift into finer-grained quartz preserving the magmatic element signature. Extensive fluid influx and hydrothermal re-placement of the recrystallised igneous quartz during subsequent uplift, deformation and/or retrogradation are the main processes in the formation of HPQ. High water/rock ratios and the infiltration of relatively low-T fluids are the most important parameters controlling its development in syn-kinematic pegmatites.

2.1.2 Pegmatites, Hydrothermal quartz veins and quartzites in Norway

A study was carried out by Müller et al., (2012) on petrological and chemical characterisation of high-purity quartz deposits. The study was carried out in Norway on the following deposits the Melkfjell quartzite, several kyanite quartzites, the Nedre Øyvollen pegmatite and the Kvalvik, Nesodden and Svanvik hydrothermal quartz veins (Fig.2.1).

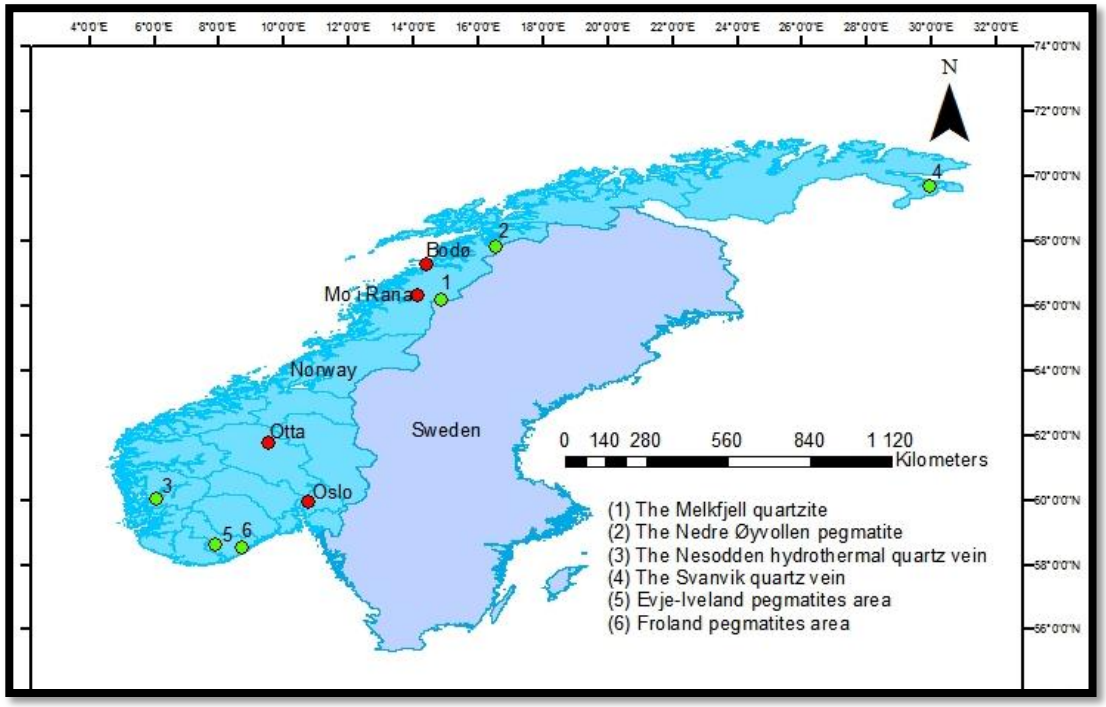

Figure 2.1 Location of some of the quartz deposits in Norway

The study covered a refined definition of HPQ, a discussion of the impurities controlling the chemical quality of HPQ products and descriptions of selected HPQ deposits in Norway, both economic and potentially economic examples. Regarding suggested definition of HPQ, Müller et al., (2012) proposed that the maximum concentration limit of each element should be: Al<30 µg/g, Ti<10 µg/g, Na<8 µg/g, K<8 µg/g, Li<5 µg/g, Ca<5 µg/g, Fe<3 µg/g, P<2 µg/g and B<1 µg/g. Impurities within quartz crystals (intracrystalline impurities) control the quality of HPQ products because they cannot be removed by conventional processing. These and other impurities include lattice-bound trace elements, submicron inclusions (<1 µm), and mineral and fluid micro inclusions (<1 µm) (Müller et al., 2012). Backscattered electron (BSE) and Cathodoluminescence (SEM-CL) imaging were used for identification of impurities and laser ablation inductively coupled plasma mass spectrometry (LA-ICP-MS) for analysis.

Müller et al., (2012) mentioned that trace element concentrations in HPQ products do not necessarily represent hundred percent lattice-bound elements if processed HPQ sand is analysed, for example by solution ICP-MS. Portions of the element concentrations might arise from inclusions or other minerals which were not entirely removed during processing. Müller et al., (2012) further stated that the analysis of inclusions or foreign minerals can be avoided by the application of in-situ micro-beam techniques on single quartz crystals such as EPMA, LA-ICP-MS or SIMS.

2.1.2.1 The Melkfjell quartzite

The study indicated that the Melkfjell quartzite is located roughly 30 km SE of Mo i Rana in Nordland county (Fig.2.1). The quartzite is part of the Kjerringfjell Group which forms the base of the Caledonian Rødingsfjell Nappe Complex where layers of quartzite are present together with mica gneisses and mica schists. According to Müller et al. (2012) CL imaging revealed that grain-boundary migration is a widespread phenomenon. The quartz of the Melkfjell quartzite revealed low concentrations of Li (mean 1.1 µg/g), B (mean 0.8 µg/g) and Al (mean 7.7 µg/g). Müller et al. (2012) further stated that the Ti concentration was found to be moderately high due to high-temperature Caledonian metamorphism and the application of the Ti-in-quartz geothermometer by Wark and Watson (2006) revealed the peak metamorphic temperature of about 520 ± 8°C (Ti = 8.76 µg/g). Ti saturation is assumed due to the common exsolution of rutile needles.

Müller et al. (2012) commented that the common occurrence of rutile needles in the Melkfjell quartz would make it very hard to achieve a low Ti content in the final, processed product and, thus only applications with low-quality requirements for Ti content are feasible. The author further stated that the common occurrence of apatite and monazite as interstitial accessories and inclusions in quartz will cause elevated P concentrations in the product, limiting possible photovoltaic applications. The author however pointed out that the quality of the quartzite is suitable for ferrosilicon

applications if contaminating rocks of amphibolite and the pegmatite dykes which cross-cuts the quartzite are properly handled (Müller et al., 2012).

Müller et al. (2012) mentioned that the metamorphic conditions of the Caledonian orogenesis produced quartz with very low Al and Li and moderate Ti. The author concluded that the protolith was relatively pure sandstone as indicated by the little amount of minor and accessory minerals. According to Müller et al. (2002b) as cited by Müller et al. (2012), moderate pressure (~3–4 kbars) and temperatures >350°C lead to the expulsion of Al and alkalis from the quartz lattice during metamorphic overprinting, resulting in low Al and Li contents in the newly formed quartz. The author further stated that the Melkfjell quartzite was exposed to pressures between 3 and 5 kbar (Stephens et al. 1985) and temperatures of 466 – 528°C (Müller and Koch-Müller 2009) and, therefore the metamorphic conditions coincide with the pressure–temperature window in which quartz purification occurs (Müller et al. 2002b). The author ratiocinates that the moderate Ti content reflects the relatively high crystallization temperature during metamorphism.

Müller et al., (2012) showed that CL imaging indicated that grain-boundary migration is widespread phenomenon in the quartzite, whereby dull luminescent grains replaced bright luminescent grains. Dull luminescent quartz is generally considered to be quartz with a low content of lattice defects and trace elements (Götze et al. 2001). The author therefore claims that the grain-boundary migration caused a further purification of the

quartz grains and further stated that in particular, the Ti content was reduced significantly by this process, from about 7 – 2 µg/g. He concluded that the displaced Ti may have crystallised as sub-micron rutile needles which are common in the Melkfjell quartz.

2.1.2.2 The Nedre Øyvollen pegmatite

The Nedre Øyvollen pegmatite is situated on the west side of Tysfjord in Nordland county, northern Norway (Fig.2.1). According to the author (Müller et al., 2012) the pegmatite is hosted by the Tysfjord granitic gneiss which is regarded to have an emplaced roughly 1.74 Ga and it is classified as a Niobium-Yttrium-Fluorine (NYF)-type pegmatite. He further stated that the deformational fabric of the granitic gneiss is considered to be of Caledonian age although the possibility that some of the foliations in the Tysfjord area could be of pre-Caledonian age cannot be excluded. It is moreover mentioned by the author that the Caledonian amphibolite-facies peak metamorphism has been put at approximately 432 Ma ago and deformation temperature was presumably in the range of 420–450°C and the pressure between 2 and 3 kbar (Müller et al., 2012).

The author explains that the quartz chemistry of the pegmatite revealed low Ti (mean 3.0 µg/g) and moderately low Al (mean 20.6 µg/g). The average Li content was found to be 4.9 µg/g and that of B to be 1.6 µg/g. The author described the Nedre Øyvollen pegmatite as one of the not many deposits in the world from which HPQ has been

produced for over a decade. The pegmatite is renowned for its large, massive quartz body, the large crystal size and the homogeneous chemistry with very low trace element concentrations and these have made it a highly productive world-class HPQ deposit (Müller et al., 2012).

The pegmatitic quartz core of the Nedre Øyvollen pegmatite consists of primary magmatic HPQ which was broadly not or only weakly affected by secondary recrystallisation due to shearing related to the Caledonian metamorphism. On contrary the author argues that the possibility that the metamorphic temperature, which was probably in the range of 420–450°C and the pressure of 2–3 kbar, may have had an effect on the trace element distribution in the quartz cannot be eliminated (Müller et al., 2012).

2.2.2.3 The Nesodden hydrothermal quartz vein

The Nesodden hydrothermal quartz vein is located in Hordaland County in western Norway (Fig.2.1). According to Müller et al. (2012) (author), the vein is situated in Proterozoic basement rocks, south of the Hardanger Fault Zone (HFZ) which is a 600 km long, SW-NE striking late Caledonian ductile shear zone. It is further explained by the author that fluids were mobilised during the extensional shearing and crystallised as hydrothermal quartz veins, such as the Nesodden and Kvalvik veins, in the vicinity of the fault. According to the author the chemistry of the quartz from Nesodden revealed

low Ti (mean 2.1 µg/g), moderately low Al (mean 18.0 µg/g) and Ge (mean 1.0 µg/g) and comparatively high Li (mean 5.7 µg/g) contents. The average B concentration was found to be roughly 1.4 µg/g. Because of the high average Li content, the Nesodden quartz is not a HPQ in the strict sense (Müller et al., 2012).

The LA-ICP-MS analyses suggest that the primary crystallised hydrothermal quartz contained low concentrations of lattice-bound trace elements. The author claims that succeeding alteration and recrystallisation linked to shearing and fluid flux may have contributed to further purification of the quartz as indicated by the low CL intensity of the secondary quartz. The author further remarks that relatively high Li and B concentrations, a high content of high-salinity fluid inclusions, common enclaves of granitic gneiss and micro-inclusions of muscovite, feldspar and calcite pose challenges in processing HPQ from the deposit (Müller et al., 2012).

2.2.2.4 The Svanvik quartz vein

The Svanvik quartz vein is located in Finnmatk County in northern Norway, close to the border with Russia (Fig.2.1). According to the author (Müller et al., 2012) the vein is hosted by grey granitic to granodioritic gneiss which has an age of 2825 ± 34 Ma. The author further explains that the vein was emplaced at an early stage of shear-zone formation, possibly during the early Proterozoic (*1.75 Ga), when the Pechenga–Varzuga Greenstone Belt was sandwiched between two converging continents.

He (author) described the quartz from Svanvik as of very low Li (mean 2.1 µg/g), Al (mean 5.3 µg/g), Ti (mean 1.1 µg/g) and Fe (mean 0.2 µg/g) concentrations. The Svanvik quartz was further described by the author as having the lowest total concentration of lattice-bound trace elements (~15 µg/g) compared to the other deposits discussed in this study. However, the author further pointed out that there are additional quartz generations mainly at the vein contacts and these contain higher trace element contents and may thus contaminate the quartz product. He further commented that cross-cutting calcite-chlorite-epidote veins, K-feldspar-quartz veins, macroscopic inclusions (>1 mm) and microscopic inclusions of calcite are the challenges for producing HPQ from this deposit.

2.2.3 Pegmatites in Evje and Froland areas in South Norway

Larsen et al. (2004) carried out a study on the distribution and petrogenetic behaviour of trace elements in granitic pegmatite quartz. The study was done in the Evje and Froland areas in South Norway (Fig.2.1). These areas feature as the most studied two pegmatite fields in South Norway. According to Larsen et al. (2004) the pegmatites in these areas formed in the Mezoproterozoic period and the granitic melts were either derived from mantle or lower crust. Rb/Sr dating on several pegmatites in these fields yielded ages between 852±12 Ma and 896±27 Ma (Larsen et al., 2004).

The author describes host rocks as constituting of amphibolite, norite and mafic gneisses and further describes the Evje pegmatites as modally zoned and typically comprising a wall zone (WZ), one or a number of intermediate zones (IZ) and one or a number of core zones (CZ). He (author) indicated that most of the quartz is homogeneous and composed of only one generation of primary igneous quartz but however, they noted that secondary replacement features occur, particularly in the Froland pegmatites where tectonic overprinting is more common and secondary quartz chiefly formed along fractures and grain edges. Larsen et al. (2004) however postulated that the preservation of primary igneous quartz suggest that the recrystallization was not pervasive and LA-HR-ICP-MS analysis confirmed that the general trace element distribution, with some pronounced exceptions, was preserved during several episodes of recrystallization.

According to Larsen et al. (2004) a total of 93 granitic pegmatites were sampled and analytical results revealed that >95% of the trace elements are comprised of Al, P, Li, Ti, Ge and Na in that order of abundance. The remaining 5% is comprised K, Fe, Be, B, Ba and Sr whereas other elements normally are present at concentrations below the detection limit. The Trace element concentration were analysed by ICP-MS and SEM-CL technique was used to unveil primary and secondary growth features

2.2.4 Another study in Froland and Evje-Iveland pegmatite fields

A study was undertaken by Müller (2011) on regional distribution of trace elements in quartz of pegmatites and its tectonomagnetic implications. According to the author the concentrations of Al, Ti, Li and Ge in samples from pegmatitic quartz of about 200 NY(F)-type pegmatites from the Froland and Evje-Iveland pegmatite fields were analysed by laser ablation inductively coupled plasma mass spectrometry (LAICP-MS). The pegmatite fields are in Bamble and Evje-Iveland pegmatite districts in South Norway (Fig.2.1). These were formed during the Sveconorwegian orogeny (1.14-0.90 Ga) and however the two fields differ in both age and tectonometamorphic setting (Müller, 2011).

The author described quartz of the Froland pegmatites as having a relatively homogeneous composition with 11.8 ±6.7 ppm Li, 1.5 ±0.8 ppm Ge, 44.7 ±22.7 ppm Al, and 7.7 ±3.3 ppm Ti. The regional distribution of the Ti, Al, Li and Ge contents of pegmatitic quartz were used to evaluate the differentiation pattern and crystallisation temperatures within both pegmatites fields. Müller (2011) states that the relative low Ti corresponds to crystallisation temperatures of 511 ±46°C according to Ti-in-quartz geothermometer by Wark and Watson (2006).

On the other hand quartz of the Evje-Iveland pegmatites was found to have more variable composition with 7.3 ±4.5 ppm Li, 3.0±2.9 ppm Ge, 81.7 ±58 ppm Al, and 21.4

±11.4 ppm Ti. The author pointed out the high average Ti as indicating crystallisation temperatures of 591 ±70°C. He further stated that the pegmatites in the two areas are defined as of relative low crystallisation temperatures and highly differentiated quartz composition are characterised as gadolinite- and columbite-rich NY(F) pegmatites.

2.2.5. Synopsis of general conclusions from above studies

Ihlen et al. (2007) found that the transformation of igneous quartz to HPQ in pegmatites is a fluid-induced process mainly occurring in syntectonic pegmatites. He further explained that extensive fluid influx and hydrothermal replacement of the crystallised igneous quartz during subsequent uplift, deformation and/or retrogradation are the main processes in the formation of HPQ. High water/rock ratios and the infiltration of relatively low-T fluids arethe most important parameters controlling its development in syntectonic pegmatites.

Müller et al. (2012) recommended LA-ICP-MS as an excellent method for analysing the concentration of lattice bound trace elements in single quartz crystals in situ. The concentrations determined correspond theoretically to the best achievable quality of the final quartz product if perfect processing is applied, removing all non-lattice-bound impurities.

In the same study the author further stated that study has demonstrated that SEM-CL is an appropriate method for visualising structures within quartz crystals that might be related to HPQ formation. These structures, which are only visible in CL, include healed micro-cracks, quartz domains affected by alteration, newly formed quartz due to grain boundary migration, etc. In the last remarks of the paper Müller et al. (2012) states that HPQ deposits in Norway showed that the processes of HPQ formation differ in the various deposits and that there is no general rule for HPQ formation.

2.2 Global Suppliers of High Purity Silica Quartz

The world's leading producer of high purity quartz is the US-based Unimin Corp./Sibelco which operates from Spruce Pine in North Carolina, USA (Haus et al., 2012; Hughes, 2013). Other suppliers are The Quartz Corp operating from Spruce Pine in North Carolina and Tysfjord area in Nordland province in northern Norway. The Quartz Corp is a merger which was realized in 2011 between Imerys and Norsk Mineral. Imerys SA merged its US-based Spruce Pine companies KT Feldspar and The Feldspar Corp. (TFC) with Norwegian Crystallites to form The Quartz Corp (Haus et al., 2012; Hughes, 2013). The global demand for ultra-pure quartz is 30,000 tons per year and the main industry supplier is Unimin Corporation which operates in Spruce Pine in North Carolina, USA (Vatalis et al., 2015; Krause, 2013). Unimin Corporation was founded in 1970, has grown from a small, local sand mining company to become a leading producer of non-metallic industrial minerals in the worldwide Sibelco Group. The Sibelco was

founded in 1872 and is a global giant in the mining and processing of silica sand and minerals. The company has 245 production units worldwide, employs a total of 8,000 employees and recorded a turnover of 1.7 billion Euros in 2004 (Vatalis et al., 2015).

Brazil was the world's main supplier of high purity quartz in the early 1970s and an embargo on exports of lump quartz imposed by the government reduced production significantly. There have been efforts in recent years to produce processed high purity quartz led by Mineracao Santa Rosa (MSR), one of the main lump quartz and lascas suppliers in Brazil (Haus et al., 2012). Lascas, is a term used to describe manually beneficiated rock crystal. Madagascar has been the other main source of lascas and is still producing from small mining operations. Deposits with potential to yield High Purity Quartz are present in Madagascar and Angola but due to poor infrastructure and lack of interest from their governments hinder development of these deposits (Haus et al., 2012).

According to ANZAPLAN's website (http://www.anzaplan.com/strategic-minerals-metals/high-purity-quartz/high-purity-quartz-resources/) high purity quartz projects are under development in Angola, Argentina, Australia, China, India, Kazakhstan, Mauretania, Norway, Saudi Arabia, Ukraine, Vietnam and Turkey to name just a few in which the company is involved. ANZAPLAN is a specialist in testing and engineering services for high-value industrial and strategic minerals and down-stream products.

Some of the world's High Purity Quartz deposits and their operating companies are given in Table 2.1 below (Moore, 2005; Hughes, 2013; Haus et al., 2012).

Table 2.1 Some High Purity Quartz deposits and their operating companies.

Company	Location
Auzminerals Resource Group (AMRG), Solar Silicon Resources Group (SSRG)	Lighthouse Silica Quartz Mine, QLD, Australia
I-Minerals	Helmer-Bovill, NW Idaho, USA
Mauritanian Minerals Co	Oum Agueneina, Mauritania
Momentive Performance Materials Inc	Geesthacht, Germany; Hebron, Ohio, USA
Nordic Mining	Kvinnherad, Hordaland, Norway
Polar Quartz	Sarapul, Russia
Polar Quartz, OJSC, RUSNANO	Yugra, western Siberia, Russia
The Quartz Corp	Spruce Pine, North Carolina, USA
The Quartz Corp (Norwegian Crystallites)	Tysfjord area, Nordland province, northern Norway
LLC Russia Quartz, (RUSNANO, KGOK JSC, Sumitomo Corporation)	Kyshtym, Chelyabinsk, Russia
Unimin Corp/Sibelco	Spruce Pine, North Carolina, USA

2.2.1 Spruce Pine Alaskite deposits, North Carolina, USA

The High Purity Silica Quartz located near the town of Spruce Pine, North Carolina, USA (Fig. 2.2) is the world's highest quality quartz deposits. The quartz is hosted by alaskites and separated from feldspar and mica to yield a quartz concentrate that is used to produce IOTA® quartz; the industry standard for quality and purity. The alaskites formed 375 million years ago from magma several kilometers below the earth's surface (Hughes, 2013). The alaskites were recognized for their extraordinary sheet mica, which was used as electrical insulation in early vacuum tube electronics and currently the Spruce Pine quartz is used for manufacture silicon-based semiconductor devices (Hughes, 2013). According to Vatalis et al., (2015), the global demand for ultra-pure quartz is 30,000 tons per year and the main industry supply is from the deposits in Spruce Pine in North Carolina, USA.

2.2.2 Norwegian Crystallites, northern Norway

The Norwegian part of The Quartz Corp; The Quartz Corp Norwegian Crystallites, from 2013 called The Quartz Corp^{II} (Vatalis et al., 2015). The company produces high-purity crystalline quartz for final high-tech applications. The Norwegian Crystallites factory is located in the mountainous Tysfjord area in Nordland province in northern Norway (Fig. 2.2). The company mines high purity quartz deposits in several locations. This raw material is purified to a high level of crystalline quartz products. The Norwegian

Crystallites has produced high purity quartz products in their Drag plant since 1996 (Vatalis et al., 2015). The company has a production capacity of 10,000-20,000 tonnes per annum (Krause, 2013).

2.2.3 Oum Agueneina Mine, Mauritania

Mauritania Minerals Co. (MMC) produces high quality quartz at the Oum Agueneina Mine located about 150 km from Nouadhibou Port on the West Sahara border (Fig. 2.2) and was estimated to contain 70 Mt of quartz (Feytis, 2010). The quartz mine has the capacity to produce 300,000 t/yr of quartz (Taib, 2013). The company targets several high tech areas for its material such as crucibles, liquid crystal displays (LCDs), halogen lighting, tubes, rods, and special glasses in high tech instruments. According to Hughes (2013) the Geological survey of Mauritania revealed a resource grade of 99.9% purity quartz capable of producing 100 – 500 000 tonnes in the first year of production.

2.2.4 The Lighthouse Quartz deposit, Far North Queensland, Australia

Solar Silicon Resources Group (SSRG) owns the Lighthouse Quartz mine located in Far North Queensland about 30 km south-west of Mount Surprise in Australia (Fig. 2.2). The Solar Silicon Resources Group is wholly owned by Auzminerals Resource Group (AMRG). Lighthouse Quartz has an AusIMM JORC-compliant resource estimate of

1.83 million tonnes (Krause, 2013; Queensland government, 2014). According to Krause (2013), the Lighthouse Quartz deposit is a large, world class, chemically consistent source of high-purity quartz product with multiple applications and a production capacity up to 50,000 tonnes per year. Lighthouse Quartz ore has a purity level of 99.8% SiO_2 and the company estimates a further resource of 3 to 5 Mt (Queensland government, 2014). The high-purity silica from Lighthouse Quartz has a huge range of applications in solar manufacturing and semiconductor manufacturing industries, including crucibles used in the manufacture of silicon wafers (Queensland government, 2014).

2.2.5 Kyshtym, LLC Russian Quartz

Kyshtym Mining (also known as KGOK or LLC Russian Quartz), which is located on the Eastern slopes of the South Ural mountains (Fig. 2.2), produced 60% of domestic high purity quartz demand in the Soviet era (Haus et al., 2012). The project is currently owned by LLC Russian Quartz, in which participatory interests belong to RUSNANO, KGOK JSC, Sumitomo Corporation. The project has a dry processing plant with a capacity of 6,000 tons per year for dry concentration (Haus et al., 2012; Moore, 2005) and 3,000 tons per annum production facility of high-purity quartz has been completed (http://www.sumitomocorp.co.jp/english/news/detail/id=27200).

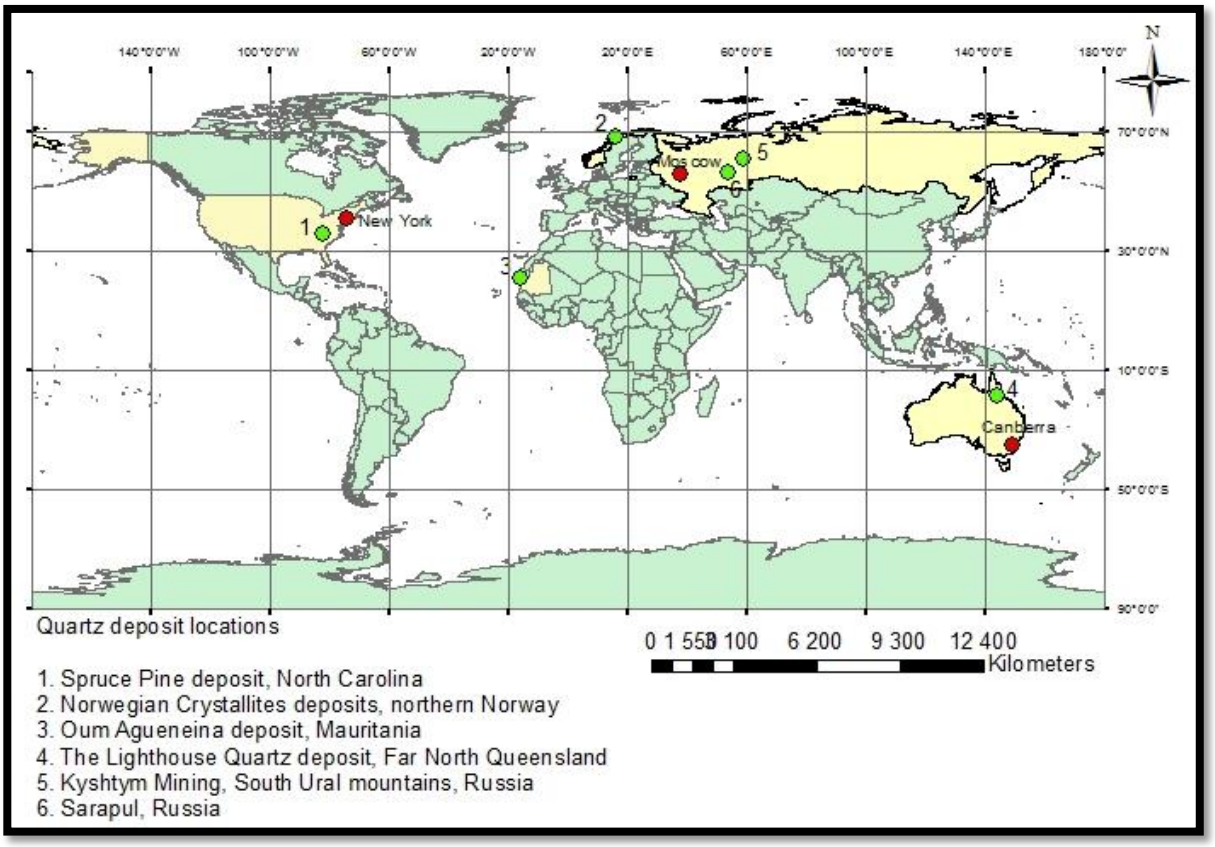

Figure 2.2 Locations of some of the global suppliers of high purity quartz.

CHAPTER 3

3. Research materials and methods

Quartz minerals were characterized in terms of growth zones, trace element associations, associated trace element concentrations, and other attributes. The SEM-CL imaging technique was used to unveil primary and secondary growth features including crystal growth zones and sequences of quartz precipitation, which reflect the crystallisation processes involved in the formation of a quartz deposit. LA–ICP-MS was used for the in-situ determination of concentrations of Na, K, Li, Al, Ca, Fe, Ti, B, P, Mg, Cr, Mn, Co, Ni, Cu, Zn, Rb, Sr and Ba in quartz grains. The analysis of these trace elements and the examination of quartz generations may play a role in bringing about a better understanding of the environment and conditions of formation of HPQ that are likely to be found within the Damara Orogenic belt. Similar studies on HPQ properties have been carried out elsewhere on deposits of similar origin (Haus, 2005; Ihlen et al., 2007; Müller et al., 2007; Müller et al., 2012; Larsen, Hendersen, Ihlen, and Jacamon, 2004; Larsen et al., 2000). These studies have been used for bench-marking procedures and comparing results of this study.

3.1 Research design

This is a quantitative study based on scientific theory to determine the purity of quartz samples from three localities: farm Alt-Seeis 133, farm Doornboom 316, and the SP14 Pegmatite intrusions; which were analysed to determine the concentrations of impurities and to determine the quartz generations. The study followed a route which enabled the researcher to achieve the following: firstly to determine whether the deposits under study meets HPQ requirements, and secondly to acquire an understanding of growth features of the quartz grains which gives a reflection of the crystallization and recrystallization processes of the quartz. Methods and procedures that were selected ensured the realisation of these goals.

3.2 Sampling

The sample set is composed of two pegmatite intrusions and two hydrothermal quartz veins from the Damara Orogenic belt which appear to have potential of hosting high purity quartz (HPQ). A total of six rock quartz samples were collected from the three different localities, with two samples collected from each locality. The selection of these localities was based on previous reports of the presence of quality quartz by earlier researchers and explorers (King, 1986; Richards, 1986) together with knowledge gathered from studies done elsewhere on similar deposits of HPQ (Haus, 2005, Ihlen et

al., 2007; Müller et al., 2007; Müller et al., 2012; Larsen et al., 2004; Larsen et al., 2000). Studies by King (1986) and Richards (1986) were on geological, mineralogical and geochemical aspects. Samples were collected using a hammer, marked, cut and delivered to the Central Analytical Facility (CAF) of the Stellenbosch University - South Africa for laboratory analyses. Samples from the Alt-Seeis deposit were marked ALT1 and ALT2, those from Doornboom were marked DB1 and DB2, and those from SP pegmatite intrusions were marked MA1 and MA2.

Sampling localities include a hydrothermal vein quartz deposit at the dormant White Ridge Mine on the farm Alt-Seeis 133 (Fig.3.1), some 80 km east of Windhoek; hydrothermal quartz veins and blows on the farm Doornboom 316, some 60 km west of Rehoboth (Fig.3.2); and SP14 Pegmatite intrusions in the Cape Cross - Uis pegmatite belt (Fig.3.3).

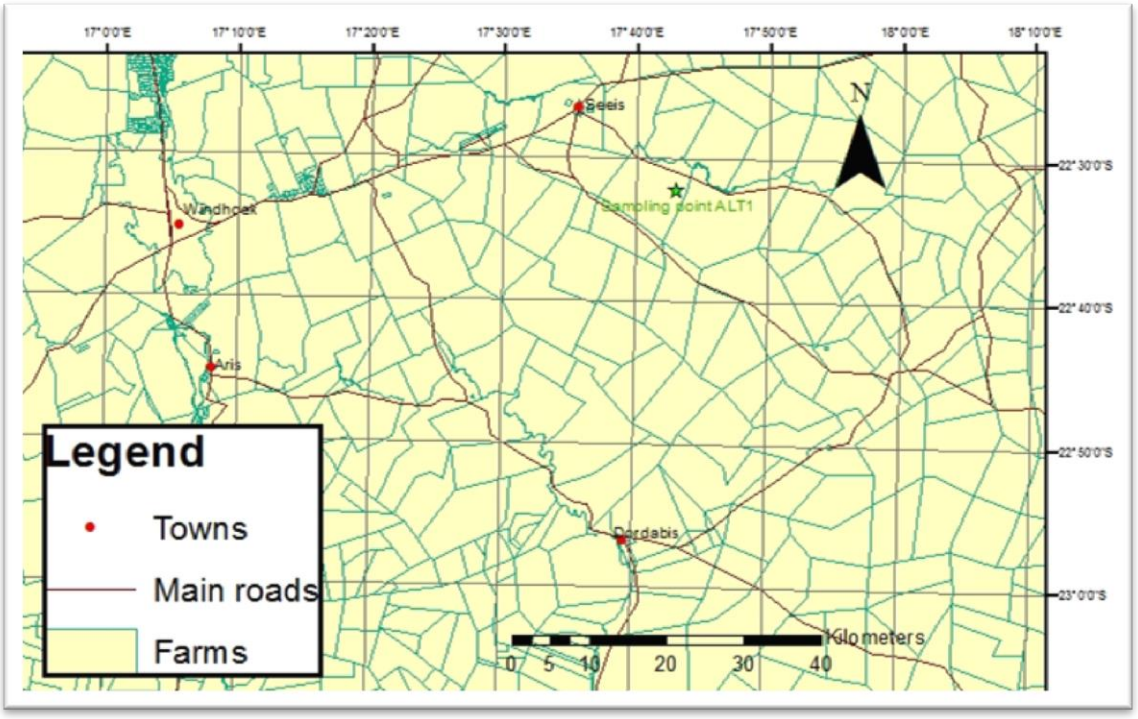

Figure 3.1 Sample locality (ALT 1 and ALT 2). The map is for orientation purposes indicating the location of the sampling point in relation to nearby villages of Dordabis and Seeis.

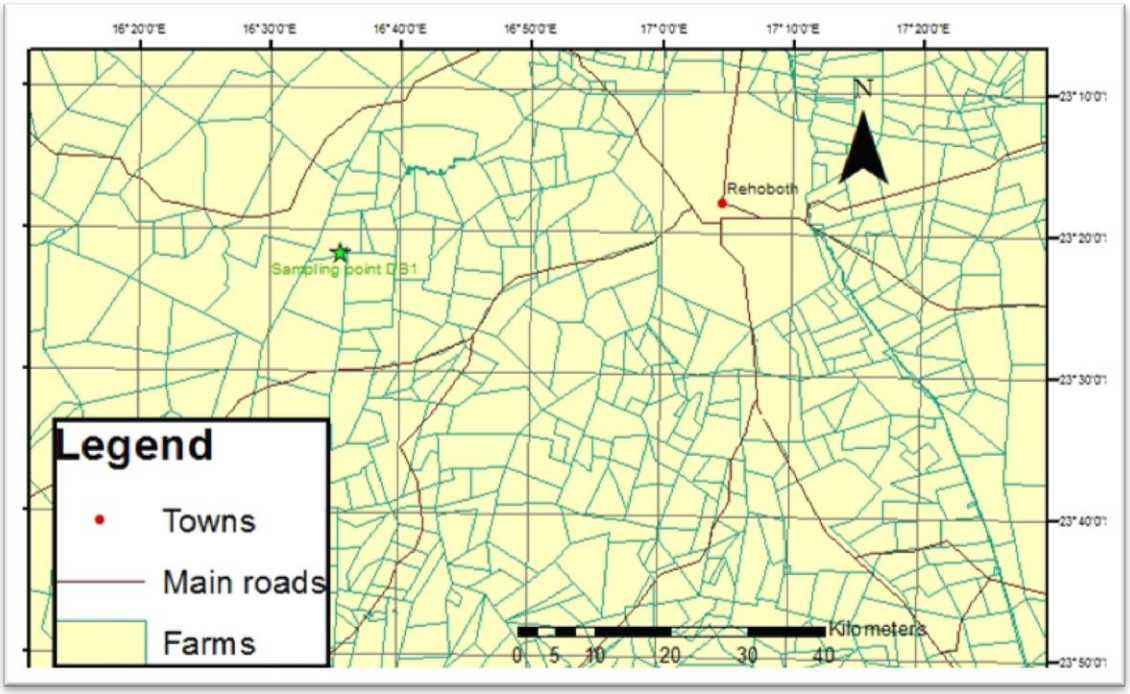

Figure 3.2 Sample locality (DB1 and DB 2). The map is for orientation purposes indicating the location of the sampling location with reference to a nearby the town of Rehoboth.

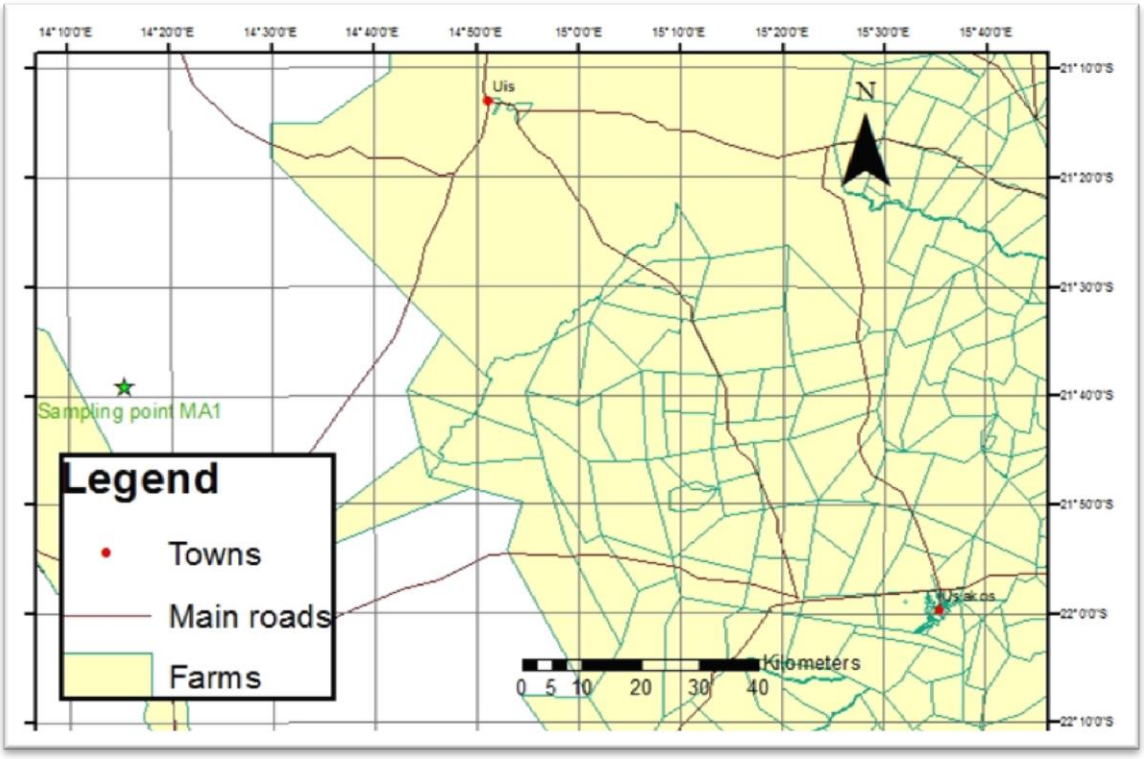

Figure 3.3 Sample locality (MA 1 and MA 2). The map is for orientation purposes indicating the location of the sampling location with reference to a nearby the town of Uis.

Sampling geographical coordinates are given in table 3.1.

Table 3.1 Sample locations and geographic coordinates of each sample.

Sample number	**Coordinates**	**Locality**	**Tectono-stratigraphic zone of the Damara Orogen**
ALT 1	22˚32'8.427" S 17˚43'6.656"E	Farm Alt Seeis 133	Southern marginal zone (SMZ)
ALT 2	22˚32'8.427" S 17˚43'6.656"E	Farm Alt Seeis 133	
DB 1	23˚21'43.211" S 16˚35'31.158"E	Farm Doorn Boom 316	
DB 2	23˚21'43.211" S 16˚35'31.158"E	Farm Doorn Boom 316	
MA 1	21˚39'12.87" S 14˚15'33.089"E	Cape Cross - Uis pegmatite belt	Northern zone (NZ)
MA 2	21˚39'12.87" S 14˚15'33.089"E	Cape Cross - Uis pegmatite belt	

3.3 Geological setting

The three study areas are located within the Damara Orogenic belt (Fig.3.4) in central Namibia which forms part of Pan-African collisional belts in southern Africa representing the formation of the Gondwana supercontinent. The Damara Orogen is a Neoproterozoic orogeny consisting of three arms, the NNW-trending coastal arm (the Kaoko Belt) extending into Angola, the NE-trending arm (the Damarara Belt) which extends through central Namibia, across Botswana to Zambezi belt (Miller, 2008) and the Gariep Belt down south. It formed as a result of continental collision between the

Congo and Kalahari cratons. The three belts converge at a triple junction centred roughly at Swakopmund (Miller, 2008). The Damara Belt has been divided into six major zones, which are, from north to south, the Northern Platform (NP), Northern Zone (NZ), Central Zone (CZ), Southern Zone (SZ), Southern Margin Zone (SMZ), and the Southern Foreland (SF) (Miller, 2008). The CZ is further divided into northern Central Zone (nCZ) and southern Central Zone (sCZ) sections (Miller, 2008).

Metamorphic grade in the orogen increases from the margins to the granite intruded areas in the west of the coastal branch and the centre of the north-east branch of the Damara belt (Miller, 1983). The convergence event of Congo Craton and the Kalahari Craton triggered volcanic eruptions which produced plutonic bodies of various ages and sizes, accompanied by pegmatites ranging in age from- early syn-tectonic to post-tectonic. Two of these pegmatites are the subject of this study together with two hydrothermal quartz veins resulting from hydrothermal fluids triggered by the effects of this orogenic event. Locations of the deposits are shown in figure 3.4 below.

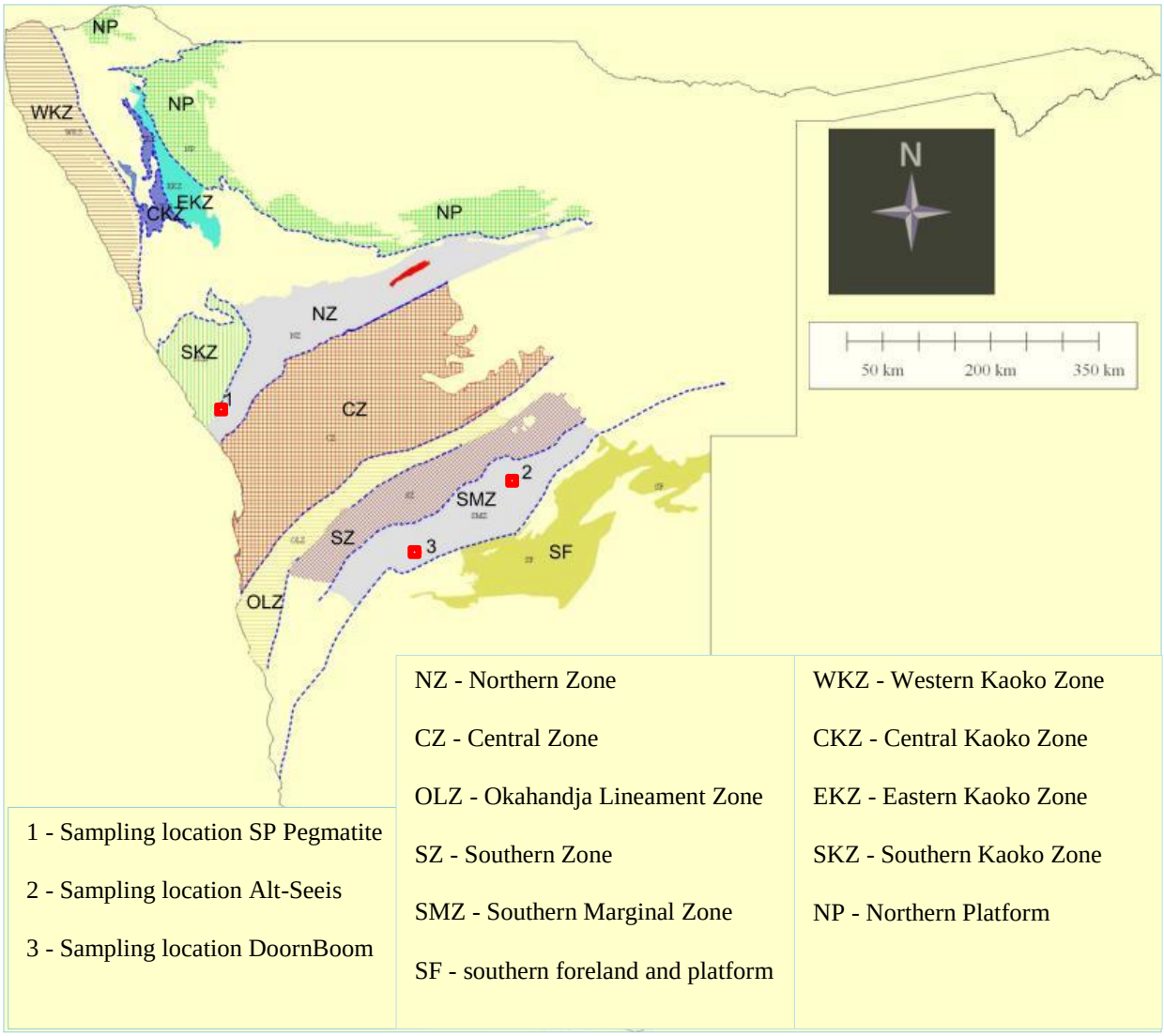

Figure 3.4 Locations of deposits of this study; SP Pegmatite intrusion marked 1 on the map is located in the Northern Zone (NZ), Alt-Seeis Hydrothermal quartz vein marked 2 on the map is located in the Southern Margin Zone (SMZ), and Doornboom Hydrothermal quartz vein marked 3 on the map is also located in the SMZ (modified after Miller, 2008)

The Damara belt comprises of over 200 plutons, plugs and stocks of granitic rocks, thousands of granite and pegmatite dykes and is approximately 74 000km^2 (Miller, 2008). A large number of these volcanic bodies are in the CZ which was the active

southern margin of the Congo Craton (Miller, 2008). Pegmatite swarms in the Damara belt were emplaced during the later stages of each of the main pulses of granitic activity. The Central Zone of the Damara Orogen is defined by high temperature, low-pressure metamorphic grade (Kasch, 1983), and abundant voluminous granitoid intrusions (Miller, 1983; Goscombe et al., 2004).

Most pegmatites of economic interest are variably zoned, in exception of the Uis stanniferous pegmatites (Diehl, 1990; Keller, 1991; Geol. Surv. Namibia, 1992). The cassiterite-rich pegmatites east of Cape Cross, those in Omaruru and Sandamap Tin Belts have a quartz core bounded by comparatively small inner cassiterite-bearing intermediate zones (Miller, 2008) (Fig.3.5). The pegmatites in the Central Zone of the Damara belt, are positioned along distinguishable belts, which are the Cape Cross – Uis pegmatite belt, the Nainais - Kohero pegmatite belt, the Sandamap - Erongo pegmatite belt, the Karibib pegmatite district and the Brandberg West - Goantagab tin belt (Geol. Surv. Namibia, 1992). A number of these pegmatites have been worked for their lithium, beryllium, cesium, tin, niobium and tantalum.

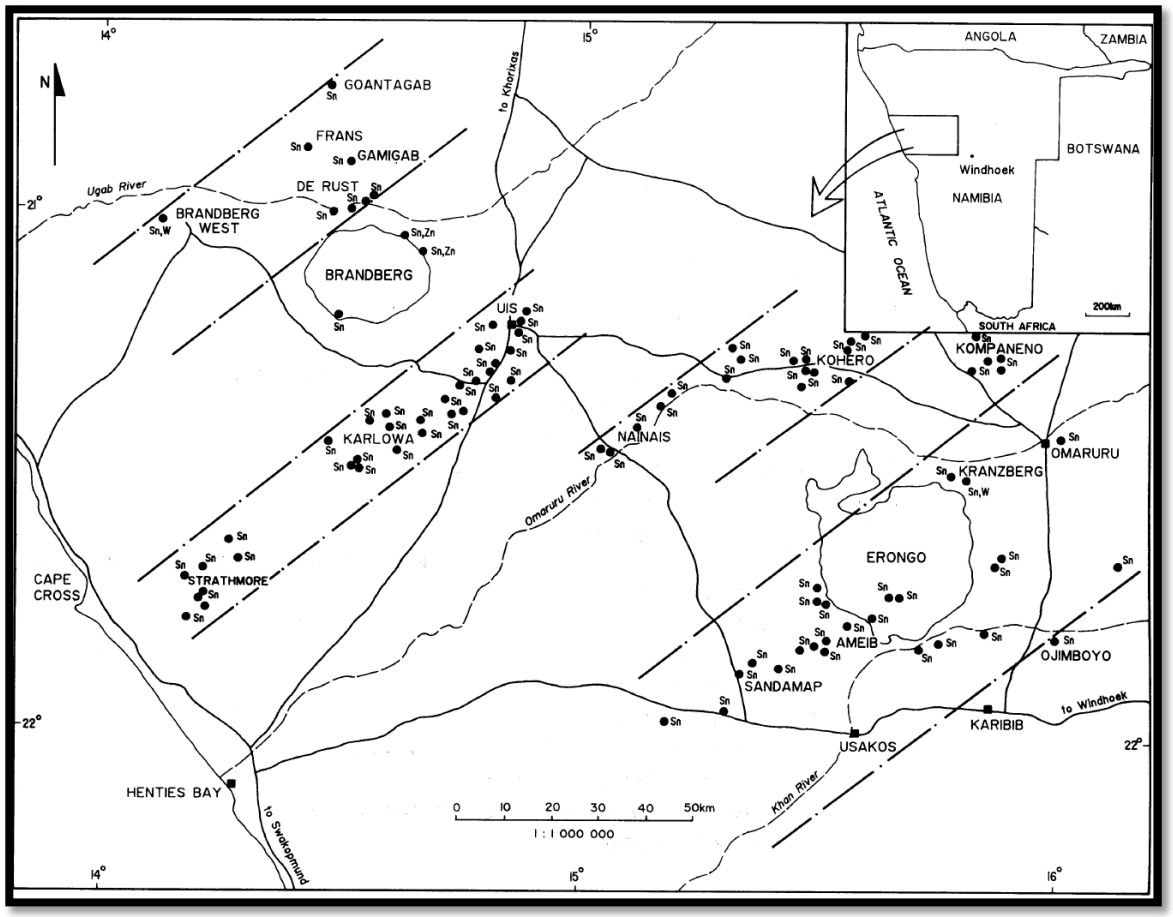

Figure 3.5 Locality map of tin occurrences in central Namibia, illustrating the alignment along northeast-trending belts (Geol. Surv. Namibia, 1992).

The internally zoned Li-Cs-Be-Rb pegmatites in Namibia which occur mainly in the Karibib - Usakos pegmatite district are characterized by massive quartz in the core zone (Keller, 1991; Geol. Surv. Namibia, 1992). This massive quartz in the core zone has been reported at pegmatites such as Rubicon and Helicon pegmatites, Dernburg pegmatite, Karlsbrunnn pegmatite, Albrechtshohe (Brockmann) pegmatite, Berger pegmatite, Kaliombo pegmatite, Okatjimukuju pegmatite (Geol. Surv. Namibia, 1992). The quartz in these pegmatites constitute a potential by-product.

The Rubicon pegmatite is located on the farm Okangava Ost 72, 30 km southeast of Karibib. According to Nex et al. (2011) the Rubicon and Helicon pegmatites are zoned lithium-cesium-tantalum (LCT) pegmatites which were worked for lithium from 1951-1994. Rubicon is the largest zoned pegmatite in the Usakos-Karibib area together with Helicon (Roering, 1963; Nex et al., 2011). The age Rubicon pegmatite is approximately 500 Ma (Nex et al., 2011). Quartz was recovered intermittently from the quartz core of the Rubikon pegmatite. Chemical analysis of the quartz gave a quartz purity of 99.460% and the impurities were found to be 0.130% Al_2O_3, 0.009% Fe_2O_3, 0.007% TiO_2, <0.001% P_2O_5, <0.001% Cr_2O_3, <0.001% MnO, 0.160% CaO, 0.004% MgO, 0.012% Na_2O, 0.003% K_2O and 0.21% was attributed to loss on ignition (LOI) (Geol. Surv. Namibia, 1992).

The tin pegmatites of the Damara belt are confined to the northern Central Zone and falls within the Cape Cross – Uis pegmatite belt where they occur in three major pegmatitic swarms and these are (from west to east) the Strathmore swarm, the Karlowa swarm, and the Uis swarm (Diehl, 1993). The Uis swarm consists of unzoned tin pegmatites while within the Strathmore swarm, and to a lesser proportion in the Karlowa swarm, zoned lithium rich tin-niobium-tantalum pegmatites occur (Diehl, 1993; Von Knorring, 1985; Wagener, 1989).

According to Nex et al. (2011), the metamorphic grade of the host rock of these pegmatites is a result of M1 metamorphism which occurred between 540 and 520 Ma and played no role on the petrological characteristics of the pegmatites besides constraining post-peak metamorphism partial melting of the crust. The synchronous emplacement of these pegmatites, affiliated with the change from ductile to brittle deformation, has implications for pegmatite classification schemes (Nex et al., 2011).

The Strathmore pegmatite swarm is considered to have over 180 rare metal pegmatites (Geol. Surv. Namibia, 1992). These pegmatites intruded the metasedimentary rocks of Amis River Formation of the Swakop Group (Geol. Surv. Namibia, 1992; Richards, 1986; Diehl, 1990). Both unzoned and zoned pegmatites types in this swarm have been intermittently worked for Sn-Nb-Ta and Li-Be bearing minerals (Nex et al., 2011).

Mineralogically the zoned pegmatites in the Strathmore- and the Karlowa swarms consist of coarse muscovite with quartz and alkali feldspar, an intermediate zone of dominantly quartz-feldspar-muscovite and a distinct quartz core (Geol. Surv. Namibia, 1992; Diehl, 1990). The Petalite Pegmatite is the largest pegmatite within the central portion of the Strathmore swarm and was worked for niobium-tantalum, cassiterite, lithium and beryllium minerals and book-mica in the past (Diehl, 1990; Geol. Surv. Namibia, 1992). SP14 Pegmatite located roughly 8.2 km east-northeast of the Petalite Pegmatite is a smaller zoned lithium-tin-niobium-tantalum bearing pegmatite.

The large unzoned, low grade pegmatites in Uis are post tectonic and have a whole rock RB-Sr age of 496±30 Ma but since the rocks are dominated by K-feldspar, this age may be closer to the mineral age than an emplacement age (Miller, 2008). Diehl (1993) puts the age of emplacement of the pegmatites in the Cape Cross – Uis pegmatite belt at 490 Ma. The ages of many post-tectonic rare-metal and tourmaline bearing pegmatites and some Sn-W veins in Brandberg West and Goantagab areas are not known but they are assumed to have been emplaced before significant cooling started. According to Miller (2008), 480 Ma is regarded to be the time when most of the central part of the Damara orogen from the NZ to the SMZ cooled down through 300°c.

Other pegmatites in the Damara Orogenic belt have various emplacement ages as given below by Miller (2008). The Uis pegmatite at K5 mine pit in the Southern Kaoko Zone has a post tectonic emplacement age of 496±30 Ma (Haack and Gohn, 1988). The Sandamap Noord and Sandamap Tin pegmatites in the Northern Central Zone have emplacement/ cooling ages of 473±23 Ma and 468±14 Ma respectively (Steven et al., 1993). The Rubicon pegmatite in the Southern Central Zone has a post tectonic mineral age of 496±30 Ma (Haack and Gohn, 1988). The Donkerhuk pegmatite in the Southern Zone has a post-tectonic emplacement age of 527±3 Ma (Haack and Gohn, 1988).

According to Miller (2008) the HPLT, syn-D2, M1 metamorphism in the SMZ and the SZ is determined to have been from 565 – 550 MA. He further stated that the age of D1 deformation for all zone north of the Okahandja Lineament is difficult to point out with

accuracy but states that it could be anywhere between 600 and 565 Ma. The Rb-Sr whole-rock dating of the Ida Dome Alaskite gave a syn-D3 age of 542±33 Ma (Marlow, 1983). 542 Ma is stated in Miller (2008) as the age of final closure of the Khomas Sea of the SZ and the age of continental collision in the Damara belt. Furthermore Miller (2008) stated the following: the age of 534±7 Ma of the anatectic red granite of the Goanikontes areas is considered to record the post-D3 peak regional metamorphism (M2) in sCZ and SZ, and peak regional metamorphism in the nCZ is considered to have occurred late to immediately post-D2. The age of D2 as obtained from a syn-D2 granite is given as 514±22 Ma (Haack et al., 1980), while that of syn-D3 Ida Dome alaskite was given as 542±33 Ma (Jacob, 2000; Marlow, 1983).

PT conditions of metamorphism of the Damara orogeny varied in each stratigraphic zone as indicated below according Miller (2008). The grade of metamorphism increases from very low in the marginal NP and SF to high in the centre of the orogenic belt. The syntectonic biotite in the northern margins of the NZ suggests a syntectonic metamorphic peak of approximately 2.5 kbar and 430 - 450°c. M1 PT conditions are estimated to have been +6 kbar and +700°c in the sCZ. The peak of M2 regional metamorphism in the sCZ was post-tectonic and PT conditions were estimated to have been 4 – 5 kbar and 650°c (Downing, 1982; Jacob, 1974; Nash, 1971; Sawyer, 1981).

Miller (2008) stated that the age of M1 metamorphism is given as 555 Ma in the SMZ which is 20 Ma older than the same event in the sCZ. He further mentioned that the peak

of M1 in SMZ and southern SZ was found to be 10 kbar and 590°C in the Omitara area and in the Gamsberg-Kuiseb River area it was found to be 9 kbar and 574°C (Hoffmann, 1987; Kasch, 1981; Hoernes and Hoffer, 1979). The PT conditions between M1 and M2 in the SZ and SMZ was calculated to be approximately 7 kbar and roughly 460°C in the Gamsberg-Kuiseb River area and approximately 8.4kbar and roughly 500°C in the Omitara area (Miller, 2008; Kasch, 1981; Sawyer, 1981). A decompression of 3 kbar resulting from erosion led to the post-tectonic M2 temperature peak and the M2 regional metamorphism was found to be at about 535 (Miller, 2008). According to Miller (2008) the peak of M2 metamorphism was post-tectonic throughout the Damara belt and has an age of 535 Ma in all except the nCZ. The nCZ is characterized by younger M2, D2, D3 events and the age of M2 metamorphism is given as 514 Ma and is syn-D2 (Miller, 2008).

A synopsis of the PT conditions and ages of metamorphism of the Damara belt are stated below as given by Miller (2008). The NP is described to have LPLT greenschist facies with peak metamorphism at 530 Ma. The NZ depicts increasing metamorphism (upper greenschist to lower amphibolites facies), with M1 metamorphism showing PT conditions of ~480°C and ~3 – 4 kbar (Hawkesworth et al., 1983). The peak of M1 is ~600 Ma and that of M2 has been determined to be 530 Ma. The nCZ is described to have been a LPHT zone with amphibolite facies and peak metamorphism is regarded to have been around 520 Ma or later. The sCZ is defined as a LPHT zone, depicting increasing metamorphism from upper amphibolite in the east (Okahandja area) to lower

granulite facies in the west (Swakopmund area) (De Kock et al., 2000, Masberg, 2000). The temperature and pressure conditions were roughly 520°C and 3.5 kbar in the east and 725°C and 5 – 6 kbar in the west. The peak metamorphism post-dates 550 Ma granites and is probably 530 Ma (Bühn et al., 1995; Downing, 1982; Jacob, 1974; Nash, 1971).

The SZ has been defined as a HPLT zone, but temperature increase westwards to the Conception Bay-Meob Bay area where migmatisation has been extreme. Greenschist facies along the southern edge in the Windhoek area to amphibolite facies along the northern edge in the Okahandja area (Hoffer, 1977; Kasch, 1981; Kasch, 1987; Sawyer, 1981). Temperature and pressure conditions have been calculated to be 570°C and 9 kbar for M1 and 580°C and 7 kbar for M2. The SMZ is described as a HPLT zone consisting of greenschist facies (Hernes and Hoffer, 1979). M1 temperature and pressure at the northern edge have been calculated to be 590°C and 10 kbar. M2 metamorphism was found to be 570°C and 8 kbar (Kasch, 1987; Sawyer, 1981). The SF is described to be a LPLT area defined by zeolite to lowest greenschist facies and the peak of metamorphism has been calculated to be 530 Ma.

3.3.1 Hydrothermal deposit on the farm Alt Seeis 133

Syn- to post-tectonic hydrothermal quartz veins of irregular shapes occur on the farm Alt Seeis 133, roughly 80 km east of Windhoek. These bodies are hosted by quartzites of the Chuos Formation and are in some parts covered by recent surficial sands of the Kalahari Group. A total number of 17 quartz bodies have been established and it is suspected that these bodies may be connected at depth (Carr, 1983). The bodies vary in size and that of the largest body is estimated to be in-excess of 50 000 t (Carr, 1983). The reserves of the two largest bodies were estimated to be 93 000 t (King, 1986). One of the bodies was mined in the mid-1980s and a total of 660t of quartz was produced from it. According to King (1986), test work indicated 7% of the total product could be marketed in the following categories: 26% transparent, 40% translucent and 34% milky. The age of these hydrothermal quartz bodies is unknown.

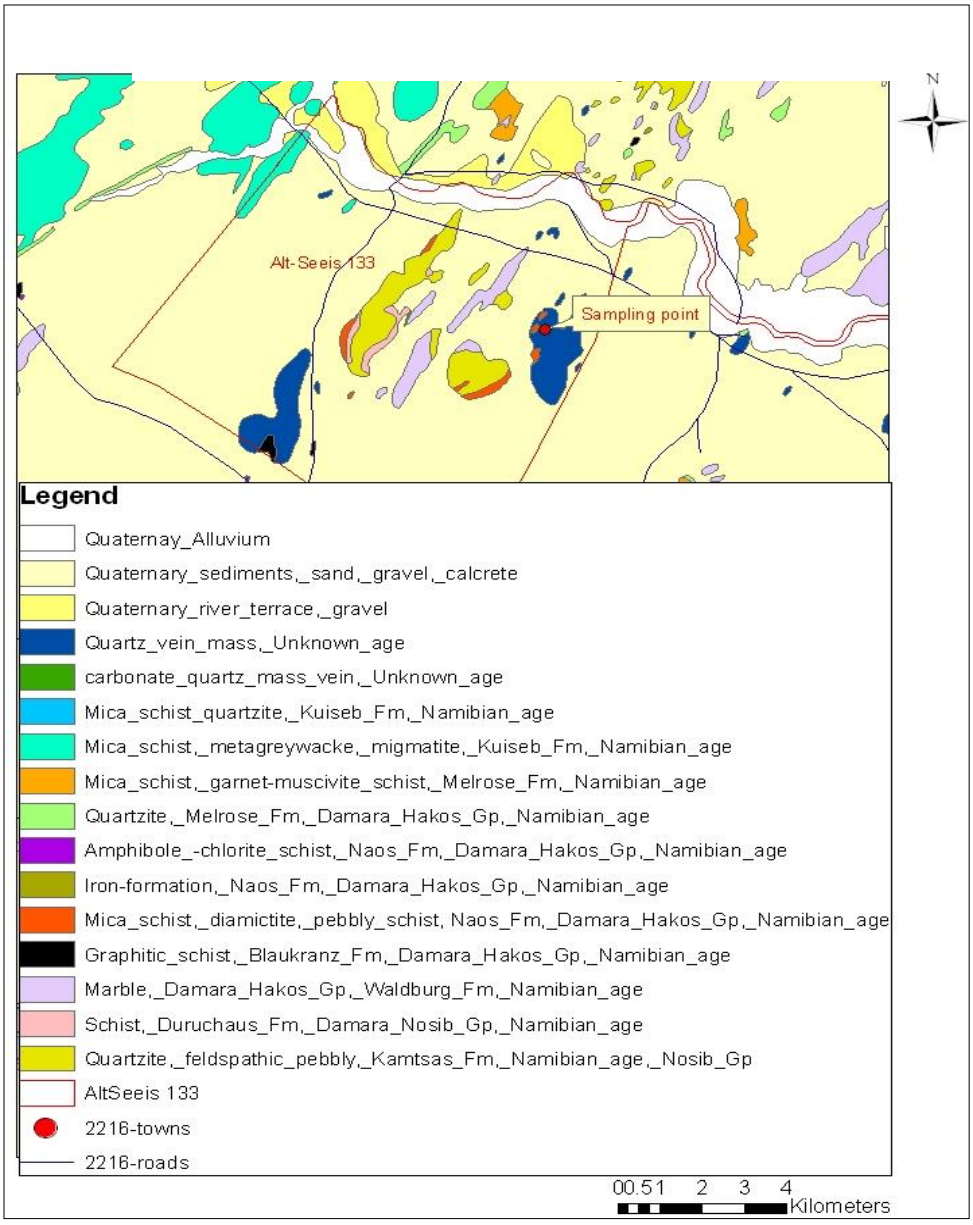

Figure 3.6 Geology of the farm Alt-Seeis 133. Sampling point is indicated. This is where samples ALT1 and ALT2 were collected.

3.3.2 Hydrothermal deposit on the farm Doornboom 316

Quartz veins and blows that are noticeable as small hills occur on the farm Doornboom 316, roughly 60 km west of Rehoboth. These quartz bodies are hosted by quartzites, schists and marbles of the Kudis Subgroup of the Damara Sequence. The age of these hydrothermal quartz bodies is also unknown.

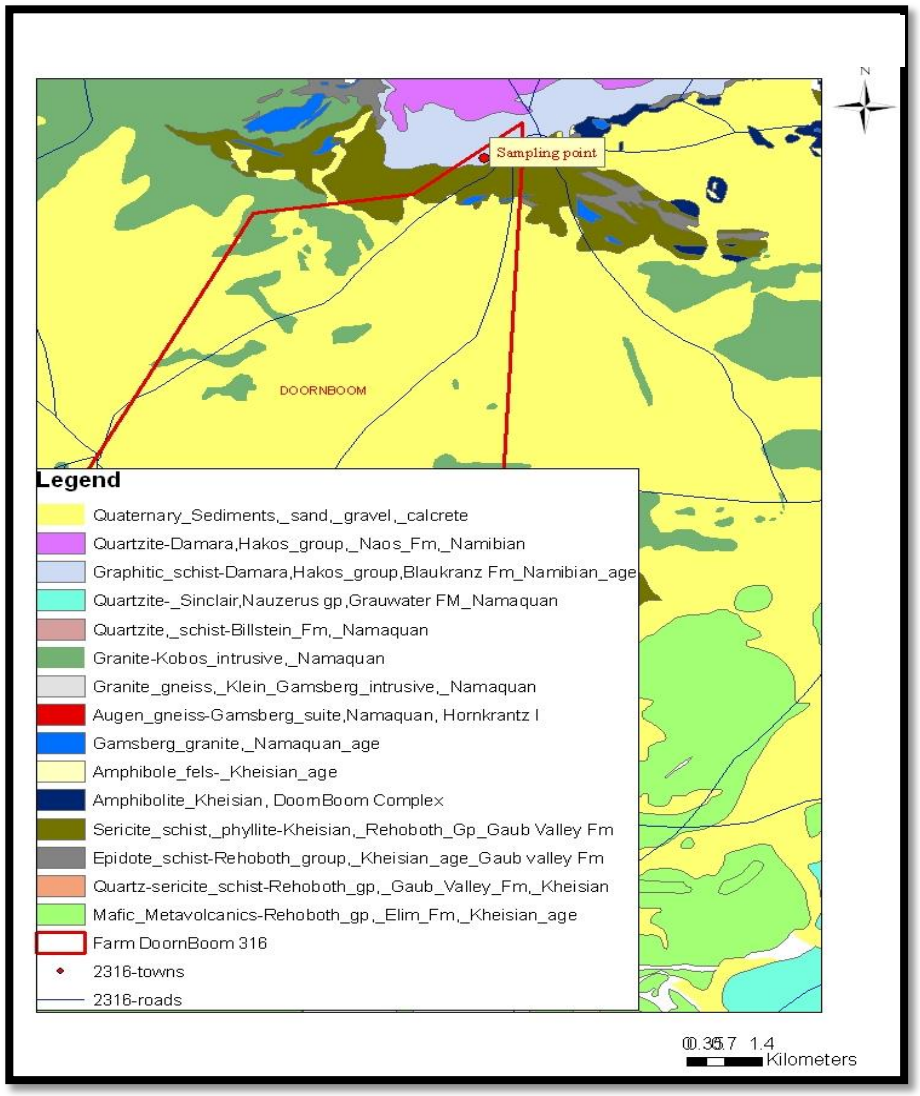

Figure 3.7 Geology of the farm Doornboom 316. Sampling location is indicated as sampling point. This is where samples DB1 and DB2 were collected.

3.3.3 SP Pegmatite Intrusions (Cape cross - Uis pegmatite belt)

The Cape Cross - Uis pegmatite belt is characterised by foliated metasedimentary rocks of the Amis River Formation, Swakop Group (Diehl, 1986, 1990). Pegmatites containing

very low concentrations of tin, niobium, tantalum, and lithium are cross-cutting the metasedimentary fabric. Structural assessments have shown that the Cape Cross - Uis pegmatite belt is purported to be a half-graben bounded by an eminent reverse fault (Autseib Fault) in the east and a series of normal, southeast-dipping faults in the west (Diehl, 1986, 1990). The pegmatites intruded though pre-existing zones of weakness created by intensive shearing and block faulting in the half-graben. Rb/Sr isotope studies of various mineral phases in pegmatites of the Cape Cross - Uis pegmatite belt indicated the emplacement age of the pegmatitic melt at 490 Ma (Diehl, 1993). According to Miller (2008) the age of the Uis pegmatites are placed at 515 – 495 Ma.

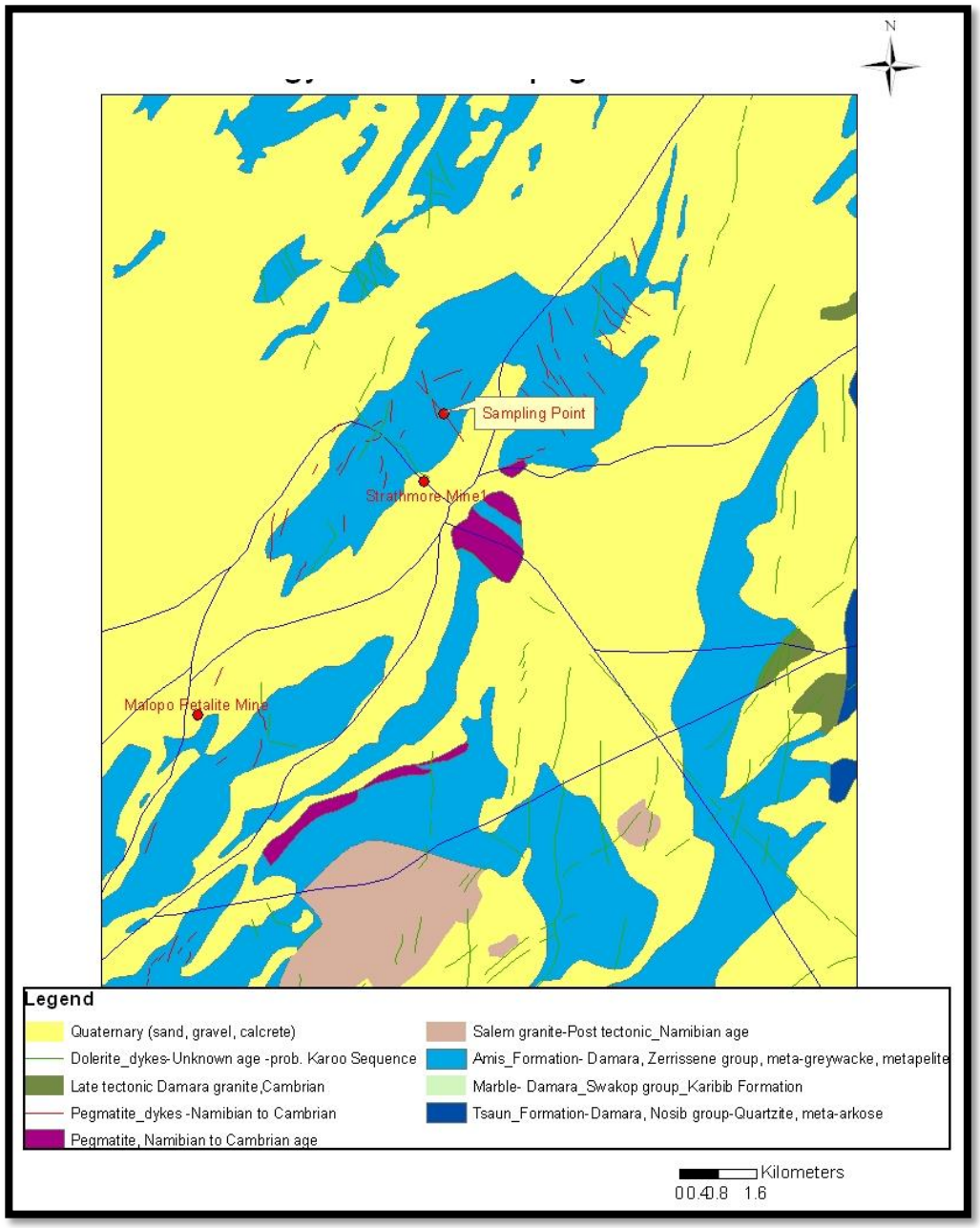

Figure 3.8 Geology of the SP14 pegmatite area. Sampling location is indicated as sampling point. This is where samples MA1 and MA2 were collected.

Figure 3.8 given below shows quartz samples from the three deposits. Samples ALT 1 and ALT 2 were sampled from the farm Alt Seeis 133, samples DB 1 and DB 2 were collected from the farm Doornboom 316 and samples identified as MA 1 and MA 2 were sampled from SP 14 in the Cape Cross – Uis pegmatite belt.

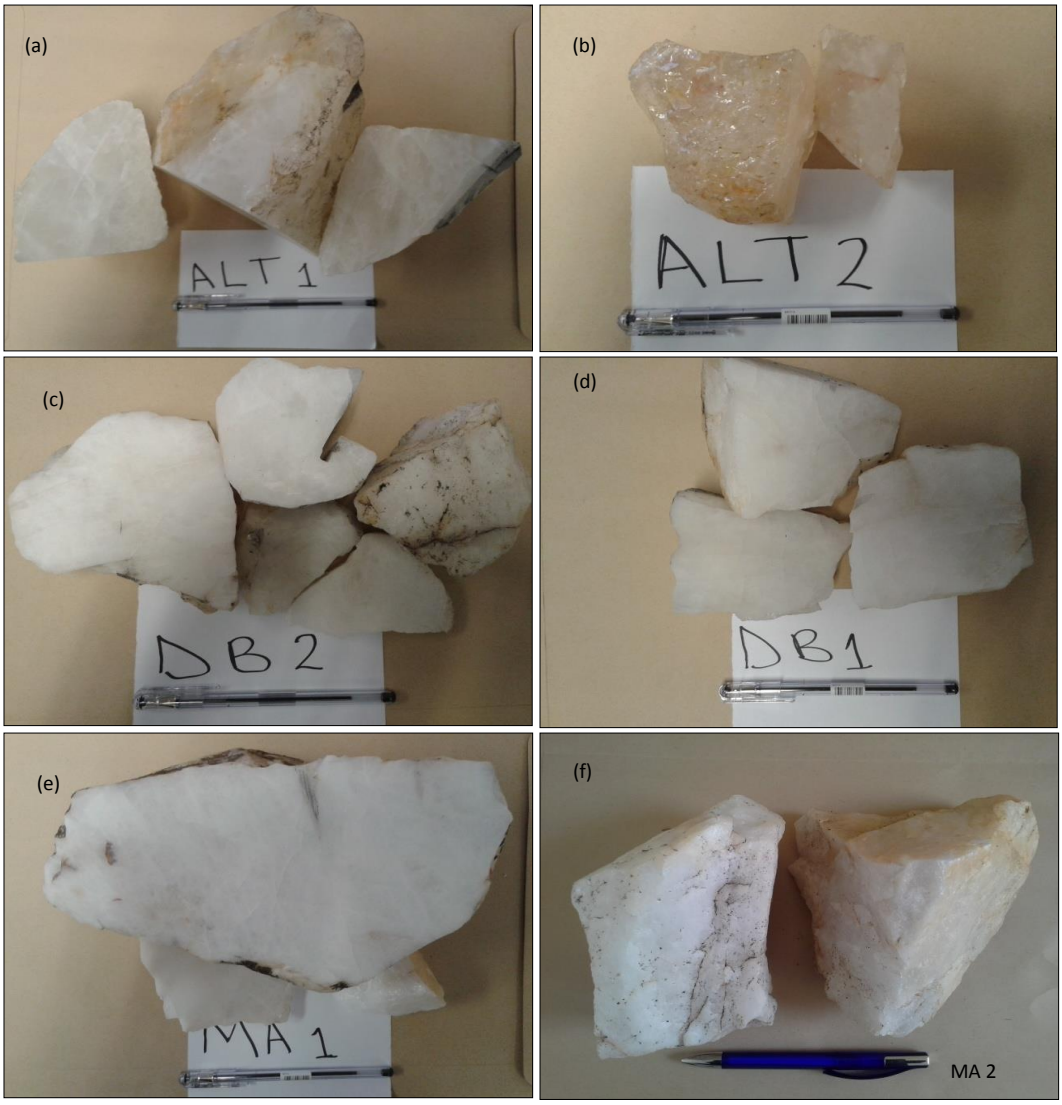

Figure 3.9 Quartz samples from Alt-Seeis. (a) and (b) show quartz samples from a hydrothermal deposit at the farm Alt-Seeis, (c) and (d) show quartz samples from a hydrothermal deposit at the farm Doornboom 316, (e) and (f) show quartz samples from two SP pegmatite intrusions in the Cape Cross - Uis pegmatite belt.

The University of Namibia has a collaborative agreement with Stellenbosch University (South Africa) and all sample analyses were carried out at the analytical laboratories of this university. Central Analytical Facility (CAF) of Stellenbosch University where sample analyses were undertaken is equipped with LA-ICP-MS and SEM-CL; equipment which were required for this study. Sample preparation was also carried out at Stellenbosch University.

3.4 Research Equipment

3.4.1 Scanning Electron Microscopy -Cathodoluminescence Imaging (SEM-CL)

Scanning Electron Microscopy - Cathodoluminescence (SEM-CL) images of quartz were obtained from polished carbon coated samples. SEM-CL imaging exposes micro-scale growth zoning (crystal growth), alteration structures, replacements, fluid driven overprints and different quartz generations which are not visible with other methods (Müller et al., 2012). Müller et al. (2012) demonstrated that SEM-CL is an appropriate method for visualizing structures within quartz crystals that might be related to HPQ formation. These structures, which are only visible in SEM-CL, include healed micro-cracks, quartz domains affected by alteration and newly formed quartz due to grain

boundary migration (retrogradation). The SEM-CL observations have indicated that the formation of secondary quartz commonly results in refinement of the quartz quality.

3.4.2 Laser Ablation Inductively Coupled Plasma Mass Spectrometry (LA-ICP-MS)

Concentrations of Na, K, Li, Al, Ca, Fe, Ti, B, P, Mg, Cr, Mn, Co, Ni, Cu, Zn, Rb, Sr and Ba were analysed in situ by LA-ICP-MS. Previous studies have shown that the first nine of the elements stated above comprise >99% of lattice bound impurities in quartz (Larsen et al., 2004), other trace elements which may be present in quartz are scarcely taken notice of because they have very little effects on silica glass properties. Müller et al. (2012) recommended that, in-situ analysis by LA-ICP-MS is an excellent method for determining the concentrations of lattice- bound trace elements in single quartz crystals. The concentrations that are determined by this method correspond theoretically to the best achievable quality of the final quartz product if perfect processing is applied, removing all non-lattice-bound impurities.

3.5 Procedures and techniques

3.5.1 Sample preparation and analysis

All sample preparation was done at the Central Analytical Facilities, University of Stellenbosch. Samples were cut into approximately 1 cm size blocks using Stuers Secotom-10. Small cuttings were embedded into individual epoxy (Stuers Specifix 40) mounts. Mounted blocks were grinded and polished using Stuers Roto Pol-35, grinding on 1200 mic grinding pad then polished on 9mic, 3mic and 1 mic polishing pads in that order. Petrographic examination of the samples using optical microscopy were not carried out on the samples before analyses due to reasons beyond the researcher's control and therefore ablation of areas which may not have been free of mineral, melt and fluid micro-inclusions could not be avoided.

3.5.1.1 SEM-CL

Images unveiling primary and secondary growth features were obtained using a Leo® 1430VP Scanning Electron Microscope with an attached Zeiss Cathodoluminescence detector at the Stellenbosch University. Prior to imaging the samples were coated with a thin layer of carbon in order to make the sample surface electrically conducting. Beam conditions during surface analysis were 20 KV and approximately 1.0 A, with a working

distance of 16 mm and a spot size of 500.Upon completion of SEM_CL imaging analyses, the concentrations of trace elements were assessed using LA-ICP-MS on the same samples.

3.5.1.2 LA-ICP-MS

In situ concentrations of Na, K, Li, Al, Ca, Fe, Ti, B, P, Mg, Cr, Mn, Co, Ni, Cu, Zn, Rb, Sr and Ba by laser-ablation inductively-coupled plasma mass spectrometry (LA-ICP-MS) with a detection limit of 0.1ppm. The analyses were carried out using an Agilent 7500ce ICP-MS with an attached Resonetics 193nmExcimer laser. The laser had an ablation time of 10 seconds background time and 20 seconds ablation time, spot size 303µm per sample, energy of 60mJ and repetition rate of 8 Hz. The ablation gas was He at 0.30L/min and ablated material were carried by mixture of argon and nitrogen at 0.9L/min argon plus 0.002L/min nitrogen.

For quality assessment a Calibration Standard with certified values and BHVO 2 Control Standard with certified values of each measured trace element were repeatedly analysed for a number of four times and error percentages calculated. A note from the laboratory is that (1) Values for Li and B are semi-quantitative, as signal was very unstable. (2) The large error for Mg, K, Ti and Fe in the control standard is because the standard values are far outside the calibration range, these large error are not expected for the values

measured in the samples. It should be noted that petrographic examination of the samples using optical microscopy were not carried out on the samples before analyses due to reasons beyond the researcher's control and therefore ablation of areas which may not have been free of mineral and fluid micro-inclusions could not be avoided.

Table 3.2 A summary of specifications of the LA ICP-MS.

Information in this table are for tables 2 to 10 given below	
Analytical conditions:	
Laser:	*ICP-MS*
Resonetics 193nm Excimer laser	Agilent 7500ce
Energy: 60mJ	Carrier gas: 0.9L/min Ar + 0.002L/min Nitrogen
Frequency: 8 Hz	
Spot: 303µm per sample	
Ablation gas: He @ 0.30L/min	
Ablation time: 10sec background, 20sec ablation	
NOTE: Values for Li and B are semi-quantitative, as signal is very unstable	
NOTE from the laboratory: The large error for Mg, K, Ti and Fe in the control standard is because the standard values are far outside the calibration range; these large errors are not expected for the values measured in the samples.	

CHAPTER 4

4. Results

4.1 SEM-CL images from Alt Seeis

Images obtained from a Scanning Electron Microscope with an attached Zeiss CL detector (SEM-CL) are given below. SEM_CL images in figures 4.1 and 4.2 below from farm Alt Seeis 133. All images show only one generation of quartz (Fig. 4.1 and Fig. 4.2) indicating that the deposit was not affected by metamorphism and as such it infers that transformation of primary quartz to HPQ did not take place.

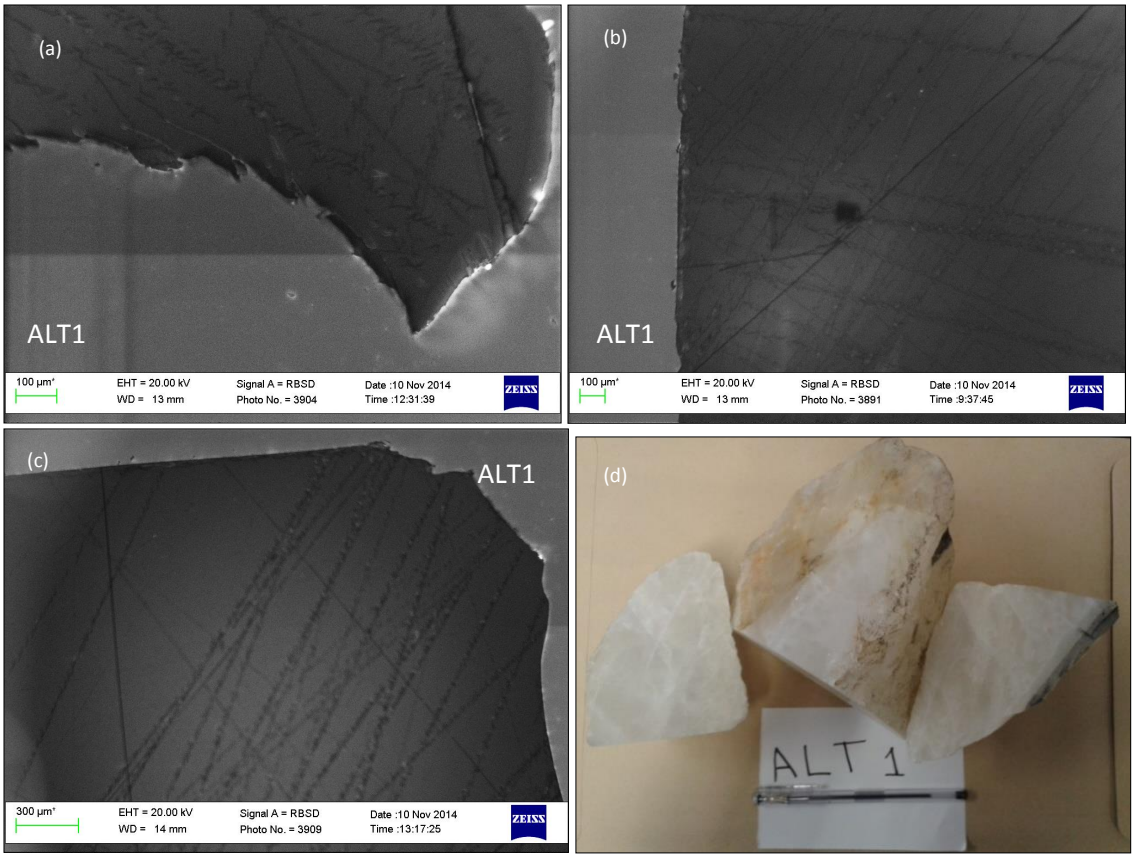

Figure 4.1 SEM-CL Images (ALT 1). (a),(b) and (c)SEM-CL images from a hydrothermal quartz deposit at the farm Alt-seeis 133 (sample ALT 1). All images show only one generation of quartz. (d) the rock samples from which the SEM-CL images were taken.

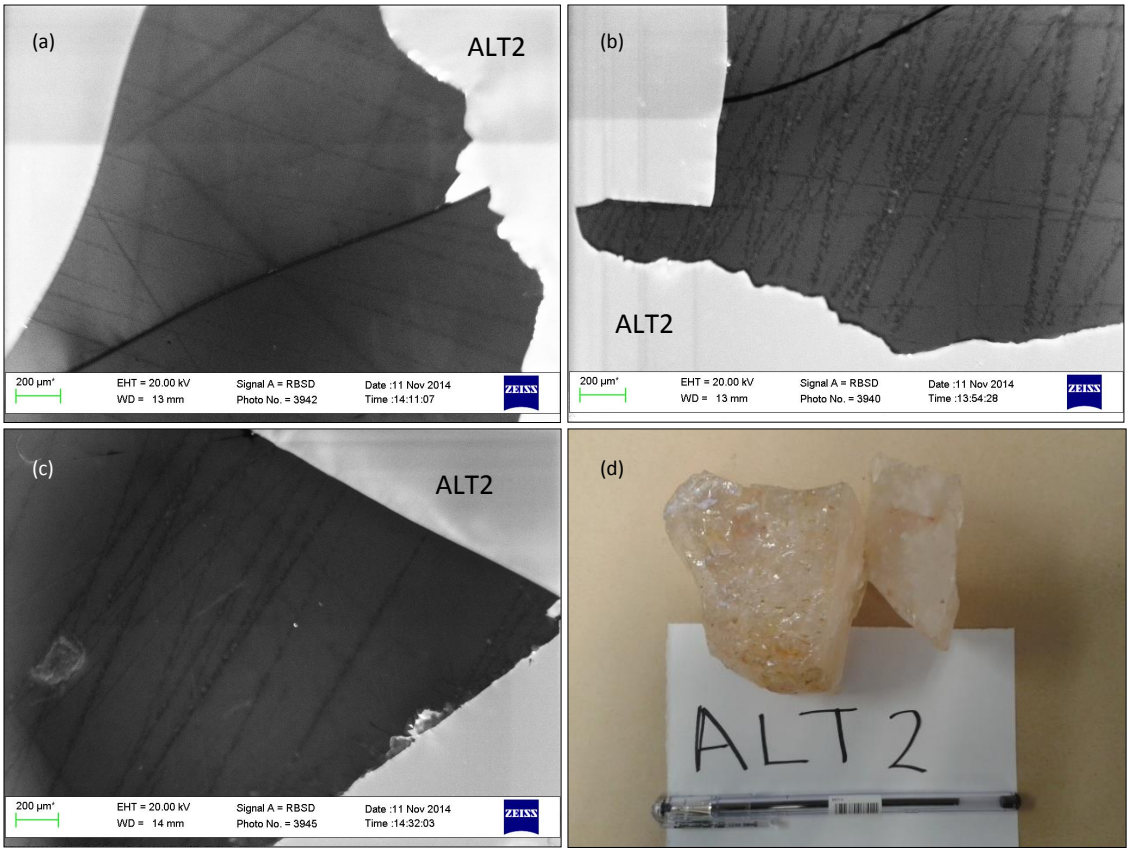

Figure 4.2 SEM-CL Images (ALT 2). (c)SEM_CL images from a hydrothermal quartz deposit at the farm Alt-seeis 133 (sample ALT 2). All images show only one generation of quartz. (d) the rock samples from which the SEM-CL images were taken.

4.2 Trace element concentrations in quartz from Alt Seeis

Quartz samples from Alt Seeis were analysed by LAICP-MS at the Central Analytical Facilities (CAF), University of Stellenbosch. In situ concentrations of Na, K, Li, Al, Ca, Fe, Ti, B, P, Mg, Cr, Mn, Co, Ni, Cu, Zn, Rb, Sr and Ba are given in table 4.1 below.

Table 4.1 shows the trace element concentrations in µg/g of sample ALT1. Three quartz grains were selected from the sample. The first quartz grain was divided into two areas

and two spots were analyzed in each area. Two spots were also analyzed in the second and the third grains. This gave a total of eight analyzed spots. The average of the eight spots for each trace element was calculated and is given in the last column of the table.

Table 4.1 Trace element concentrations (µg/g) of quartz from Alt Seeis for sample ALT 1.

Trace element	**Grain3_Area2**		**Grain3_Area3**		**Grain4_Area1**		**Grain6_Area1**		**Average**
	Spot 1 µg/g	Spot 2 µg/g	Spot 1 µg/g	Spot 2 µg/g	Spot 1 µg/g	Spot 2 µg/g	Spot 1 µg/g	Spot 2 µg/g	µg/g
Li	76.71	132.59	229.76	162.21	215.46	259.71	152.17	192.51	**177.64**
B	29.07	139.42	125.78	169.19	166.27	125.70	179.16	184.20	**139.85**
Na	81.78	65.42	59.81	94.97	94.66	77.20	62.42	79.99	**77.03**
Mg	5.46	11.71	14.91	13.83	15.10	14.33	9.00	14.16	**12.31**
Al	108.06	104.35	164.74	168.58	207.49	195.16	115.96	169.20	**154.19**
P	10.55	11.60	13.59	9.58	13.21	13.97	10.36	12.31	**11.90**
K	6.30	4.52	9.02	14.72	14.56	10.63	13.76	13.58	**10.89**
Ca	403.37	352.53	589.47	557.36	738.80	711.48	699.03	587.51	**579.94**
Ti	25.64	24.27	27.79	27.67	30.23	31.21	25.27	34.63	**28.34**
Cr	0.29	0.39	0.55	0.61	0.63	0.72	0.58	0.99	**0.59**
Mn	1.51	0.41	<0.36	<0.40	0.82	1.10	<0.37	0.44	**0.86**
Fe	0.45	0.43	0.62	0.77	0.93	0.87	0.61	0.71	**0.67**
Co	0.10	0.16	0.14	0.20	0.26	0.24	0.22	0.19	**0.19**
Ni	27.70	22.53	26.20	32.25	38.57	44.29	24.95	29.04	**30.69**
Cu	1.77	1.56	1.88	2.65	2.78	2.80	4.12	4.95	**2.81**
Zn	4.20	3.17	2.85	3.62	6.41	4.44	3.96	4.18	**4.10**
Rb	0.08	0.06	0.11	0.11	0.11	0.12	0.06	0.11	**0.10**
Sr	0.33	1.90	1.44	0.90	2.03	2.10	0.85	1.33	**1.36**
Ba	0.31	0.47	0.61	0.91	0.99	0.95	0.62	0.72	**0.70**

Table 4.2 shows the trace element concentrations in µg/g of sample ALT2. Three quartz grains were selected from the sample and in the first two grains two spots were analyzed

in each grain. The third quartz grain was divided into two areas and two spots were analyzed in each area. This gave a total of eight analyzed spots. The average of the eight spots for each trace element was calculated and is given in the last column of the table.

Table 4.2 Trace element concentrations (µg/g) of quartz from Alt Seeis for sample ALT 2.

Trace element	Grain1_Area4		Grain2_Area2		Grain4_Area2		Grain4_Area1		Average
	Spot 1 µg/g	Spot 2 µg/g	Spot 1 µg/g	Spot 2 µg/g	Spot 1 µg/g	Spot 2 µg/g	Spot 1 µg/g	Spot 2 µg/g	µg/g
Li	96.99	49.20	28.92	67.24	76.90	68.32	42.60	62.86	**61.63**
B	68.80	54.38	22.64	67.99	45.93	36.81	17.65	28.71	**42.86**
Na	67.37	52.81	61.18	44.06	74.81	43.25	43.40	30.36	**52.16**
Mg	9.77	8.51	7.23	4.78	5.47	5.83	5.02	4.04	**6.33**
Al	70.37	109.75	58.76	47.14	54.36	53.55	52.68	56.01	**62.83**
P	10.59	9.34	8.97	10.15	8.09	7.53	8.14	6.14	**8.62**
K	9.50	6.77	8.13	9.52	10.51	10.31	8.24	4.63	**8.45**
Ca	586.40	574.75	414.82	445.65	464.73	531.98	390.87	315.40	**465.58**
Ti	28.68	21.97	24.12	23.90	25.48	22.71	22.08	22.01	**23.87**
Cr	0.40	0.25	0.35	0.60	0.39	0.34	0.27	0.28	**0.36**
Mn	0.74	<0.36	1.00	2.23	<0.34	0.78	1.46	<0.32	**1.24**
Fe	0.46	0.39	0.41	0.28	0.37	0.34	0.29	0.29	**0.35**
Co	0.10	0.11	0.09	0.09	0.07	0.08	0.08	0.06	**0.09**
Ni	13.39	12.69	10.07	7.77	14.42	4.01	9.43	12.94	**10.59**
Cu	2.10	1.69	1.89	4.04	3.17	2.25	1.02	1.02	**2.15**
Zn	2.81	2.17	1.91	2.76	2.18	1.40	2.38	1.47	**2.14**
Rb	0.06	0.04	0.06	0.05	0.06	0.06	0.04	0.08	**0.06**
Sr	0.76	0.36	0.53	0.36	0.77	0.46	0.37	0.37	**0.50**
Ba	0.46	0.35	0.60	0.43	0.57	0.36	0.28	0.39	**0.43**

4.2.1 Quartz chemistry of the Alt-Seeis hydrothermal vein quartz

The quartz at Alt-Seeis hydrothermal vein quartz deposit is characterized by very low Fe concentration (averages for both ALT1 and ALT2 being <0.8 µg/g). Average concentrations for ALT1 are relatively higher than that of ALT2 for trace elements which constitute HPQ definition. The only element that gave very high average values is calcium (579.9 µg/g for ALT1 and 465.6 µg/g ALT2). The average concentrations of other trace elements are relatively moderately low though still higher than the required HPQ limits: Averages for phosphorus in ALT1 and ALT2 are for each <12 µg/g while for Ti, concentration averages are both <29 µg/g. Potassium gave low average values in both samples with ALT1 averaging 10.9 µg/g and ALT2 averaging 8.5 µg/g. Other alkali metals (Li and Na) gave averages that are slightly higher than that of potassium (Na gave 77 µg/g and 52.2 µg/g for ALT1 and ALT2 respectively). Lithium averages were calculated as 177.6 µg/g for ALT1 and 61.6 µg/g for ALT2. The average concentrations of the two samples for boron were found to be 139.8 µg/g for ALT1 which is slightly high and 42.9 µg/g for ALT2 which is relatively low.

4.3 SEM-CL images from Cape Cross – Uis pegmatite belt

Images were obtained from a Scanning Electron Microscope with an attached Zeiss CL detector (SEM-CL) and are given below.

SEM_CL images of MA1 sample from the Cape Cross - Uis pegmatite belt show that primary quartz (PQ) has only been partially replaced and is still in abundance (Fig. 4.3). Replacement is very limited and is only along fractures. The other sample (MA 2) exhibits no secondary quartz generation implying that no transformation took place.

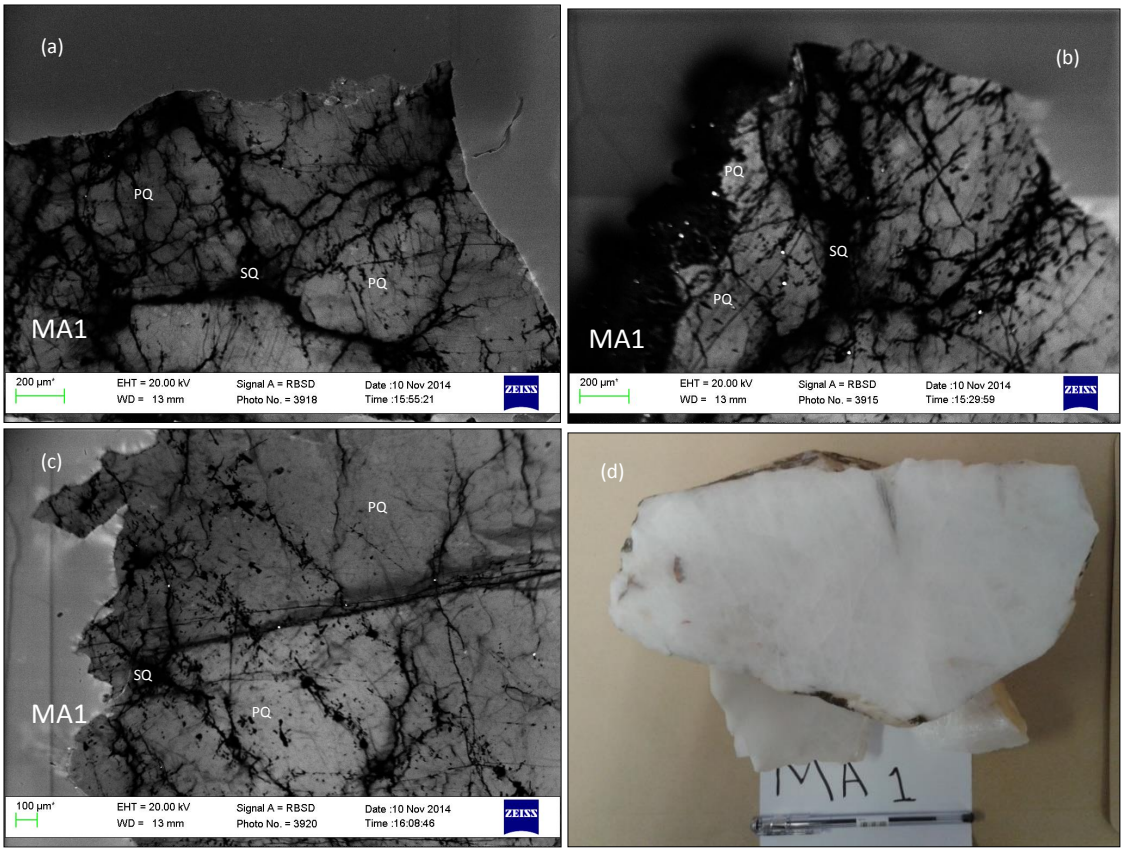

Figure 4.3 SEM-CL Images (MA 1). (a), (b) and (c) SEM_CL images from SP14 Pegmatite intrusion in the Cape Cross - Uis pegmatite belt (Sample MA 1). All images show two generations of quartz; primary quartz (PQ) was replaced to some very limited extent by secondary quartz (SQ)and the secondary quartz is limited to fractures. (d) the rock samples from which the SEM-CL images were taken.

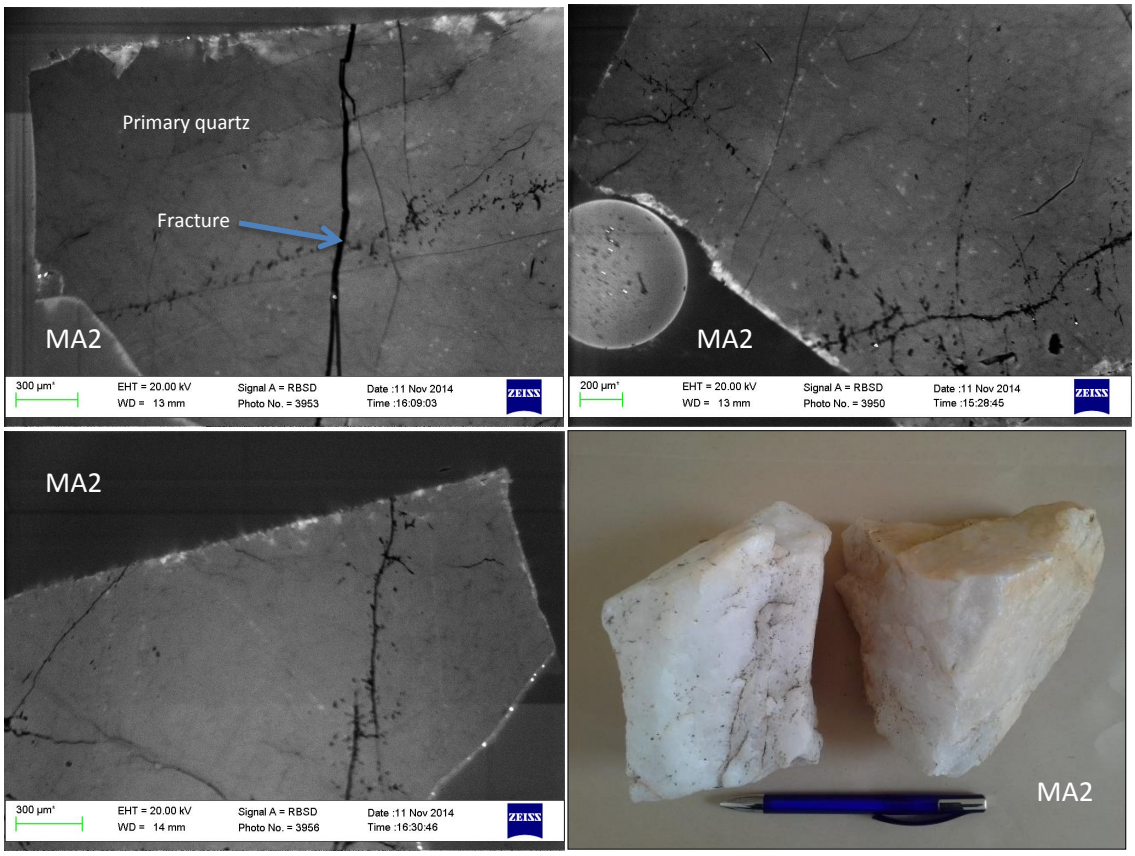

Figure 4.4 SEM-CL Images (MA 2). (a), (b) and (c) SEM_CL images from one of the SP14 Pegmatite intrusion in the Cape Cross - Uis pegmatite belt (sample MA 2). All images are depicting a single generation of quartz. (d) the rock samples from which the SEM-CL images were taken.

4.4 Trace element concentrations in quartz from Cape Cross – Uis pegmatite belt

Quartz samples from SP 14 in the Cape Cross – Uis pegmatite belt were analysed by LAICP-MS at the Central Analytical Facilities (CAF), University of Stellenbosch. In situ concentrations of Na, K, Li, Al, Ca, Fe, Ti, B, P, Mg, Cr, Mn, Co, Ni, Cu, Zn, Rb, Sr and Ba are given in table 4.3 below.

Table 4.3 shows the trace element concentrations in µg/g of sample MA1. Two quartz grains were selected from the sample and in the first grain two spots were analyzed. The second quartz grain was divided into three areas and in each area two spots were analyzed. This gave a total of eight analyzed spots. The average of the eight spots for each trace element was calculated and is given in the last column of the table.

Table 4.3 Trace element concentrations (µg/g) of quartz from Cape Cross – Uis pegmatite belt for sample MA 1.

Trace element	Grain1_Area3		Grain3_Area2		Grain3_Area6		Grain3_Area4		Average
	Spot 1 µg/g	Spot 2 µg/g	Spot 1 µg/g	Spot 2 µg/g	Spot 1 µg/g	Spot 2 µg/g	Spot 1 µg/g	Spot 2 µg/g	µg/g
Li	94.40	212.12	152.08	249.20	336.72	215.50	127.39	225.59	201.63
B	65.31	178.82	48.96	101.39	126.50	150.72	137.54	138.99	118.53
Na	97.34	165.77	88.38	117.38	252.39	111.28	147.51	146.93	140.87
Mg	29.25	14.14	12.55	10.25	29.18	8.03	7.30	8.98	14.96
Al	718.95	635.76	474.76	577.95	617.86	624.98	683.75	907.53	655.19
P	10.72	10.08	9.64	12.88	37.31	8.72	10.99	19.74	15.01
K	90.20	30.26	33.10	43.38	94.13	77.40	84.50	111.93	70.61
Ca	333.88	455.15	537.83	635.19	667.53	533.29	363.47	579.94	513.29
Ti	30.47	29.57	32.05	37.42	61.30	29.89	34.00	36.66	36.42
Cr	0.30	0.47	0.41	0.47	3.69	0.33	0.51	0.51	0.84
Mn	<0.40	<0.34	<0.36	<0.36	5.83	1.03	1.13	<0.38	2.66
Fe	1.90	0.91	1.70	2.38	1.99	1.70	2.05	2.73	1.92
Co	0.15	0.19	0.15	0.19	0.31	0.13	0.11	0.20	0.18
Ni	17.42	33.17	23.82	30.02	41.00	26.36	16.70	28.76	27.16
Cu	1.54	1.55	2.10	2.77	17.90	2.29	3.54	1.91	4.20
Zn	4.01	3.73	3.45	6.45	18.49	3.84	5.99	4.73	6.34
Rb	1.17	0.22	0.55	0.79	0.91	1.15	1.27	1.85	0.99
Sr	0.71	1.34	0.88	0.81	7.91	1.03	1.17	0.88	1.84
Ba	0.66	0.98	0.55	0.80	2.09	0.56	0.43	0.80	0.86

Table 4.4 below shows the trace element concentrations in µg/g of sample MA2. Two quartz grains were selected from the sample and each grain was divided into two areas. Then two spots in each area were analyzed, giving a total of eight analyzed spots. The average of the eight spots for each trace element was calculated and is given in the last column of the table.

Table 4.4 Trace element concentrations (µg/g) of quartz from Cape Cross – Uis pegmatite belt for sample MA 2.

Trace element	Grain5_Area1		Grain5_Area2		Grain1_Area1		Grain1_Area2		Average
	Spot 1 µg/g	Spot 2 µg/g	Spot 1 µg/g	Spot 2 µg/g	Spot 1 µg/g	Spot 2 µg/g	Spot 1 µg/g	Spot 2 µg/g	µg/g
Li	170.91	215.91	203.41	87.83	211.51	245.41	129.14	192.51	182.08
B	105.93	87.46	91.75	79.41	154.77	249.08	133.65	96.61	124.83
Na	435.71	374.80	242.92	420.10	265.21	263.72	391.31	353.21	343.37
Mg	9.59	18.54	13.21	13.85	11.72	16.45	11.92	9.12	13.05
Al	633.00	594.30	544.59	732.32	569.09	628.97	591.86	554.29	606.05
P	10.45	16.84	14.54	15.88	14.38	19.08	15.87	15.56	15.33
K	18.54	11.79	30.51	15.66	33.71	40.37	22.51	21.97	24.38
Ca	594.23	585.53	826.01	715.45	719.39	783.01	665.41	751.08	705.01
Ti	39.34	40.23	34.08	44.18	37.32	37.14	40.18	37.93	38.80
Cr	0.59	0.53	0.55	0.83	0.60	0.55	0.52	0.75	0.61
Mn	1.35	0.92	<0.36	1.75	2.27	<0.40	<0.36	1.65	1.59
Fe	0.71	0.88	0.90	0.65	1.08	1.45	0.94	0.95	0.95
Co	0.16	0.20	0.18	0.18	0.19	0.22	0.20	0.23	0.20
Ni	31.78	21.95	26.12	26.73	32.09	32.01	32.85	28.13	28.96
Cu	1.99	2.03	2.02	2.47	3.23	3.25	2.23	6.71	2.99
Zn	3.40	5.07	4.91	4.46	4.05	5.67	4.87	6.68	4.89
Rb	0.19	0.20	0.75	0.14	0.93	1.07	0.38	0.16	0.48
Sr	1.56	1.29	1.50	1.54	1.19	2.22	1.40	1.07	1.47
Ba	0.66	0.95	0.82	1.04	1.03	3.97	0.99	0.99	1.30

4.4.1 Quartz chemistry of the Cape Cross – Uis pegmatite belt

The quartz from Cape Cross – Uis pegmatite belt is characterized by low Fe concentration (both MA 1 and MA 2 gave averages of <2 µg/g). The two averages for phosphorus (P) are both <15.4 µg/g while Ti's average concentrations are both <38.9 µg/g. Alkali metals (Li, Na and K) gave very high concentration values with the mean for each being above 70 µg/g with Na giving the highest mean of 343.4 µg/g (Table 4.4). Calcium and aluminium gave very high average values of above 500 µg/g and 600 µg/g respectively. Boron gave average concentrations of 118.5 µg/g and 124.8 µg/g for samples MA1 and MA2 respectively.

4.5 SEM-CL images from Doornboom

Images obtained from a Scanning Electron Microscope with an attached Zeiss CL detector (SEM-CL) are given below. Images for both DB 1 and DB 2 show two generations of quartz; higher luminescent quartz (PQ) show partial but limited replacements and is still in abundance indicating the limited effect of metamorphism.

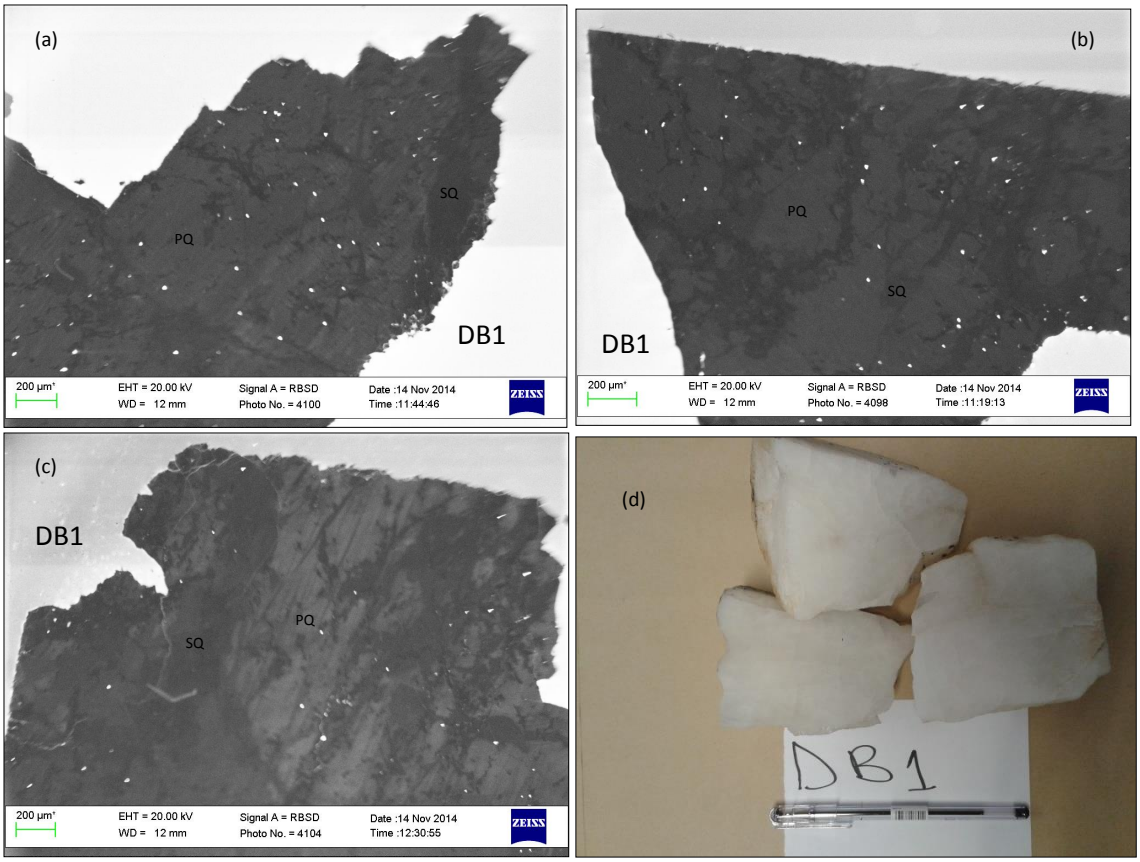

Figure 4.5 SEM-CL Images (DB1). (a), (b) and (c) SEM_CL images from a hydrothermal quartz deposit at the farm Doornboom 316 (Sample DB 1). All images show two generations of quartz; higher luminescent quartz (PQ) which was partially replaced by a generation of quartz with lower luminescent quartz (SQ). (d) the rock samples from which the SEM-CL images were taken.

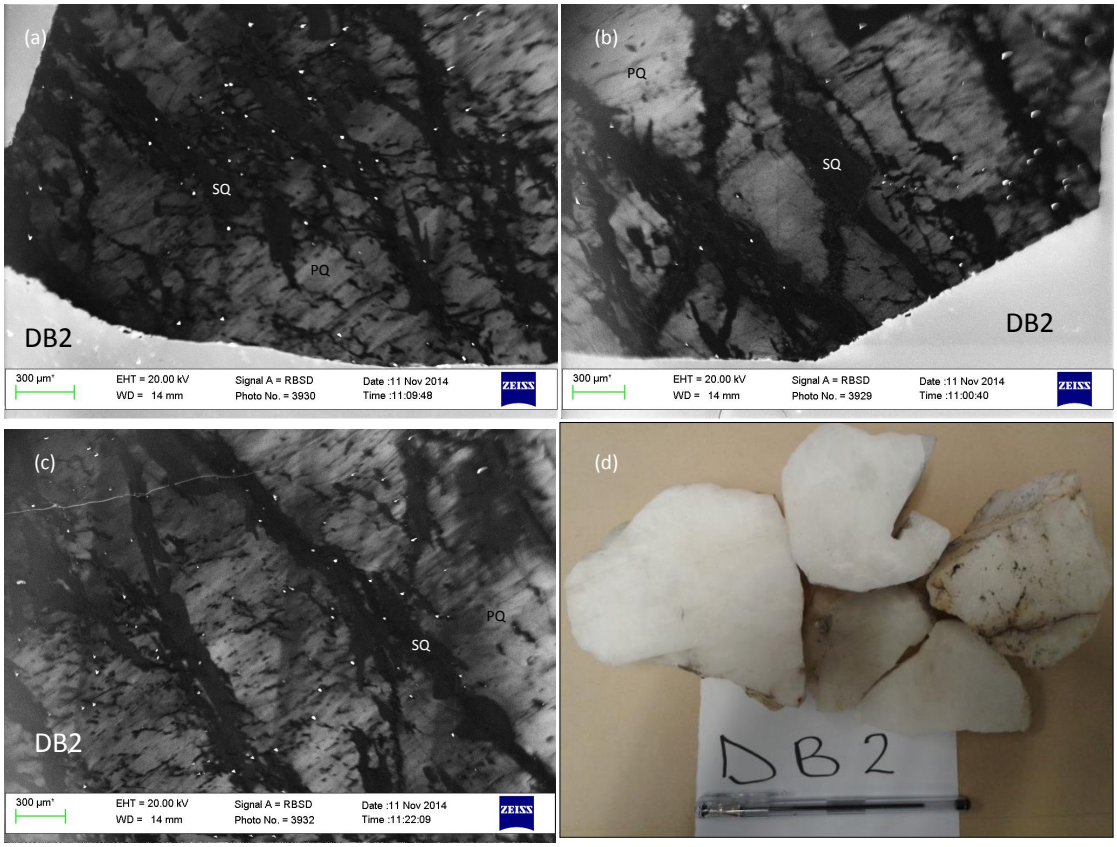

Figure 4.6 SEM-CL Images (DB2). (a), (b) and (c) SEM_CL images from a hydrothermal quartz deposit at the farm Doornboom 316 (Sample DB 2). All images show two generations of quartz; higher luminescent quartz (PQ) which was partially replaced by a generation of quartz with lower luminescent quartz (SQ). (d) the rock samples from which the SEM-CL images were taken.

4.6 Trace element concentrations in quartz from Doornboom

Table 4.5 shows the trace element concentrations in µg/g of sample DB1. Three quartz grains were selected from the sample and from the first grain two spots were analyzed and also two spots in the second quartz grain. The third quartz grain was divided into two areas; two spots were analyzed in the first area and three spots in the second area.

This gave a total of nine analyzed spots. The average of the nine spots for each trace element was calculated and is given in the last column of the table.

Table 4.5 Trace element concentrations (µg/g) of quartz from the Doornboom for sample DB 1.

Trace element	Grain1_Area1		Grain3_Area1		Grain4_Area1		Grain4_Area2			Average
	Spot 1 µg/g	Spot 2 µg/g	Spot 1 µg/g	Spot 2 µg/g	Spot 1 µg/g	Spot 2 µg/g	Spot 1 µg/g	Spot 2 µg/g	Spot 3 µg/g	µg/g
Li	249.48	197.38	255.23	280.61	184.40	266.95	283.59	199.84	138.01	228.39
B	158.38	132.98	194.39	244.41	96.00	120.52	179.45	98.89	70.96	144.00
Na	999.49	2187.75	2916.82	3407.0	674.89	587.02	1475.5	898.12	961.20	1567.53
Mg	17.03	26.26	15.60	17.22	8.09	8.80	12.69	11.95	7.95	13.95
Al	170.92	419.90	185.38	232.35	79.56	213.52	170.22	188.52	136.01	199.60
P	16.04	26.61	14.11	12.17	8.64	12.86	16.72	12.28	35.05	17.16
K	58.78	161.35	140.08	132.66	94.70	83.61	141.11	109.89	135.89	117.56
Ca	704.54	665.56	582.44	573.77	523.22	726.12	651.33	530.93	1101.6	673.25
Ti	32.44	50.34	29.66	26.41	31.77	25.71	24.78	31.08	25.65	30.87
Cr	0.65	1.87	0.50	0.70	0.44	0.51	0.36	0.60	0.58	0.69
Mn	3.37	2.60	1.51	<0.36	2.83	<0.41	<0.43	1.69	<0.33	2.40
Fe	0.90	1.51	0.75	0.70	0.49	0.65	1.09	0.80	1.85	0.97
Co	0.21	0.40	0.24	0.22	0.10	0.24	0.18	0.22	0.17	0.22
Ni	34.67	47.41	33.48	45.36	20.67	41.02	30.87	36.76	20.22	34.50
Cu	3.21	11.21	3.43	4.55	3.96	4.08	2.67	4.88	4.35	4.70
Zn	4.75	14.11	4.36	6.88	4.03	3.97	3.13	4.19	2.68	5.34
Rb	0.33	0.87	0.62	0.40	0.18	0.49	0.60	0.54	0.29	0.48
Sr	1.43	1.73	1.83	1.30	0.71	1.09	1.16	1.23	1.10	1.29
Ba	1.04	1.96	1.05	1.25	0.64	1.21	1.13	0.80	0.80	1.10

Table 4.6 below shows the trace element concentrations in µg/g of sample DB2. Two quartz grains were selected from the sample and each grain was divided into two areas.

Then two spots in each area were analyzed, giving a total of eight analyzed spots. The average of the eight spots for each trace element was calculated and is given in the last column of the table.

Table 4.6 Trace element concentrations (µg/g) of quartz from the Doornboom for sample DB 2.

Trace element	Grain1_Area1		Grain1_Area3		Grain2_Area1		Grain2_Area4		Average
	Spot 1 µg/g	Spot 2 µg/g	Spot 1 µg/g	Spot 2 µg/g	Spot 1 µg/g	Spot 2 µg/g	Spot 1 µg/g	Spot 2 µg/g	µg/g
Li	204.04	144.50	163.29	211.39	100.42	250.08	145.15	199.27	177.27
B	127.51	122.09	117.70	181.19	67.58	141.46	89.33	196.82	130.46
Na	318.33	673.36	389.17	2114.87	249.95	1740.09	258.55	387.12	766.43
Mg	14.49	14.32	11.09	15.54	14.05	18.33	9.63	17.60	14.38
Al	268.12	254.77	125.88	226.35	182.04	311.73	143.12	174.42	210.80
P	14.60	10.74	10.20	17.08	13.56	17.26	12.60	19.72	14.47
K	31.40	86.12	89.86	106.42	34.81	108.64	30.30	60.25	68.48
Ca	588.31	667.77	571.29	918.52	747.53	924.42	660.86	883.95	745.33
Ti	28.62	26.11	23.67	31.62	34.36	35.97	28.03	36.52	30.61
Cr	0.90	0.68	0.52	0.77	0.57	0.89	0.51	0.82	0.71
Mn	2.55	<0.33	<0.33	2.64	1.96	3.18	1.13	1.51	2.16
Fe	0.96	0.76	0.39	0.81	0.67	0.94	0.53	1.26	0.79
Co	0.23	0.93	0.19	0.34	0.27	0.62	0.15	0.27	0.37
Ni	44.34	27.69	19.17	34.34	17.96	38.17	26.89	26.88	29.43
Cu	2.69	3.56	1.87	2.65	4.21	4.26	2.13	3.96	3.17
Zn	4.77	4.87	4.02	4.09	5.05	5.77	3.46	8.88	5.11
Rb	0.38	0.33	0.20	0.46	0.21	0.63	0.21	0.28	0.34
Sr	1.51	3.33	1.65	1.59	2.39	1.64	0.70	1.60	1.80
Ba	1.26	1.41	1.06	1.52	1.21	1.31	0.70	1.35	1.23

4.6.1 Quartz chemistry of Doornboom hydrothermal vein quartz

The lowest trace element concentration (out of the nine which makes up the HPQ definition) at Doornboom hydrothermal vein quartz is Fe which gave a mean of 1 µg/g for sample DB1 and 0.8 µg/g for sample DB2. The second lowest mean trace element concentration is phosphorus (P) followed by titanium (Ti) with DB1 giving a mean of 17.2µg/g for P and 30.9 µg/g for Ti whereas DB2 gave a mean of 14.5 µg/g for P and 30.6 µg/g for Ti. Alkali metals (Li, Na and K) gave very high concentration values with the mean of each sample being above 100 µg/g. Na gave the highest mean of above 1500 µg/g (Table 4.7). High calcium and boron mean concentrations were also recorded and are all above 100 µg/g.

Table 4.7 Average concentrations of trace elements of all analysed samples. Included in the table are only those trace elements which are included in high purity quartz definition (HPQ) - Those trace elements which when present in excessive amounts affect end-use applications of quartz.

	Trace element average concentrations in µg/g										Required
Sample ID	**Li**	**B**	**Na**	**Al**	**P**	**K**	**Ca**	**Ti**	**Fe**	**Total conc.**	as /HPQ def.
DB1	228.4	144.0	1567.5	199.6	17.2	117.6	673.3	30.9	1.0	2979.3	50.0
DB2	177.3	130.5	766.4	210.8	14.5	68.5	745.3	30.6	0.8	2144.6	50.0
ALT1	177.6	139.8	77.0	154.2	11.9	10.9	579.9	28.3	0.7	1180.5	50.0
ALT2	61.6	42.9	52.2	62.8	8.6	8.5	465.6	23.9	0.4	726.3	50.0
MA1	201.6	118.5	140.9	655.2	15.0	70.6	513.3	36.4	1.9	1753.5	50.0
MA2	182.1	124.8	343.4	606.1	15.3	24.4	705.0	38.8	0.9	2040.8	50.0

Figure 4.7 below is a graphic representation of the average conditions from all three deposits.

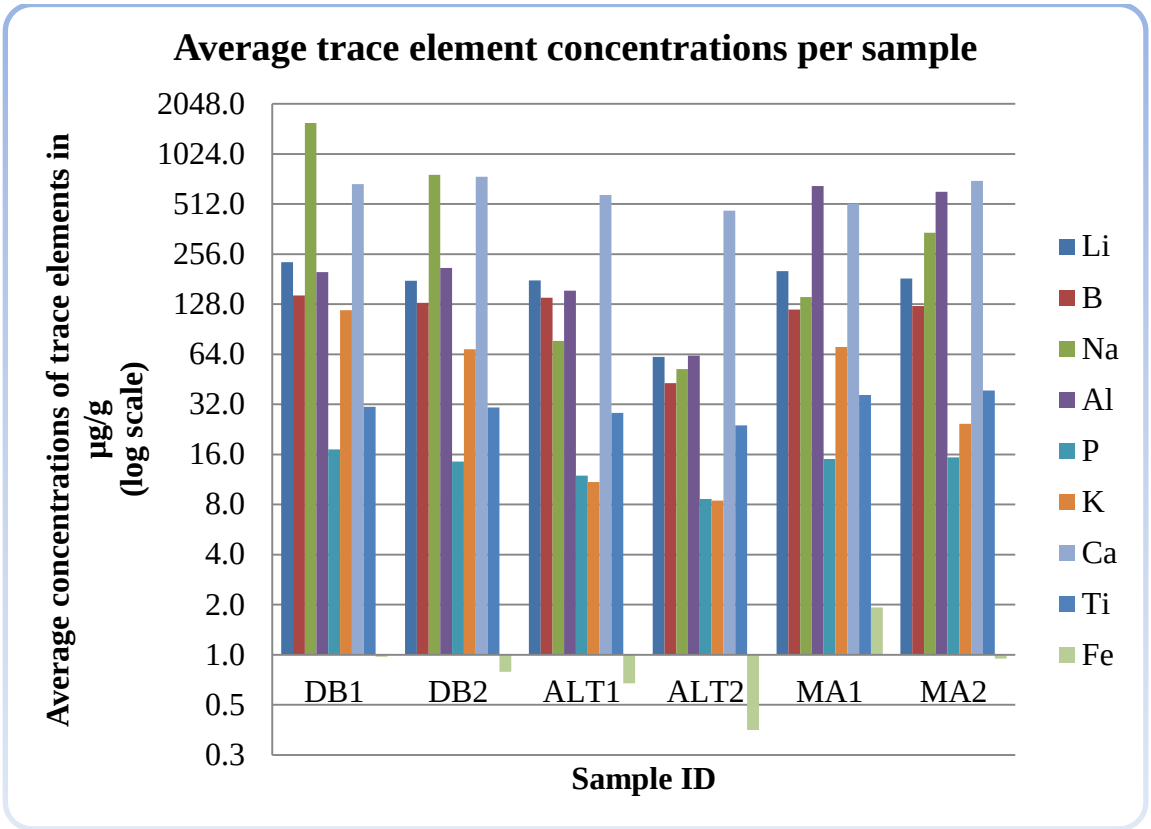

Figure 4.7 Average concentrations column chart. Average concentrations of trace elements per analysed sample. Samples depicted in the chart are DB1, DB2, ALT1, ALT2, MA1 and MA2. The trace element concentration (µg/g) on the Y-axis is on a logarithmic scale. It should be noted that Fe concentration columns are pointing the opposite of the rest; the reason is that the concentration are below 1µg/g i.e. the concentration of Fe in sample ALT2 is 0.4 µg/g, that in MA2 is 0.9 µg/g, that in ALT1 is 0.7 µg/g, that in DB2 is 0.8 µg/g and that in DB1 is 1 µg/g and it is the reason it is almost unnoticeable.

There are some notable similarities and variations when comparing average trace element concentrations in different samples from different localities (Fig. 4.7 and Fig. 4.8). The variations are quite pronounced for Na and Al concentrations. Na concentration is much higher in samples from Doornboom in comparison to samples from other localities (Fig. 4.8), giving a margin of not < 400 ppm (calculated as the difference between lowest average concentration at Doornboom and highest average concentration from other localities). Samples from the Cape Cross – Uis pegmatite belt contains much higher Al concentrations than samples from other localities giving (Fig. 4.8) a margin of not < 350 ppm, (calculated as the difference between lowest average concentration at the Cape Cross – Uis pegmatite belt and highest average concentration from other localities).

Similarities in concentrations from all the three localities are very pronounced for P, Ti and Ca (Fig. 4.8). The margins between concentrations for each of the three elements across the localities are quite small (Fig. 4.8). The other thing to note is that Li and B are depicting a similar trend; they are either low or high at each locality (Fig. 4.8).

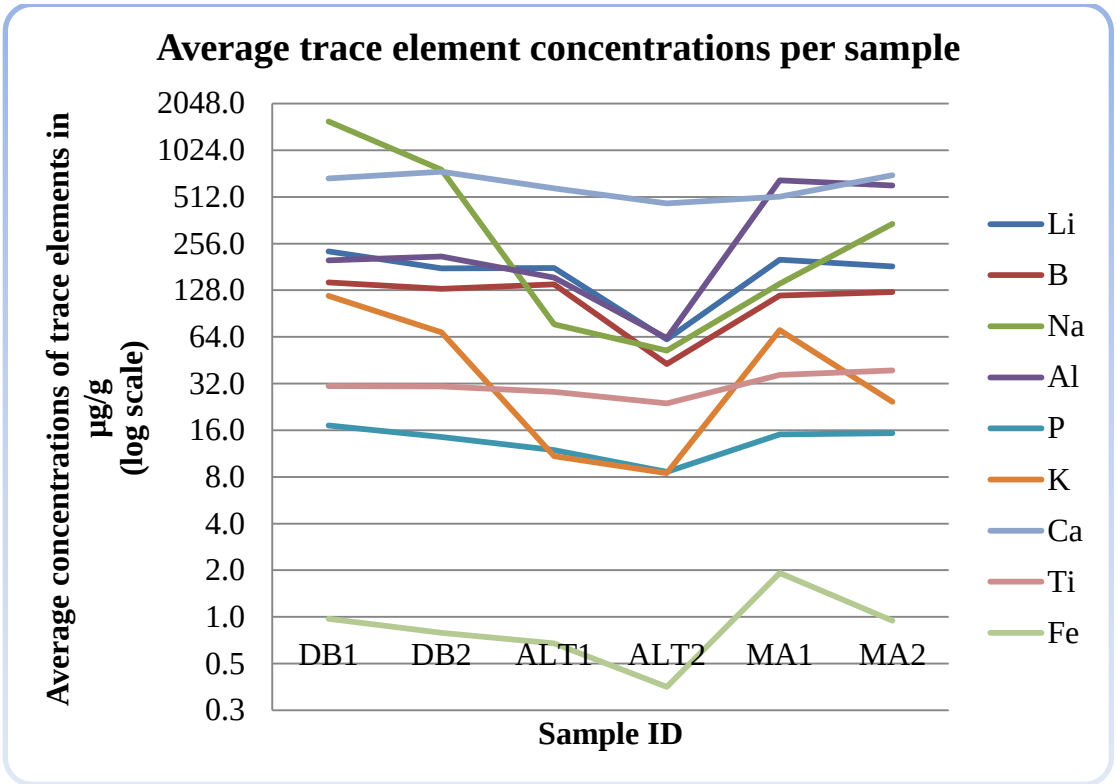

Figure 4.8 Average concentrations line chart. The graph is for purposes for depicting variations and similarities in concentrations from different localities.

In terms of trace element abundance in each sample, pie charts in figure 4.9 given below illustrate how much each element accounts for in the overall composition. In samples from Doornboom, Na and Ca are the dominant trace elements with each accounting for more than 20% (Fig. 4.9). Calcium (Ca) is the dominant trace element in samples from Alt Seeis, accounting for more than 45% of the concentration (Fig. 4.9). Calcium and aluminium are the dominant trace elements in samples from the Cape Cross - Uis pegmatite belt, with each accounting for more than 25% (Fig. 4.9). The general observation is that the content of Ca is high across all localities.

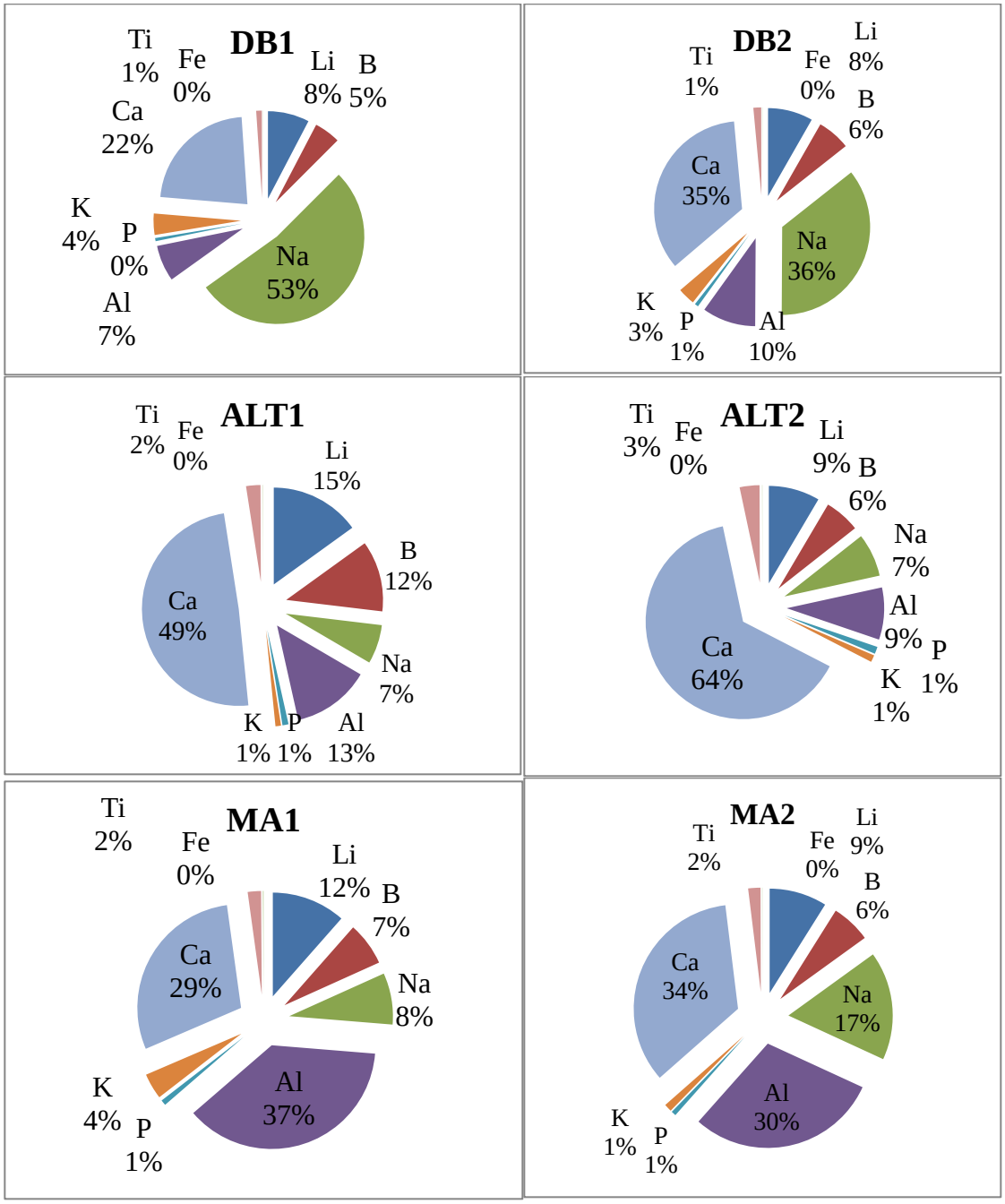

Figure 4.9 Average concentrations pie chart. Percentages of average concentrations of trace elements per sample. The pie charts indicate the concentrations of samples DB1, DB2, ALT1, ALT2, MA1 and MA2 to give a more clear representation of the amount of trace elements in each sample.

4.7 Statistical data analysis

Statistical Analysis of the concentrations in quartz was carried out and are as follows: F-test, T-test and correlation. The F test was carried to test the null hypothesis. The null hypothesis is that the variances of trace elements concentrations between samples from different localities are equal. The samples are expected to come from the same population considering the fact the genesis of the rock bodies under study are linked to the Damara Belt orogeny.

4.7.1 F and T-tests

F-tests were done to compare the variances of trace element content between samples from different localities i.e. an F-test on calcium concentrations between samples from Doornboom hydrothermal vein quartz and samples from Alt-Seeis hydrothermal vein quartz. The T-test was undertaken to determine mean differences of trace element concentrations between samples from different locations. The tables below are examples of the tables obtained from Excel 2010 during calculation of the F and the T tests.

Table 4.8 Calculation example of the F and the T tests; the table on left hand side contains concentrations of calcium from Doornboom (DB) and Alt-Seeis (ALT) and on the right of the concentration table are the F-test and T-test results calculated from the concentrations.

Ca concentration(µg/g)	
DB 1 and 2	ALT 1 and 2
704.54	403.37
665.56	352.53
582.44	589.47
573.77	557.36
523.22	738.80
726.12	711.48
651.33	699.03
530.93	587.51
1101.36	586.40
588.31	574.75
667.77	414.82
571.29	445.65
918.52	464.73
747.53	531.98
924.42	390.87
660.86	315.40
883.95	

F-Test Two-Sample for Variances

	Variable 1	*Variable 2*
Mean	707.172	522.759
Variance	26242.942	16975.163
Observations	17	16
df	16	15
F	1.546	
P(F<=f) one-tail	0.202	
F Critical one-tail	2.385	

t-Test: Two-Sample Assuming Equal Variances

	Variable 1	*Variable 2*
Mean	707.172	522.759
Variance	26242.942	16975.163
Observations	17	16
Pooled Variance	21758.533	
Hypothesized Mean Difference	0	
df	31	
t Stat	3.589	
P(T<=t) one-tail	0.001	
t Critical one-tail	1.696	
P(T<=t) two-tail	0.001	
t Critical two-tail	2.040	

The results of the one way analysis of variance are tabulated in table 4.9:

An example of how the table given below should be read (Row 1):

A one-way variance analysis of Ca concentrations of samples from Doornboom (M = 707.17, SD = 162.00) and Alt-Seeis (M = 522.76, SD = 130.29) revealed that the variances of the two populations are equal. F(16,15) = 1.55, p = 0.20.

Where M = mean, SD = standard deviation, F = the F-value, p = the p-value or probability value and (16,15) are the degrees of freedom (df).

Table 4.9 Tabulated results of the F-test. The test was carried out to compare the variances of trace element content between samples from different localities.

Trace element and sample ID	Mean	SD	df	F	p	Variances of the two populations
Ca conc. in DB (1 and 2)	707.17	162.00	(16,15)	1.55	0.20	Equal
Ca conc. in ALT (1 and 2)	522.76	130.29				
Ca conc. in DB (1 and 2)	707.17	162.00	(16,15)	1.31	0.30	Equal
Ca conc. in MA (1 and 2)	609.15	141.52				
Ca conc. in MA (1 and 2)	609.15	141.52	(15,15)	1.18	0.38	Equal
Ca conc. in ALT (1 and 2)	522.76	130.29				
Ti conc. in DB (1 and 2)	30.75	6.39	(16,15)	3.02	< 0.05	Not equal
Ti conc. in ALT (1 and 2)	26.10	3.68				
Ti conc. in MA (1 and 2)	37.61	7.54	(15,16)	1.4	0.26	Equal
Ti conc. in DB (1 and 2)	30.75	6.39				
Ti conc. in MA (1 and 2)	37.61	7.54	(15,15)	4.21	< 0.05	Not equal
Ti conc. in ALT (1 and 2)	26.10	3.68				
Fe conc. in DB (1 and 2)	0.89	0.37	(16,15)	3.11	< 0.05	Not equal

Fe conc. in ALT (1 and 2)	0.51	0.21				
Fe conc. in MA (1 and 2)	1.43	0.64	(15,16)	2.98	< 0.05	Not equal
Fe conc. in DB (1 and 2)	0.89	0.37				
Fe conc. in MA (1 and 2)	1.43	0.64	(15,15)	9.28	< 0.05	Not equal
Fe conc. in ALT (1 and 2)	0.51	0.21				
K conc. in DB (1 and 2)	94.46	40.92	(16,15)	156.94	< 0.05	Not equal
K conc. in ALT (1 and 2)	9.67	3.27				
K conc. in DB (1 and 2)	94.46	40.92	(16,15)	1.58	0.19	Equal
K conc. in MA (1 and 2)	47.50	32.52				
K conc. in MA (1 and 2)	47.50	32.52	(15,15)	99.14	< 0.05	Not equal
K conc. in ALT (1 and 2)	9.67	3.27				
P conc. in DB (1 and 2)	15.90	6.47	(16,15)	8.23	< 0.05	Not equal
P conc. in ALT (1 and 2)	10.26	2.26				
P conc. in MA (1 and 2)	15.17	6.80	(15,16)	1.12	0.42	Equal
P conc. in DB (1 and 2)	15.90	6.47				
P conc. in MA (1 and 2)	15.17	6.80	(15,15)	9.09	< 0.05	Not equal
P conc. in ALT (1 and 2)	10.26	2.26				
Li conc. in ALT (1 and 2)	119.63	73.57	(15,16)	1.83	0.12	Equal
Li conc. in DB (1 and 2)	204.33	54.34				
Li conc. in MA (1 and 2)	191.85	63.65	(15,16)	1.37	0.27	Equal
Li conc. in DB (1 and 2)	204.33	54.34				
Li conc. in ALT (1 and 2)	119.63	73.57	(15,15)	1.34	0.29	Equal
Li conc. in MA (1 and 2)	191.85	63.65				
B conc. in ALT (1 and 2)	91.36	62.23	(15,16)	1.62	0.17	Equal
B conc. in DB (1 and 2)	137.63	48.86				
B conc. in DB (1 and 2)	137.63	48.86	(16,15)	1	0.5	Equal
B conc. in MA (1 and 2)	121.68	48.83				
B conc. in ALT (1 and 2)	91.36	62.23	(15,15)	1.62	0.18	Equal
B conc. in MA (1 and 2)	121.68	48.83				
Al conc. in DB (1 and 2)	204.87	79.21	(16,15)	2	0.1	Equal
Al conc. in ALT (1 and 2)	108.51	56.19				
Al conc. in MA (1 and 2)	630.62	98.24	(15,16)	1.54	0.2	Equal
Al conc. in DB (1 and 2)	204.87	79.21				

Al conc. in MA (1 and 2) Al conc. in ALT (1 and 2)	630.62 108.51	98.24 56.19	(15,15)	3.06	0.05	Equal
Na conc. in DB (1 and 2) Na conc. in ALT (1 and 2)	1190.50 64.60	968.20 18.81	(16,15)	2649.45	< 0.05	Not equal
Na conc. in DB (1 and 2) Na conc. in MA (1 and 2)	1190.50 242.10	968.20 122.09	(16,15)	62.89	< 0.05	Not equal
Na conc. in MA (1 and 2) Na conc. in ALT (1 and 2)	242.10 64.60	122.09 18.81	(15,15)	42.13	< 0.05	Not equal

A noteworthy observation from Table 4.9 given above is that the standard deviation of sodium and calcium are relatively high, this may be attributed atomic clusters or the presence of mineral, melt and fluid micro-inclusions as given in detail under discussion of this study.

T-tests of independent Groups were carried out and the results are tabulated in Table 4.10:

An example of how the table given below should be read (Row 1):

An independent-samples t-test was conducted to compare the mean concentrations of Ca in samples from Doornboom (M = 707.17, SD = 162.00) and Alt-Seeis (M = 522.76, SD = 130.29). The result suggests that there is a significant difference between the concentrations of the two groups. $t(31) = 3.59$, $p < 0.05$.

Where M = mean, SD = standard deviation, t = the t-value, p = the p-value or probability value and (31) is the degrees of freedom (df).

Table 4.10 Tabulated results of the T-test. The test was carried out to determine if trace element concentrations from different localities are significantly different from each other.

Trace element and sample ID	Mean	SD	df	t	p	Remark
Ca conc. in DB (1 and 2)	707.17	162.00	31	3.59	< 0.05	Significant difference
Ca conc. in ALT (1 and 2)	522.76	130.29				
Ca conc. in DB (1 and 2)	707.17	162.00	30	1.85	0.07	No significant difference
Ca conc. in MA (1 and 2)	609.15	141.52				
Ca conc. in MA (1 and 2)	609.15	141.52	30	1.80	0.08	No significant difference
Ca conc. in ALT (1 and 2)	522.76	130.29				
Ti conc. in DB (1 and 2)	30.75	6.39	26	2.58	< 0.05	Significant difference
Ti conc. in ALT (1 and 2)	26.10	3.68				
Ti conc. in MA (1 and 2)	37.61	7.54	31	2.83	< 0.05	Significant difference
Ti conc. in DB (1 and 2)	30.75	6.39				
Ti conc. in MA (1 and 2)	37.61	7.54	22	5.48	< 0.05	Significant difference
Ti conc. in ALT (1 and 2)	26.10	3.68				
Fe conc. in DB (1 and 2)	0.89	0.37	26	3.55	< 0.05	Significant difference
Fe conc. in ALT (1 and 2)	0.51	0.21				
Fe conc. in MA (1 and 2)	1.43	0.64	24	2.96	< 0.05	Significant difference
Fe conc. in DB (1 and 2)	0.89	0.37				
Fe conc. in MA (1 and 2)	1.43	0.64	18	5.42	< 0.05	Significant difference
Fe conc. in ALT (1 and 2)	0.51	0.21				
K conc. in DB (1 and 2)	94.46	40.92	16	8.51	< 0.05	Significant difference
K conc. in ALT (1 and 2)	9.67	3.27				
K conc. in DB (1 and 2)	94.46	40.92	31	3.63	< 0.05	Significant difference
K conc. in MA (1 and 2)	47.50	32.52				
K conc. in MA (1 and 2)	47.50	32.52	15	4.63	< 0.05	Significant difference

K conc. in ALT (1 and 2)	9.67	3.27				
P conc. in DB (1 and 2)	15.90	6.47	20	3.38	< 0.05	Significant difference
P conc. in ALT (1 and 2)	10.26	2.26				
P conc. in MA (1 and 2)	15.17	6.80	31	-0.32	0.75	No significant difference
P conc. in DB (1 and 2)	15.90	6.47				
P conc. in MA (1 and 2)	15.17	6.80	18	2.74	< 0.05	Significant difference
P conc. in ALT (1 and 2)	10.26	2.26				
Li conc. in ALT (1 and 2)	119.63	73.57	31	-3.78	< 0.05	Significant difference
Li conc. in DB (1 and 2)	204.33	54.34				
Li conc. in MA (1 and 2)	191.85	63.65	31	-0.61	0.55	No significant difference
Li conc. in DB (1 and 2)	204.33	54.34				
Li conc. in ALT (1 and 2)	119.63	73.57	30	-2.97	< 0.05	Significant difference
Li conc. in MA (1 and 2)	191.85	63.65				
B conc. in ALT (1 and 2)	91.36	62.23	31	-2.38	< 0.05	Significant difference
B conc. in DB (1 and 2)	137.63	48.86				
B conc. in DB (1 and 2)	137.63	48.86	31	0.94	0.36	No significant difference
B conc. in MA (1 and 2)	121.68	48.83				
B conc. in ALT (1 and 2)	91.36	62.23	30	-1.53	0.14	No significant difference
B conc. in MA (1 and 2)	121.68	48.83				
Al conc. in DB (1 and 2)	204.87	79.21	31	4.01	< 0.05	Significant difference
Al conc. in ALT (1 and 2)	108.51	56.19				
Al conc. in MA (1 and 2)	630.62	98.24	31	13.74	< 0.05	Significant difference
Al conc. in DB (1 and 2)	204.87	79.21				
Al conc. in MA (1 and 2)	630.62	98.24	24	18.45	< 0.05	Significant difference
Al conc. in ALT (1 and 2)	108.51	56.19				
Na conc. in DB (1 and 2)	1190.50	968.20	16	4.79	< 0.05	Significant difference
Na conc. in ALT (1 and 2)	64.60	18.81				
Na conc. in DB (1 and 2)	1190.50	968.20	17	4.00	< 0.05	Significant difference
Na conc. in MA (1 and 2)	242.10	122.09				
Na conc. in MA (1 and 2)	242.10	122.09	16	5.75	< 0.05	Significant difference
Na conc. in ALT (1 and 2)	64.60	18.81				

4.7.2 Correlation coefficient

Correlation coefficients of trace elements in each sample were calculated using MS Excel and the results are tabulated in Table 4.12. This was done to check whether there was any relationship between trace elements from the same locality.

Table 4.11 Relationship between the correlation coefficient and the strength of correlation as given by Dancey and Reidy's (2004). Generally the higher the correlation coefficient, the stronger the relationship between the groups being analysed.

Value of the Correlation Coefficient	Strength of Correlation
1	Perfect
0.7 - 0.9	Strong
0.4 - 0.6	Moderate
0.1 - 0.3	Weak
0	Zero

Correlation coefficient analysis reveals that there is lot of concentration correlations in each sample (Table 4.12) and to be briefly looked at here are only strong correlations that are observed in both samples at a given locality. For example strong correlations that are observed in both samples from Alt Seeis (ALT 1 and ALT 2). Table 4.12 shows that there is a strong correlation between Fe and Ca, and also a strong correlation between Ti and Fe in both ALT 1 and ALT 2. For samples from Doornboom three strong correlations are observed in both DB 1 and DB 2. These correlations are between

B and Li, P and Ca and between Fe and P (Table 4.12). The observed strong correlation in samples from the Cape Cross – Uis pegmatite belt (MA1 and MA 2) are between Na and Li, Ti and Li and between Na and Ti (Table 4.12). Table 4.12 below should be read with reference to table 4.11 which indicates the relationship between coefficient and the allocated colour (indicating strength).

Table 4.12 Correlation coefficients of trace elements in each sample. The table should be used check any relationship between trace elements from the same locality.

Sample ID: ALT1

	Li7	***B11***	***Na23***	***Al27***	***P31***	***K39***	***Ca44***	***Ti47***	***Fe56***
Li7	1.000								
B11	0.459	1.000							
Na23	-0.006	0.056	1.000						
Al27	**0.841**	0.384	**0.520**	1.000					
P31	**0.800**	0.036	-0.169	**0.617**	1.000				
K39	0.418	**0.707**	0.487	**0.618**	-0.066	1.000			
Ca44	**0.734**	**0.525**	0.173	**0.725**	0.417	**0.785**	1.000		
Ti47	**0.637**	0.371	0.386	**0.761**	**0.531**	**0.530**	**0.512**	1.000	
Fe56	**0.765**	0.493	**0.575**	**0.945**	0.441	**0.768**	**0.841**	**0.682**	1.000

Sample ID: ALT2

	Li7	***B11***	***Na23***	***Al27***	***P31***	***K39***	***Ca44***	***Ti47***	***Fe56***
Li7	1.000								
B11	**0.698**	1.000							
Na23	0.281	0.328	1.000						
Al27	-0.093	0.290	0.175	1.000					
P31	0.226	**0.713**	**0.516**	0.292	1.000				
K39	0.400	0.349	**0.579**	-0.333	0.439	1.000			
Ca44	0.439	**0.655**	**0.507**	**0.583**	**0.633**	0.497	1.000		
Ti47	**0.683**	**0.570**	**0.741**	-0.081	**0.602**	**0.525**	0.456	1.000	
Fe56	0.246	0.335	**0.754**	0.493	**0.526**	0.239	**0.680**	**0.691**	1.000

Sample ID: DB1

	Li7	*B11*	*Na23*	*Al27*	*P31*	*K39*	*Ca44*	*Ti47*	*Fe56*
Li7	1.000								
B11	**0.821**	1.000							
Na23	0.413	**0.823**	1.000						
Al27	0.110	0.224	0.435	1.000					
P31	**-0.579**	-0.370	-0.036	0.301	1.000				
K39	-0.124	0.209	**0.603**	0.485	0.466	1.000			
Ca44	-0.478	-0.432	-0.281	-0.082	**0.855**	0.093	1.000		
Ti47	-0.298	-0.134	0.142	**0.754**	0.249	0.279	-0.188	1.000	
Fe56	**-0.546**	-0.342	-0.029	0.334	**0.985**	**0.520**	**0.791**	0.278	1.000

Sample ID: DB2

	Li7	*B11*	*Na23*	*Al27*	*P31*	*K39*	*Ca44*	*Ti47*	*Fe56*
Li7	1.000								
B11	**0.733**	1.000							
Na23	**0.656**	**0.515**	1.000						
Al27	**0.588**	0.236	**0.551**	1.000					
P31	**0.647**	**0.723**	0.438	0.321	1.000				
K39	**0.536**	**0.515**	**0.795**	0.350	0.137	1.000			
Ca44	**0.520**	**0.604**	**0.718**	0.357	**0.831**	0.482	1.000		
Ti47	0.342	0.353	0.313	0.317	**0.864**	0.021	**0.834**	1.000	
Fe56	**0.559**	**0.694**	0.191	**0.501**	**0.844**	0.022	**0.586**	**0.710**	1.000

Sample ID: MA1

	Li7	*B11*	*Na23*	*Al27*	*P31*	*K39*	*Ca44*	*Ti47*	*Fe56*
Li7	1.000								
B11	0.408	1.000							
Na23	**0.740**	**0.501**	1.000						
Al27	-0.049	0.357	0.141	1.000					
P31	**0.758**	0.114	**0.868**	0.165	1.000				
K39	0.077	0.118	0.311	**0.764**	0.478	1.000			
Ca44	**0.883**	0.071	0.412	-0.170	**0.600**	-0.037	1.000		
Ti47	**0.764**	0.043	**0.844**	-0.030	**0.971**	0.359	**0.628**	1.000	
Fe56	0.141	-0.243	-0.018	0.500	0.319	**0.619**	0.340	0.293	1.000

Sample ID: MA2

	Li7	*B11*	*Na23*	*Al27*	*P31*	*K39*	*Ca44*	*Ti47*	*Fe56*
Li7	1.000								
B11	**0.521**	1.000							
Na23	**-0.702**	**-0.508**	1.000						
Al27	**-0.617**	-0.029	**0.558**	1.000					
P31	0.250	0.489	-0.366	0.068	1.000				
K39	**0.561**	**0.810**	**-0.841**	-0.322	0.296	1.000			
Ca44	0.219	0.313	**-0.750**	-0.229	0.365	**0.714**	1.000		
Ti47	-0.751	-0.314	**0.819**	**0.810**	0.038	**-0.687**	**-0.560**	1.000	
Fe	0.721	0.915	**-0.712**	**-0.325**	0.636	**0.829**	**0.456**	-0.521	1.00

CHAPTER 5

5. Discussion

Research work similar to this study have been carried out elsewhere on deposits of similar origin (Haus, 2005; Ihlen et al., 2007; Müller et al.,2007; Müller et al., 2012; Larsen, Hendersen, Ihlen, and Jacamon, 2004; Larsen et al. 2000). These studies have been used for bench-marking procedures and comparing results of this study.

5.1 Quartz structures

Samples under this study indicate that the growth of secondary quartz is very limited and absent in some samples (Fig.4.1 - Fig. 4.6). This infers that the transformation of primary quartz to HPQ is negligible and it as such translates into meaning that metamorphic conditions did not play a role in the chemistry of trace element in quartz.

5.2 Causes of high trace element concentrations

A number of factors presumably played a role in the chemistry of trace elements in quartz under this study. These are factors such as melt and hydrothermal fluid composition, fluid inclusions, etc. Analysed spots were not checked for melt and fluid inclusions before analysis and their presence may elevate trace element concentrations in quartz. Melt inclusions for example may contain high concentrations of F, Cl, B, P, Li, Cs, and Rb (Thomas et al., 2006).

According to Müller et al. (2012) trace elements concentrations are chiefly regulated by the crystallization temperature (Wark, and Watson, 2006), the extent of melt fractionation in igneous and pegmatitic quartz (Müller et al., 2002a; Larsen et al., 2004; Breiter, and Müller, 2009; Jacamon, and Larsen, 2009; Müller et al., 2010a; Beurlen et al., 2011) and the chemistry and acidity of the fluid from which the quartz crystallized in diagenetic and hydrothermal quartz (Rusk et al., 2008; Jourdan et al., 2009; Müller et al., 2010b).

According to Müller et al. (2003), Larsen et al. (2004a,b), Spear and Wark (2004), Wark et al. (2004), Wark and Watson (2006) as cited in Müller et al. (2007), the concentration of Ti is a reflection of temperature during metamorphism. In this study metamorphism seem not to have played a major role in refining the quartz as evidenced by very limited

secondary quartz generations or their absence in some CL images. Therefore the Ti concentrations in this study are presumably a reflection of the fluid composition. Moderate pressure (~3–4 kbar) and temperatures (>350°C) during metamorphism, produces low Al and Li contents in the newly formed quartz (Müller et al., 2002b; Müller et al., 2012) . Deposits under this study are post – tectonic and were as such not affected by major metamorphic events. Therefore it is generally assumed that the trace element concentrations obtained in this study is a reflection of fluid composition. Favourable conditions existed in the Northern Central zone before emplacement of the intrusions under this study (intrusions in the Cape Cross – Uis pegmatite belt). These conditions have been calculated to have existed during M1 and M2 metamorphisms than roughly 530 and more Ma (Miller, 2008), whereas as the emplacement age of the pegmatites in the Cape Cross – Uis pegmatite belt has been put ~ 490 (Diehl, 1993).

The SMZ where two of the deposits (the Alt-Seeis hydrothermal vein quartz and the Doornboom hydrothermal vein quartz deposits) under this study are located is characterized by high pressure and low temperature with metamorphism peaks of 10 kbar and 590°c for M1 and 8 kbar and 570°c for M2 (Miller, 2008). Cl images of samples from these deposits show very limited presence of secondary quartz generations. Even though the ages of these deposits are not known, these deposits seem to have been deposited in the late stages of tectonism. This is evidenced from lack and in

some image parts, the absence of secondary quartz generations. Therefore the concentration in these deposits are also linked to fluid composition

5.3 Element correlations

T-test results carried out show that there are no significant differences with regard concentrations of Ca, Li, B, and P in samples from Doornboom hydrothermal quartz and SP14 pegmatite quartz. The F test also suggests that there are no variances in the trace element concentrations between the two deposits. This revelation may be explained by the assumption that the aqueous solutions of hydrothermal vein quartz and the pegmatite melts are from the same source rock. Diel (1993) stated that high 87Sr/ 86Sr initial ratios in the melts of the Cape cross – Uis pegmatites reflect partial melting of basement rocks. As such an assumption that the pegmatite melts and the hydrothermal aqueous solutions emanated from the same crustal rocks may have support.

A strong relationship was also revealed by the T-test results in the concentrations of Ca and B between samples from Cape Cross – Uis pegmatite belt and those from Alt Seeis hydrothermal vein quartz. It is noted from the correlation tables (Table 4.12) that both positive and negative correlations exist between elements but there was no distinctive pattern picked-out which could be linked to literature.

5.4 Economic appraisal

5.4.1 Economic appraisal of the Alt-Seeis hydrothermal vein quartz

The total trace element content (1180.5 µg/g for ALT1 and 726.3 µg/g for ALT2) of the Alt-Seeis hydrothermal vein quartz deposit though relatively low in comparison to the other two deposits in this study exceeds the requirement limit (50 µg/g) of HPQ deposits as per HPQ definition. The only trace element meeting the HPQ definition requirement is Fe and as such only applications requiring low Fe content may be feasible.

It should however be noted that petrographic examination of the samples using optical microscopy was not carried out before analysis. Petrographic examination allows the selection of quartz centres that are free of mineral, melt and fluid micro-inclusions for ablation and this was not carried out due to non-availability of equipment at the time of analysis. These inclusions if present may elevate the concentrations of quartz quality determining trace elements.

The inclusions being referred to here are intra-crystalline submicron inclusions (<1 µm), intra-crystalline mineral and fluid micro inclusions (>1 µm) and inter-crystalline impurities which may be present within grain boundaries as micro-crystals or mineral

coatings. Silicate melt inclusions are small blebs (~1-300 μm) of silicate melt that are trapped within igneous and pegmatitic quartz (Frezzotti, 2001; Webster, 2006).

5.4.2 Economic appraisal of quartz from Cape Cross – Uis pegmatite belt

According to the HPQ definition the SP14 pegmatite intrusions do not meet the requirement of a high purity quartz deposit. With the exception of iron (Fe) all the trace elements which determine the purity of quartz as per HPQ definition are far above the required limits. Nevertheless it should be noted with caution here that petrographic examination of the samples to check for inclusions was not carried out before analysis. The effects of these inclusions are as stated above under 'Economic appraisal of the Alt-Seeis hydrothermal vein quartz. Melt inclusions in pegmatitic quartz can contain high concentrations of F, Cl, B, P, Li, Cs, and Rb (Thomas et al., 2006).

5.4.3 Economic appraisal of the Doornboom hydrothermal vein quartz

The concentrations of eight out of the nine trace elements which determines quality of quartz and the definition of high purity quartz (HPQ) are all above the required limit as per HPQ definition. The only trace element meeting the required content as per HPQ definition is Fe with an average concentration of <1.1 μg/g whereas the requirement is <3 μg/g.

CHAPTER 6

6. Conclusions and recommendations

6.1 Conclusions

Analytical results revealed that all the three deposits under this study do not meet HPQ requirement and are thus not HPQ deposits. The HPQ requirement for each trace element is given as Al <30 μg g^{-1}, Ti <10 μg g^{-1}, Na <8 μg g^{-1}, K <8 μg g^{-1}, Li <5 μg g^{-1}, Ca <5μg g^{-1}, Fe <3 μg g^{-1}, P <2 μg g^{-1} and B <1 μg g^{-1}. Overally, Alt-Seeis hydrothermal vein quartz deposit has given a relatively the lowest concentration for each trace element in comparison to the other two deposits in this study. Analytical results obtained by LA-ICP-MS showed very low Fe concentrations in all the three deposits with all samples giving an average of <2μg g^{-1}.

Calcium content was very high in all samples from the three deposits (averaging 450 – 750μg/g) and these high values are seemingly associated with the chemistry of the fluids and composition of the melt from which the quartz crystallized. Titanium content in all samples is relatively low which may also be a reflection of fluid and melt composition. Titanium content in all samples was found to be averaging between 20 and 31μg g^{-1}. Very high Al and alkalis concentration were recorded in all the samples under study.

Aluminium and alkali metals (Li, Na and K) concentrations were relatively high in all the deposits with fewer exceptions. Average values of lithium were noted as being between 170 and 230μg g^{-1}, those of sodium as being between 70 and 1600μg g^{-1}, and those of potassium as being between 65 and 120μg g^{-1}, while aluminium average values were found to be between 150 and 660μg g^{-1}. Exceptions were exhibited by sample ALT2 from the hydrothermal vein deposit at the farm Alt-Seeis 133, in which all the alkali metals and aluminium average values were found to be less than 63μg g^{-1}.

Al and alkalis concentration values in the samples may also be attributed to fluid composition. Temperature conditions in the SMZ seem to have been favourable for transformation of quartz to HPQ but these conditions existed presumably before the emplacement of the deposits under study. Similarly temperature and pressure conditions which support transformation of quartz to HPQ existed before the emplacement pegmatite intrusions located in the Cape Cross – Uis pegmatite belt.

SEM-CL images indicate that secondary quartz generation was absent in some samples and only very minimal in others. This infers that that transformation of quartz to HPQ as a result of metamorphism was negligible or even absent. Samples from Doornboom hydrothermal quartz and one of the samples from SP14 pegmatite intrusion exhibited minimal secondary quartz generation limited to fractures whereas samples from Alt-

Seeis hydrothermal vein quartz and one of the samples from SP14 pegmatite intrusion contained no secondary quartz. This implies that metamorphic conditions did not play a role in the chemistry of trace elements in the quartz under study. This is also supported by the post tectonic emplacement age of the pegmatites under study.

Overall one of the samples from Alt-Seeis hydrothermal vein quartz ALT2 gave the lowest average concentration values on all trace elements. Samples from other deposits yielded very high trace element content. However a beneficiation study on these deposits is recommended to establish possible feasible industrial applications. It may be possible to upgrade the quartz from some of the deposits because this study did not establish as to whether all the trace element concentrations detected were lattice bound or not. Statistical interpretation of analytical results of pegmatite intrusions from Cape Cross - Uis pegmatite belt and those from Doornboom indicate significant compositional similarities. It is as a result assumed that the melts of the pegmatite intrusions from Cape Cross - Uis pegmatite belt and the aqueous solutions of the hydrothermal vein quartz of Doornboom emanated from the same source rock.

6.2 Recommendations

Results of this study revealed that post tectonic quartz hosting deposits in this orogenic belt have a high content of trace elements. The chemistry of these post tectonic deposits has not been affected by metamorphism. As studies have shown elsewhere that some favourable metamorphic conditions can transform primary quartz to HPQ, it is recommended that an HPQ study be carried out on syn- or pre-tectonic quartz hosting deposits. Such deposits should have been affected by metamorphism. The ages of these deposits should be pre-dating favourable metamorphic conditions. It is also highly recommended that spots to be ablated by LA-ICP-MS should first be examined for inclusions before analysis.

The second suggestion for future studies is to find out as to whether deposits dealt with herein can be beneficiated to meet requirements of some of the industrial applications. This would include studies determining whether the impurities detected in these deposits are lattice bound or interstitial. If the majority of impurities in these deposits are interstitial, then removing them using conventional processing methods such as initial crushing, optical sorting, comminution, classification to product particle size, autogenous grinding, electrodynamic fragmentation, attrition, magnetic separation, high tension separation, flotation acid washing, leaching, hot chlorination and calcinations should be considered as a research project.

REFERENCES

Ahrendt, H., Hunziker, J.C. and Weber, K. (1977). Age and degree of metamorphism and time of nappe emplacement along the southern margin of the Damara Orogen/Namibia (SW-Africa). *Geol. Rdsch*., **67**, 719- 742.

Baldwin, J.R. (1993). *Lithium and tantalum mineralization in rare-element pegmatites from southern Africa*. Unpubl. Ph.D. thesis, Univ. St. Andrews, 314 pp.

Beurlen, H., Müller, A., Silva, D., and Da Silva, M. R. R. (2011). Petrogenetic significance of trace-element data analyzed with LA-ICP-MS in quartz from the Borborema pegmatite province, north eastern Brazil. *Mineral Mag 75*, 2703–2719.

Blaine, J.L. (1977). Tectonic evolution of the Waldau Ridge structure and the Okahandja Lineament in part of the Central Damara Orogen, west of Okahandja, South West Africa. *Bull. Precambr. Res. Unit, Univ. Cape Town*, **21**, 99 pp.

Blankenburg, H. -J., Götze, J., and Schulz, J. (1994).Quarzrohstoffe. Deutscher Verlagfür Grundstoffindustrie, Leipzig-Stuttgart.

Breiter, K., and Müller, A. (2009). Evolution of rare-metal granitic magmas documented by quartz chemistry. *Eur J Mineral 21*, 335–346.

Broccardo, L., Kinnaird, J. A., and Nex, P. A. M. (2011). Preliminary fluid inclusion results from the Rubicon pegmatite, Karibib, Namibia. *Asociación Geológica Argentina, Serie D, publicación especial No 14*, 45-48.

Brouard, S., Breton, J., and Girardet, G. (1995). Small alkali metal clusters on (001) quartz surface: adsorption and diffusion. *J Molecular Struct. (Theochem) 334*, 145–153.

Bruhn, F., Bruckschen, P., Meijer, J., Stephan, A., Richter, D. K., and Veizer, J. (1996). Cathodoluminescence investigations and trace-element analysis of quartz by micro-PIXE: implications for diagenetic and provenance studies in sandstone. *Can. Mineral, 34*, 1223-1232.

Bühn, B., Okrusch, M., Woermann, E., Lehnert, K. and Hoernes, S. (1995). Metamorphic evolution of Neoproterozoic manganese formations and their country rocks at Otjosondu, Namibia. *J. Petrol*., **36**, 463-496.

Carr, R. G. (1983). Report on the preliminary investigation of the No 1 quartz body located on claim No 3, Alt Seeis. Unpubl. rep. Hochland Mining Co. (Pty) Ltd.

Cohen, A. J., and Makar, L. N. (1985). Dynamic biaxial absorption spectra of Ti^{3+} and Fe^{2+} in a natural rose quartz crystal. *Mineralogical Magazine, 49*, 709-715.

Dancey, C., and Reidy, J. (2004). Statistics without Maths for Psychology: using SPSS for Windows, London: Prentice Hall.

De Kock, G.S., Eglington, B., Armstrong, R.A., Harmer, R.E. and Walraven, F. (2000). U-Pb and Pb-Pb ages of the Naauwpoort rhyolite, Kawakeup leptite and Okongava Diorite: implications for the onset of rifting and orogenesis in the Damara belt, Namibia. *Communs geol. Surv. Namibia, Henno Martin Vol*., **12**, 81-88.

De Waal, S.A. (1966). *The Alberta Complex, a metamorphosed layered intrusion north of Nauchas, South West Africa, the surrounding granites and repeated folding in the younger Damara System*. Unpubl. D.Sc. thesis, Univ. Pretoria, 203 pp.

Diehl, B.J.M. (1986). Preliminary report on the Cape Cross - Uis pegmatite field. *Communs geol. Surv. S.W. Afr./ Namibia,* **2**, 39-45.

Diehl, B.J.M. (1990). Pegmatites of the Cape Cross - Uis Pegmatite Belt, Namibia: Geology, Mineralisation, Rb-Sr Characteritics and Petrogenesis of Rare Metal Pegmatites. Geol. Surv. Namibia. Open File rep, EO 083.

Diehl, M. (1993). Rare metal pegmatites of the Cape Cross – pegmatite belt, Namibia: geology, mineralization, rubidium-strotium characteristics and petrogenesis. *Journal of African Earth Sciences. 17(2),* 167-181. DOI: 10.1016/0899-5362(93)90033-M.

Downing, K.N. (1982). *The evolution of the Okahandja Lineament and its significance in Damaran tectonics (Namibia).* Unpubl. Ph.D. thesis, Univ. Leeds, 242 pp.

Feytis, A. (2010, May). Mauritanian quartz: *Industrial Minerals, no. 512*, 75.

Flicstein, J., and Schieber, M. (1974). Micro segregation of impurities in hydrothermally-grown quartz crystals. *J Cryst Growth 24 (25),* 603–609.

Frezzotti, M. L. (2001). Silicate-melt inclusions in magmatic rocks: applications to petrology. *Lithos 55*, 273–299.

Frondel, C. (1962). *The System of Mineralogy (vol.3). Silica minerals*, Wiley, New York

Geological Survey of Namibia. (1992). Lithium. In: Mineral Resources of Namibia.

Geological Survey of Namibia. (1992). Quartz. In: Mineral Resources of Namibia.

Geological Survey of Namibia. (1992). Tin. In: Mineral Resources of Namibia.

Goscombe, B., Gray, D. and Hand, M. (2004). Variation in metamorphic style along the northern margin of the Damara Orogen. *J. Petrol.* ***45***(6): 1261-1295.

Götze, J. (2009). Chemistry, textures and physical properties of quartz geological interpretation and technical application. *Mineral Mag 73*, 645–671.

Götze, J. (2012). Mineralogy, geochemistry and cathodoluminescence of authigenic quartz from different sedimentary rocks. In: J. Götze and R. Möckern, (Eds.), *Quartz: Deposits, Mineralogy and Analytics*, (pp. 287–306). Berlin, Heidelberg: Springer.

Götze, J., Plötze, M., and Habermann, D. (2001). Origin, spectral characteristics and practical applications of the Cathodoluminescence (CL) of quartz—a review. *Mineral Petrol*, *71*, 225–250.

Haack, U. and Gohn, E. 1988. Rb-Sr data on some pegmatites in the Damara Orogen, Namibia. *Communs geol. Surv. S.W. Afr./Namibia*, **4**, 13-17.

Haack, U., Gohn, E. and KLlein, J.A. (1980). Rb/Sr ages of granitic rocks along the middle reaches of the Omaruru River and the timing of orogenetic events in the Damara Belt (Namibia). *Contrib. Miner. Petrol*., **74**, 349-360.

Harben, P. W. (2002). The industrial mineral handybook—a guide to markets, specifications and prices (4thed.). Industrial Mineral Information. Worcester Park.

Hartmann, O., Hoffer, E. and Haack, U. (1983). Regional metamorphism in the Damara Orogen: interaction of crustal motion and heat transfer, 233-241. *In*: Miller, R.McG. (Ed.) *Evolution of the Damara Orogen of South West Africa/Namibia*. Spec. Publ. geol. Soc. S. Afr., **11**, 515 pp.

Hassan, F., and Cohen, A. J. (1974). Biaxial color centers in amethyst quartz. *American Mineralogist, 59,* 709-718.

Haus, R. (2005). High demands on high purity—processing of high purity quartz and diatomite. *Industrial Minerals*, 62–67.

Haus, R., Prinz, S., and Priess, C. (2012). Assessment of High Purity Quartz Resources (J. Götze andR. Möckel Eds.), *Quartz: Deposits, Mineralogy and Analytics*, 29-51.Springer Geology. DOI: 10.1007/978-3-642-22161-3_2.

Hawkesworth, C.J., Gledhill, A.R., Roddick, J.C., Miller, R.McG. and Kröner, A. (1983). Rb-Sr and 40Ar/39Ar studies bearing on models for the thermal evolution of the Damara Belt, Namibia, 323-338. *In*: Miller, R.McG. (Ed.) *Evolution of the Damara Orogen of South West Africa/Namibia*. Spec. Publ. geol. Soc. S. Afr., **11**, 515 pp.

Hoernes, S. and Hoffer, E. (1979). Equilibrium relations of prograde metamorphic mineral assemblages. A stable isotope study of rocks of the Damara Orogen, from Namibia. *Contrib. Miner. Petrol*., **68**, 377-389.

Hoffer, E. (1983). Compositional variations of minerals in metapelites involved in low- to medium grade isograd reactions in the southern Damara Orogen, South

West Africa, 745-765. *In*: Martin, H. and Eder, F.W., (Eds) *Intracontinental Fold Belts*. Springer Verlag, Berlin, 945 pp.

Hoffmann, C. (1976). Granites and migmatites of the Damara belt, South West Africa. Petrography and melting experiments. *Geol. Rdsch*., **65**, 939-966.

Hoffmann, K.-H. (1987). Stratigraphic subdivision and sedimentary facies of the Duruchaus Formation in the Geelkop Dome and Nauaspoort-Wortelpoort area northof Rehoboth, southern Damara Belt. *Communs geol. Surv. S.W. Afr./Namibia*, **3**, 9-18.

Hughes, E. (Ed) (2013, December). Projects in the pipeline High Purity Quartz. *Industrial Minerals,* 22- 25.

Humphries, S. E. (1984). The mobility of the rare earth elements in the crust. In: Henderson P. (Ed.), *Rare Earth element geochemistry.*515-341. Elsevier, Amsterdam.

Hyrsl, J., and Niedermayr, G. (2003). Magic world: inclusions in quartz—Geheimnisvolle Welt: Einschlüsseim Quarz. Bode Verlag GmbH, Haltern.

Ihlen, P. M., Muller, A., Larsen, R. B., and Henderson I. (2007). *Transformation of igneous quartz to high-purity quartz in granitic pegmatites of South Norway Granitic Pegmatites. Paper presented at the State of the Art – International Symposium,* Porto, Portugal. Retrieved from http://www.fc.up.pt/peg2007/files/ihlen.pdf

IOTA. (2011). *IOTA_high purity quartz.* Retrieved from http://www.iotaquartz.com/techiota4data.html

Jacob, R.E. (1974). Geology and metamorphic petrology of part of the Damara Orogen along the lower Swakop River, South West Africa. *Bull. Precambr. Res. Unit, Univ. Cape Town,* **17**, 185 pp.

Jacob, R.E., Moore, J.M. and Armstrong, R.A. 2000. Zircon and titanite age etermination from igneousrocks in the Karibib District, Namibia: implications for Navachab vein-style gold mineralization, *Communs geol. Surv. Namibia*, **12**, 157-166.

Jacamon, F., and Larsen, R. B. (2009). Trace element evolution of quartz in the charnockitic Kleivan granite, SW Norway: the Ge/Ti ratio of quartz as an index of igneous differentiation. *Lithos 107,* 281–191.

Jourdan, A. -L., Vennemann, T.W., Mullis, J., Ramseyer, K., and Spiers, C.J. (2009). Evidence of growth and sector zoning in hydrothermal quartz from Alpine veins. *Eur J Mineral 21,* 219–231.

Karnin, W.D. (1980). Petrographic and geochemical investigations on the Tsoabismund pegmatite dyke, South West Africa/Namibia. *Neues Jb. Miner., Mh.*, **5**, 193-208.

Kasch, K.W. (1981). The structural geology, metamorphic petrology and tectonothermal evolution of the southern Damara belt around Omitara, SWA/Namibia. *Bull. Precambr. Res. Unit, Univ. Cape Town*, **27**, 333 pp.

Kasch, K.W. (1983a). Regional P-T variations in the Damara Orogen with particular reference to early high-pressure metamorphism along the Southern Margin,

243-253. *In*: Miller, R.McG. (Ed.) *Evolution of the Damara Orogen of South West Africa/Namibia*. Spec. Publ. geol. Soc. S. Afr., **11**, 515 pp.

Kasch, K.W. (1987). Metamorphism of pelites in the Upper Black Nossob River area of the Damara Orogen. *Communs geol. Surv. S.W. Afr./Namibia*, **3**, 63-81.

Keller, P. (1991). The occurrence of Li-Fe-Mn phosphate minerals in granitic pegmatites of Namibia. *Communs geol. Surv. Namibia, 7* (1991) 21-35

Kheloufi, A., Fathi, M., Rahab, H., Kefaifi, A, Keffous, A., and Medjahed, S.A. (2013). Characterization and Quartz Enrichment of the Hoggar deposit intended for the electrometallurgy. (S. Pierucci and J.J. Klemeš Eds.), *Chemical Engineering Transactions, 32*, 889-894, DOI:10.3303/CET1332149

King, A. J. (1986). *Alt Seeis quartz deposits - final report on reserve evaluation drilling July - August 1986.* Unpubl. rep. A.J. King Associates.

Krause, R.. (2013). Overview of Overview of Auzminerals. Auzminerals Resource Group (AMRG) [Pdf]. Retrieved from https://www.ausimm.com.au/content/docs/branch/2013/09_auzmin_rg_ausimm_krause_8feb2013.pdf

Kronz, A., Van den Kerkhof, A. M., and Müller, A. (2012). Analysis of Low Element Concentrations in Quartz by Electron Microprobe. In: J. Götze and R. Möckel (eds.), *Quartz: Deposits, Mineralogy and Analytics, Springer Geology*, (p.191-217) Berlin Heidelberg: Springer-Verlag DOI: 10.1007/978-3-642-22161-3_9

Larsen, R. B., Hendersen, I., Ihlen, P. M., and Jacamon, F. (2004). Distribution and petrogenic behaviour of trace elements in granitic pegmatite quartz from South Norway. *Contributions to Mineralogy and Petrology, 147(5),* 615-628.

Larsen, R.B., Jacamon, F., Ihlen, P.M., and Henderson, I. (2004b). Natural refinement of quartz raw materials for the production of polycrystalline silicon. In: Pecchio M et al (eds) Applied Mineralogy—developments in science and technology, vol. 2. ICAM-BR, Sao Paulo, pp 693–696.

Larsen, R. B., and Polvé, M. (1998). *Trace element distribution in pegmatitic quartz: petrogenetic applications to granite pegmatites in South-Norway (extended abstract). 17th Meeting International Mineralogical Association,* Toronto, Canada.

Larsen, R. B., Polvé, M., and Juve, G. (2000). Granitic pegmatite quartz from Evje-Iveland: trace element chemistry and implications for high purity quartz formation. *Bulletin Geological Survey Norway, 436*, 57–65.

Leeder, O, Thomas, R, and Klemm, W. (1987). Einschlüsse in Mineralen. VEB Deutscher Grundstoffverlag, Leipzig.

Macey, P., and Harris, C. (2006): Stable isotope and fluid inclusion evidence for the origin of the Brandberg West area Sn–W vein deposits, NW Namibia. *Mineralium Deposita 41*, 671-690.

Marlow, A. (1983). Geology and Rb-Sr geochronology of mineralized and radioactive granites and alaskites, Namibia, 289-298. *In*: Miller, R.McG. (Ed.)

Evolution of the Damara Orogen of South West Africa/Namibia. Spec. Publ. geol. Soc. S. Afr., **11**, 515 pp.

Masberg, P. (2000). Garnet growth in medium-pressure granulite facies metapelites from the central Damara Orogen: igneous metamorphic history, 11 5-124. *In*: Miller, R.McG. (Ed.) *Henno Martin Commemorative Volume, Communs geol. Surv. Namibia*, **12**, 414 pp.

Masberg, P., Hoffer, E. and Hoernes, S. (1992). Microfabrics indicating granulite-facies metamorphism in the low-pressure central Damara Orogen, Namibia. *Precambr. Res*., **55**, 243-257.

McLaren, A. C., Cook, R. F., Hyde S. T., and Tobin, R. C., (1983). The mechanism of the formation and growth of water bubbles and associated dislocation loops in synthetic quartz. *PhysChem Miner 9*, 79–94.

Meinhold, G. (2010). Rutile and its applications in the earth sciences. *Earth Sci Rev 102*, 1–28.

Miller, R. McG. (1983). The Pan-African Damara Orogen of South West Africa/ Namibia. In: R. McG Miller (Ed.), Evolution of the Damara Orogen of South West Africa/ Namibia. The geological Society of South Africa. *Spec. Publication No.11, 431 – 515.*

Miller, R. McG. (2008). The Geology of Namibia, Neoproterozoic to lower paleoproterozoic (2). Geological survey of Namibia.

Moore P. (2005). High purity quartz. *Industrial Miner*als 8, 54–57.

Müller, A. (2011). Regional distribution of trace elements in quartz of South Norwagian pegmatites and its tectonomagnetic implications. *Asociación Geológica Argentina, Serie D, publicación especial No 14,* 139-140

Müller, A., René, M., Behr, H. –J., and Kronz, A. (2003). Trace elements and cathodoluminescence of igneous quartz in topaz granites from the Hub Stock (Slavkovskỳ Les Mts., Czech Republic). *Mineral Petrol 79,* 167–191.

Müller, A., Behr, H. –J., Van den Kerkhof, A. M., Kronz, A., and Koch-Müller, M. (2010a). The evolution of late-Hercynian granites and rhyolites documented by quartz—a review. *Earth Environ Sci Trans Royal Soc Edinburgh 100,* 185–204.

Müller, A., Herrington, R., Armstrong, R., Seltmann, R., Kirwin, D. J., Stenina, N. G., and Kronz, A. (2010b). Trace elements and cathodoluminescence of quartz in stockwork veins of Mongolian porphyry-style deposits. *Mineralium Deposita 45,*707–727.

Müller, A., and Ihlen, P. M. (2007). *Chemical signature of quartz and feldspar in polygeneration pegmatites in Froland, Norway. Granitic Pegmatite*s. *Paper presented at the State of the Art – International Symposium,* Porto, Portugal. Retrieved from www.fc.up.pt/peg2007/files/muller.pdf

Müller A., Ihlen P. M. and Kronz A. (2005). Potential resources of quartz and feldspar raw material in Sørland IV: Relationships between quartz, feldspar and mica chemistry and pegmatite type. *Geological survey of Norway report, 075,* pp. 104.

Müller, A., Ihlen, P. M., and Kronz, A. (2008a). Quartz chemistry in polygeneration Sveco Norwegian pegmatites, Froland, Norway. Eur *J Mineral 20,* 447–463.

Müller, A., Ihlen, P. M., Wanvik, J. E., and Flem, B. (2007). High-purity quartz mineralisation in kyanite quartzites, Norway. *Mineralium Deposita*, *42,* 523–535.

Müller, A., and Koch-Müller, M. (2009). Hydrogen speciation and trace element contents of igneous, hydrothermal and metamorphic quartz from Norway. *Mineral Mag 73,* 569–583.

Müller, A., Kronz, A., and Breiter, K. (2002a). Trace elements and growth patterns in quartz: a fingerprint of the evolution of the subvolcanic Podlesi Granite System (KrušneHory, Czech Republic). *Bull Czech GeolSurv 77,* 135–145.

Müller, A., Lennox, P., and Trzebski, R. (2002b). Cathodoluminescence and micro-structural evidence for crystallisation and deformation processes of granites in the Eastern Lachlan Fold Belt (SE Australia). Contributions Mineral Petrol 143, 510–524.

Müller, A., Wanvik, J. E., and Ihlen, P. M. (2012). Petrological and Chemical Characterisation of High-Purity quartz Deposits with Examples from Norway. In: J. Götze and R. Möckern, (Eds.), *Quartz: Deposits, Mineralogy and Analytics, Springer Geology*,(pp.71–118) Berlin Heidelberg: Springer-Verlag DOI: 10.1007/978-3-642-22161-3_4

Nash, C.R. (1971). Metamorphic petrology of the SJ Area, Swakopmund District, South West Africa. *Bull. Precambr. Res.Unit, Univ. Cape Town*, **9**, 77 pp.

Nex, P. A. M., Kinnaird, J. A., and Broccardo, L. (2011). Regional zonation of pegmatites and synchronous mineralization in the Central Zone of the Damara Orogen, Namibia. *Asociación Geológica Argentina, Serie D, publicación especial No 14*, 145-147.

Norwegian Crystallites AS. (2011). Retrieved from http://norcryst.no/

Ollila, J. T. (1987). Genetic aspects of Sn, Li, Be, Nb-Ta pegmatites and Sn-W vein deposits of the Damaraland orogeny, Namibia. Bulletin of the Geological Society of Finland 59, Part 1, 21–34.

Pearce, J. A. (1983). Role of the sub-continental lithosphere in magma genesis at active continental margins. In: C. J. Hawkesworth and M. J. Norry (Eds.), *Continental basalts and mantle xenoliths. (pp.* 230-249). Shiva, Nantwich.

Platiasa, S., Vatalisa, K. I., and Charalabidisa, G. (2013). Innovative processing techniques for the production of a critical raw material the high purity quartz. *Procedia Economics and Finance,* 5, 597 – 604. Retrieved from www.elsevier.com/locate/procedia

Puhan, D. (1983). Temperature and pressure of metamorphism in the central Damara Orogen, 219-223. *In*: Miller, R.McG, (Ed.) *Evolution of the Damara Orogen of South West Africa/Namibia*. Spec. Publ. geol. Soc. S. Afr., **11**, 515 pp.

Queensland Government. (2014). Queensland's metalliferous and industrial minerals 2014. Retrieved from https://www.dnrm.qld.gov.au/__data/assets/pdf_file/0005/271922/metalliferous-industrial-minerals-2014-part-3.pdf

Ramseyer, K., and Mullis, J. (1990). Factors influencing short-lived blue cathodoluminescence of - quartz. *Am Mineral 75*, 791–800.

Richards, T.E. (1986). Geological characteristics of rare metal pegmatites of the Uis Type in the Damara Orogen, South West Africa/Namibia, 1845-1862. *In*: Anhaeusser, C.R. and Maske, S. (Eds) *Mineral deposits of Southern Africa,* **2**. Geol. Soc. S. Afr., Johannesburg.

Roda, E., Keller, P., Pesquera, A. and Fontan, F. (2007). Micas of the muscovite-lepidolite series from Karibib pegmatites, Namibia. *Min. Mag. 71:* 41- 62.

Roedder, E. (1984). Fluid inclusions. *Reviews in mineralogy,12*. Mineralogical Society of America, Washington.

Roering, C. (1963). Pegmatite investigations in the Karibib District, South West Africa. Ph.D thesis (unpublished), University of the Witwatersrand, pp130.

Rollinson, H. R. (1993). Using geochemical Data: Evaluation, presentation, interpretation. Longman Group UK.

Rusk, B. G., Lowers, H. A., and Reed, M. H. (2008). Trace elements in hydrothermal quartz: relationships to cathodoluminescence textures and insights into vein formation. *Geology 36,* 547–550.

Sawyer, E.W. (1981). Damaran structural and metamorphic geology of an area south-east of Walvis Bay, South West Africa/Namibia. *Mem. geol. Surv. S.W. Afr*., **7**, 83 pp.

Simon, K. (2001). Does δD from fluid inclusion in quartz reflect the original hydrothermal fluid? *ChemGeol 177*, 483–495.

Spear, F. S., and Wark, D. (2004). TITANiQ: potential applications of the Ti in- quartz (+rutile) thermometer in metamorphic rocks. Eos Trans AGU, Joint Assembly Suppl, Abstract 85: JA491.

Sprunt, E. S. (1981). Causes of quartz cathodoluminescence colours. *Scanning Electron Microscopy*, 525-535.

Steven, N.M., Armstrong, R.A. and Moore, J.M. 1993. New Rb-Sr data from the Central Zone of the Damara Orogen, Namibia. *Communs geol. Surv. Namibia*, **8**, (1992/93), 5-14.

Stephens, M. B., Gustavson, M., Ramberg, I. B., and Zachrisson, E. (1985). The Caledonides of central north Scandinavia—a tectonostratigraphic overview. In: D. G Gee, B. A Sturt (Eds.), *The Caledonide Orogen—Scandinavia and Related Areas.* (pp. 135–162) Wiley, New York.

Taib, M. (2013). The Mineral Industry of Mauritania. U.S. Geological Survey Minerals Yearbook. Retrieved from http://minerals.usgs.gov/minerals/pubs/country/2013/myb3-2013-mr.pdf

Thomas, R., Webster, J. D., and Davidson, P. (2006). Understanding pegmatite formation: the melt and fluid inclusion approach. In: Webster J. D. (Ed.),

Melt inclusions in plutonic rocks. Short Course Series 36, (pp.189–210) Mineralogical Association of Canada.

Van den Kerkhof, A. M., and Hein, U. F. (2001). Fluid inclusion petrography. *Lithos 55*, 27-47.

Van den Kerkhof, A. M., Kronz, A., Simon, K., and Scherer, T. (2004). Fluid-controlled quartz recovery in granulite as revealed by cathodoluminescence and trace element analysis (Bamble sector, Norway). *Contributions Mineral Petrol 146*, 637–652.

Van den Kerkhof, A. M., Scherer, T., and Riganti, A. (1996). *Cathodoluminescence and EPR analysis of Archean quarzites from the Nondweni Greenstone Belt, South Africa.In "Abstracts SLMS International Conference on Cathodoluminescence", Nancy, 75.*

Vatalis, K.I., Charalambides, G., Benetis, N. P. 2015. Market of high purity quartz innovative applications. *Procedia Economics and Finance **24*** 734 – 742

Von Knorring, O. (1985). Some mineralogical, geochemical and economic aspects of lithium pegmatites from the Karibib - Cape Cross pegmatite field in South West Africa/Namibia. *Communs geol. Surv. S.W. Afr./ Namibia*, **1**, 79-84.

Wagener, G.F. (1989). Systematic variation in the tin content of pegmatites in western central Namibia. *J. geochem. Explor*., **34**, 1-19.

Wark, D. A., and Watson, E. B. (2006). TitaniQ: a titanium-in-quartz geothermometer. *Contributions Mineral Petrol 152*, 743–754.

Wark, D. A., Anderson, A. T., and Watson, E. B. (2004). Probing Ti in quartz: application of the TITANiQ thermometer to the Bishop Tuff. Eos Trans AGU, Joint Assembly Suppl, Abstract 85: JA494.

Watson, N.I. (1982). Regional geology of areas 211 5 C and 211 5 DC. *Open File Rep. geol. Surv. Namibia*, RG 5, 59 pp.

Webster, J. D. (Ed.) (2006). Melt inclusions in plutonic rocks. *Short Course Series 36*, Mineralogical Association of Canada, Montreal, Canada.

Weil, J. A. (1984). A review of electron spin spectroscopy and its application to the study of paramagnetic defects in crystalline quartz. *PhysChem Miner 10*, 149–165.

Weil, J. A. (1993). A review of the EPR spectroscopy of the point defects in a-quartz: The decade1982–1992. In: C. R. Helms and B. E. Deal (Eds.), *Physics and Chemistry of SiO2 and the Si-SiO2 interface 2*.(pp. 131–144). Plenum Press, New York.

Appendix 1 Calibration standard analysis

The information given in the table below is for the calibration standard sample which has known certified values for each element as indicated in column two of the table. The calibration standard was repeatedly analyzed four times and values obtained are given in column three to six under titles Calibration standard repl1, 2, 3 and 4. The averages of the repeated measurements are given in the second last column. The errors in terms of percentages for each element are given in the last column. A note from the analysing laboratory is that: Values for Li and B are semi-quantitative, as signal was very unstable.

SAMPLE ID: CALIBRATION STANDARD

Trace element	Calibration standard certified value µg/g	Calibration standard repl 1 µg/g	Calibration standard repl 2 µg/g	Calibration standard repl 3 µg/g	Calibration standard repl 4 µg/g	Average Calibration standard µg/g	% Error
Li7	42	14.84	60.77	85.02	23.6	46.1	9.7
B11	35	16.56	42.09	73.64	21.7	38.5	10.0
Na23	103 859.3	101698.94	101688.5	101364.61	101860.74	101653.2	2.1
Mg24	77.44	61.91	69.07	71.92	64.37	66.8	13.7
Al27	11166.7	11132.85	10611.3	10816.11	10729.56	10822.5	3.1

P31	51	42.2	47.39	49.81	43.44	45.7	10.4
K39	66.3	70.52	58.81	67.48	59.45	64.1	3.4
Ca44	85048.5	86218.88	84552.46	85563.62	84775.49	85277.6	0.3
Ti47	44	38.75	45.18	46.7	41.38	43.0	2.3
Cr53	36	37.55	36	36.61	36.37	36.6	1.8
Mn55	38	38.93	38.53	39.04	38.45	38.7	1.9
Fe56	51	41.24	53.17	58.25	44.77	49.4	3.2
Co59	35	35.76	35.43	35.45	35.57	35.6	1.6
Ni60	38.8	33.8	39.06	45.18	34.29	38.1	1.8
Cu65	37	37.78	37.81	37.79	37.81	37.8	2.2
Zn66	38	37.92	38.99	40.94	37.6	38.9	2.3
Rb85	31.4	32.4	31.12	31.34	31.57	31.6	0.7
Sr88	78.4	77.53	78.3	79.79	77.21	78.2	0.2
Ba137	39.7	40.96	38.73	39.59	39.26	39.6	0.2

Appendix 2 Control standard analysis.

BHVO 2 stated in the table below is a control standard sample with known certified values for each element as indicated in column two of the table. The BHVO2 control standard was repeatedly analyzed four times and obtained values are given in column three to six under titles Calibration standard repl1, 2, 3 and 4. The averages of the repeated measurements are given in the second last column. The errors in terms of percentages for each element are given in the last column. A note from the analysing laboratory is that: The large errors for Mg, K, Ti and Fe in the control standard is because the standard values are far outside the calibration range, these large errors are not expected for the values measured in the samples. Another note is that: Values for Li and B are semi-quantitative, as signal is very unstable.

SAMPLE ID: BHVO 2 CONTROL STANDARD							
Trace element	BHVO 2 Control standard certified value µg/g	Calibration standard repl 1 µg/g	Calibration standard repl 2 µg/g	Calibration standard repl 3 µg/g	Calibration standard repl 4 µg/g	**Average BHVO 2 control standard** µg/g	**% Error**
Li7	**4.4**	1.67	13.12	31.15	64	**27.5**	524.7

B11		9.12	14.72	20.07	45.12		
Na23	**17 804.5**	15195.86	15356.66	15196.14	15326.53	**15268.8**	14.2
Mg24	**42 999.3**	30202.27	30750.01	32023.85	32345.88	**31330.5**	27.1
Al27	**71 974.9**	73439.77	73013.67	72562.27	71756.98	**72693.2**	1.0
P31	**1 265.5**	1084.02	1107.09	1128.64	1134.36	**1113.5**	12.0
K39	**4 233.8**	2579.03	2632.98	2646.99	2680.75	**2634.9**	37.8
Ca44	**81475**	81199.84	80866.98	80221.16	79518.09	**80451.5**	1.3
Ti47	**16300**	9062.51	9447.48	10223.63	10446.55	**9795.0**	39.9
Cr53	**293**	264.88	269.22	273.53	273.7	**270.3**	7.7
Mn55	**1345**	1232.68	1243.48	1252.82	1253.38	**1245.6**	7.4
Fe56	**79 036**	52692.9	56071.84	62145.9	64345.27	**58814.0**	25.6
Co59	**44**	44.07	44.71	44.47	44.49	**44.4**	1.0
Ni60	**116**	87.08	92.28	97.22	100.7	**94.3**	18.7
Cu65	**127**	121.31	123.71	124.26	125.78	**123.8**	2.5
Zn66	**102**	97.79	101.42	104.78	107.63	**102.9**	0.9
Rb85	**9.2**	8.27	8.45	8.58	8.76	**8.5**	7.4
Sr88	**396**	378.54	379.26	382.04	377.38	**379.3**	4.2
Ba137	**131**	121.88	123.49	123.96	125.41	**123.7**	5.6